MODELS FOR TRANSIENT ANALYSES IN ADVANCED TEST REACTORS

Von der Fakultät für Energie-, Verfahrens- und Biotechnik
der Universität Stuttgart
zur Erlangung der Würde eines
Doktor-Ingenieurs (Dr. -Ing.) genehmigte Abhandlung

Vorgelegt von

Fabrizio Gabrielli

aus Rom, Italien

Haupberichter:	Prof. G. Lohnert, Ph.D.
Mitberichter:	Prof. Dr. P. Ravetto

Tag der mündlichen Prüfung: 22. Februar 2011

Institut für Kernenergetik und Energiesysteme der Universität Stuttgart

2011

to my wife Angelica and my daughter Benedetta
I love you!

Acknowledgments

I wish to thank several people who played a fundamental role in achieving this important goal in my professional life. When I think about them, I realize myself how much I was lucky to have encountered so many good persons.
First, I would like to thank my group leader, Dr. Werner Maschek. He believed in my technical capabilities in a particular period of my life and accepted me in his team. He was always available and supportive in my work, and I know that his door is always open for me. Apart his great scientific qualities, I found in him a great friend and this is much more important for me.
Furthermore I wish to thank Dr. Andrei Rineiski who has the greatest responsibility in this work, after me of course. He proposed the subject and guided me in completing the detailed studies, by means of fairly long discussions. Each time I was amazed by his enthusiasm in teaching me in a collaborative environment. His mind is a treasure chest of excellent ideas and I learned a lot by following them. Almost every day he gave me at least one example of his friendship.
There is also another 'column' who I wish to thank: Dr. Edgar Kiefhaber. He was a fundamental scientific resource for me because his of great experience in the neutronics and reactor physics field. He shared with me his knowledge and experience with patience, politeness, and passion. I wish to thank him for having spent a huge amount of time in reviewing this work and other papers I wrote in my limited English.
There is another unforgettable person whom I wish to thank: Prof. Günther Lohnert. He accepted me as his student and he gave me the possibility to get a Ph.D., which for me was a sort of dream. I thank him for his support and encouragement by pushing me to do my very best in order to make the optimum job. Each comment or suggestion from him had this final target.
I wish to thank Prof. Piero Ravetto for his help and support since I entered in the world of the nuclear research. I always found in him full availability, kindness, and a 'contagious' enthusiasm.
Special thanks to all my colleagues of the 'Partitioning and Transmutation' team at Karlsruhe Institute of Technology: Aleksandra, Claudia, Danilo, Eva, Michael, Shisheng, Xue-Nong, and Walter for their support and for the help with the German language to me and my family. A personal special thank to Claudia who is a sort of sister to me.
I would like to thank Prof. Thomas Schulenberg, director of Institute for Nuclear and Energy Technologies of the Karlsruhe Institute of Technology for offering me to perform this thesis work.
A special thought goes to my parents who did their very best in growing me up. They gave me the instruments to build my professional life and taught me the basic moral values to face the life.
There is a person that is the 'cornerstone' of my life since the first time I met her. This extraordinary person is my wife, Angelica. She continuously supports and encourages me, and she taught me that working hard makes everything possible in life. She followed me in another country and I well know that it was rather difficult for her at the beginning. My wife did not give me only this. She gave me a very particular gift, our marvellous daughter, Benedetta. This thesis is therefore dedicated to my ladies.

Table of Contents

Abstract

Several strategies are developed worldwide to respond to the world's increasing demand for electricity. Modern nuclear facilities are under construction or in the planning phase. In parallel, advanced nuclear reactor concepts are being developed to achieve sustainability, minimize waste, and ensure uranium resources. To optimize the performance of components (fuels and structures) of these systems, significant efforts are under way to design new Material Test Reactors facilities in Europe which employ water as a coolant. Safety provisions and the analyses of severe accidents are key points in the determination of sound designs. In this frame, the SIMMER multiphysics code systems is a very attractive tool as it can simulate transients and phenomena within and beyond the design basis in a tightly coupled way. This thesis is primarily focused upon the extension of the SIMMER multigroup cross-sections processing scheme (based on the Bondarenko method) for a proper heterogeneity treatment in the analyses of water-cooled thermal neutron systems. Since the SIMMER code was originally developed for liquid metal-cooled fast reactors analyses, the effect of heterogeneity had been neglected. As a result, the application of the code to water-cooled systems leads to a significant overestimation of the reactivity feedbacks and in turn to non-conservative results. To treat the heterogeneity, the multigroup cross-sections should be computed by properly taking account of the resonance self-shielding effects and the fine intra-cell flux distribution in space group-wise. In this thesis, significant improvements of the SIMMER cross-section processing scheme are described. A new formulation of the background cross-section, based on the Bell and Wigner correlations, is introduced and pre-calculated reduction factors (Effective Mean Chord Lengths) are used to take proper account of the resonance self-shielding effects of non-fuel isotopes. Moreover, pre-calculated parameters are applied to the non-fuel multigroup neutron cross-sections to take account of the different neutron spectra in the fuel and non-fuel regions. These techniques have been validated in the present work for a wide range of water-cooled thermal systems near steady-state conditions by benchmarking the extended SIMMER version against the reference neutronics codes and experimental results, for the criticality, the kinetic parameters, and the main reactivity effects. In this work, it is proven that the deployment of the new approach leads to more accurate SIMMER results for a large variety of situations during a transient. It is also shown that these parameters can be evaluated for few representative reactor states and that they can be interpolated more easily than the microscopic cross-sections as is usually done in the safety codes for LWRs. Thus, the employment of the Bondarenko method and of the pre-calculated parameters provides a very efficient SIMMER cross-section processing scheme during transient simulations.

Zusammenfassung

Weltweit werden unterschiedliche Strategien verfolgt, um den künftigen steigenden Bedarf an elektrischer Energie befriedigen zu können. Diesem Ziel dienen verschiedene Versionen moderner Reaktoranlagen, die sich in der Konstruktions- oder Planungsphase befinden. Parallel dazu werden fortschrittliche Reaktorkonzepte entwickelt, um Nachhaltigkeit zu gewährleisten, und den Verbrauch von Uranreserven und die Menge an nuklearem Abfall zu minimieren. Um das Materialverhalten der Komponenten (Brennstoff und Strukturelemente) dieser Systeme zu optimieren, gibt es erhebliche Anstrengungen in Europa, Materialtestreaktoranlagen zu entwickeln, die Wasser als Kühlmittel benutzen. Die Analyse schwerer Unfälle ist ein entscheidender Gesichtspunkt bei der Entwicklung sicherer Reactoren. Im Rahmen derartiger Untersuchungen bietet das „multi-physics" SIMMER-Programmpaket attraktive Aspekte, da es ermöglicht, transiente Vorgänge auch jenseits des Auslegungsunfalls zu simulieren, bei denen verschiedenartige Phänomene mit Hilfe von eng gekoppelten Rechenverfahren untersucht werden können. Die vorliegende Arbeit befasst sich wird in erster Linie mit der Verbesserung des in SIMMER angewendeten Berechnungsverfahrens zur Heterogenitätsbehandlung, basierend auf der sog. Bondarenko-Methode zur Bestimmung von Multigruppen-Wirkungsquerschnitten für thermische Systeme. Da SIMMER ursprünglich für die Analyse von Unfällen in flüssigmetallgekühlten Reaktoren entwickelt und eingesetzt wurde, wurde zunächst der Heterogenitätseffekt vernachlässigt, da er für derartige Reaktoren weniger wichtig ist. Dies hatte zur Folge, dass bei der Anwendung für wassergekühlte Reaktoren die Reaktivitätsrüchwirkungen stark überschätzt wurden und die Ergebnisse nicht-konservativ waren. Um diesen Mangel zu beheben, müssen die Resonanzselbstabschirmungseffekte und die räumliche Flussfeinverteilung energiegruppenweise im Detail berücksichtigt werden. Die dazu in dieser Arbeit durchgeführten wesentlichen Verbesserungen bei der Bestimmung effektiver Gruppenwirkungsquerschnitte werden beschrieben. Auf der Grundlage der Bell- und Wiegner- Beziehungen wird ein neuartiger Untergrundquerschnitt eingeführt, der (mit Hilfe vorherberechneter Factoren unter Verwendung von „Effective Mean Chord Lenghts") die Berücksichtigung von Resonanzselbstabschirmungseffekten der Nicht-Brennstoffisotope ermöglicht. Entsprechende vorherbestimmte Parameter erlauben es auβerdem, den Einfluss der Unterschiede in den Neutronenspektren zwischen dem Brennstoff-Bereich und den Nichtbrennstoff-Bereichen zu berücksichtigen. Die neuentwickelten Berechnungsmethoden wurden für einen groβen Bereich von thermischen Systemen in der Nähe von normalen Betriebszuständen validiert. Dazu wurde die weiterentwickelte SIMMER Version an Referenz-Neutronik-Codes und, soweit verfügbar, an Experimenten getestet und hinsichtlich Kritikalität, kinetischen Parametern und wichtigen Reactivitätseffekten überprüft. Es wird gezeigt, dass das verbesserte Verfahren genauere SIMMER Ergebnisse für eine Vielzhal von Unfallabläufen liefert. Darüberhinaus wird nachgewiesen, dass die für einige wenige repräsentative Reaktorzustände ermittelten und tabellierten Parameter eine einfache Interpolation ermöglichen im Vergleich mit den üblichen mikroskopischen Wirkungsquerschnitten, die in Sicherheitscodes für Leichtwasserreaktoren verwendet werden. Insgesamt ermöglicht die Verwendung der erweiterten Bondarenko-Methode und der zugehörigen vorausberechneten Parameter ein effizientes Berechnungsverfahren in SIMMER für geeignete effekive Gruppenwirkungsquerschnitte bei der Simulation von Reaktortransienten in thermischen Systemen.

Chapter 1. Introduction

1.1 Background

Research reactors are nuclear installations acting as neutron sources dedicated to fundamental and applied research. More than 500 such reactors have been built worldwide, with low power research reactors often used for training and education purposes. Material Testing Reactors (MTRs) operate at higher power levels and are mainly intended for:

- studies of fuel and material behaviour under irradiation for later application in various commercial nuclear reactor types;
- analyses and characterization of materials;
- irradiations for industrial and medical applications.

MTRs have provided essential support for nuclear power programs in many countries over the last 40 years. Combined with hot laboratories for post-irradiation examinations, they are an essential part of nuclear research facilities for R&D in the fission reactor domain. MTRs have been used to address development and qualification, under irradiation, of materials and fuels with compositions, dimensions, and environmental conditions relevant for nuclear power plants. Such programs were performed to optimize and demonstrate safe operation of a range of different commercial power reactors (AGR, BWR, PWR, MAGNOX and VVER). The majority of these Generation-II plants are now reaching the end of their planned lives (~30 years), but it is anticipated that some operators will seek and acquire licenses to extend these lifetimes.

Several countries in Europe, America, and Asia have initiated multinational efforts, such as the Generation-IV International Forum (GIF) [1] and the IAEA International Project on Innovative Nuclear Reactor (INPRO) [2], which aimed at the development of advanced reactor technology that should be able to respond to the world's increasing electricity demand while simultaneously being safer, more competitive, and more proliferation resistant.

Generation-III light-water reactors (EPR and advanced LWRs), which represent optimized versions of conventional energy facilities, are under construction or in the planning stages in several countries, often to augment existing nuclear power plants with safer reactor systems. In parallel, with the implementation of these cutting-edge LWR technologies, it is seemed essential to begin development of advanced nuclear technologies for the longer term: metal- and gas- cooled fast reactors, high temperature reactors, molten-salt reactors, and accelerator driven systems. Key technologies for such advanced systems, in addition to enhanced safety features, encompass fuel burn-up extension, structural materials operating at high temperature, fast neutron resistant fuels and structural materials, and advanced fuel recycling processes. The understanding of the mechanisms governing the material behaviour under irradiation is critical for the control of the most relevant parameters.

Currently, only a small fraction of the operating MTRs have enough power to perform representative irradiations of materials and fuels (> 10 MWth). Existing MTRs in Europe will be more than 50 years old in the coming decade and will face an increasing probability of shut-down (Table 1, [3]). As a result, there is a general consensus about the need to renew MTRs in Europe.

Country	Reactor	First Criticality	Power (MWth)
Czech Republic	LVR15	1957	10
Norway	Halden	1960	19
Netherland	HFR	1961	45
Belgium	BR2	1961	60
France	OSIRIS	1966	70
Sweden	R2	1960	50

Table 1. The main European Material Test Reactors

In order to address this issue, the Jules Horowitz Reactor (JHR) project [4, 5, 6] has been launched as a new MTR which will be in operation in 2014 at Cadarache (France). JHR is a 100 MW tank pool reactor which will offer modern irradiation experimental

capabilities for studying material and fuel behavior under irradiation for a wide range of nuclear systems. The reactor (see Figure 1) is designed to provide a flexible experimental capability able to create up to 16 dpa-Fe/year for in-core and for in-reflector irradiated samples which is about twice the material damage per year than currently available in European MTRs.

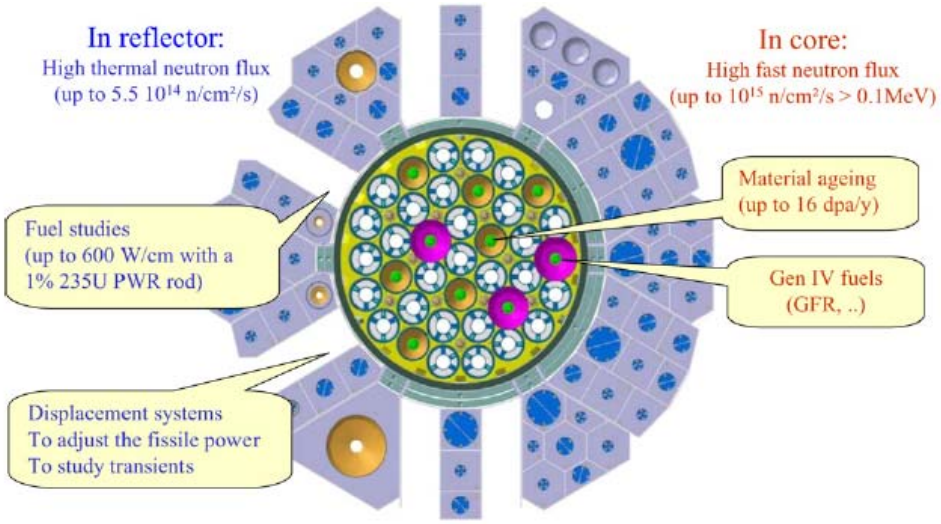

Figure 1. JHR core layout and experimental devices location

JHR will be operated with a high density low enriched fuel (U enrichment below 20%, density 8 g/cm^3), requiring the development of U-Mo fuel. As a back-up solution, the JHR may be started, if necessary, with a U_3Si_2 fuel with a higher enrichment (typically 27%), for a limited period of time. The fuel element is composed of a set of curved plates assembled with stiffeners with a layout similar to those usually employed in many material test reactors in Europe and in the United States [7].

1.2 Motivation

On the basis of the Mastered Severe Accident, the French safety methodology defines, beyond the four classical safety categories, several accident scenarios for which it has to be demonstrated that no harmful radiological or mechanical consequences will result.

The so-called BORAX accident is the reference Mastered Severe Accident to be taken into account in the containment design of JHR [6]. This accident consists of a steam explosion following the introduction of a large amount of reactivity in the core by means of a sudden ejection of the control rod corresponding to a short reactor period.

The nomenclature is obtained from the BORAX-I (Boiling Reactor Experiment) facility [8, 9] where an unexpected full destruction of the reactor occurred during an experimental test in 1954. In the 50's and 60's, large non-destructive tests and integral core destructive tests were performed in the framework of light water reactor development at the National Reactor Testing station in Idaho (USA), namely, the BORAX-I and the Special Power Excursion Reactor Tests (SPERT) [10, 11]. The aim of these tests was the simulation of reactivity-induced accidents (RIA) using enriched aluminium plate-type fuel in water-reflected and moderated reactor systems to better understand and evaluate reactivity compensating mechanisms during transients in these systems.

These experiments provided understanding of the phenomenology of the transient. If the reactivity injection is sufficiently high, the aluminium of the fuel plates starts to melt, while the water coolant in the core remains relatively cold. Under such conditions, the fuel-coolant interaction (FCI) may then induce the formation of a water steam bubble, which expands in the primary circuit producing pressure waves.

In France, the lessons learned from the BORAX accident are taken into account in the safety evaluation and design of research reactors. The BORAX accident actually is treated as an extension of the Design Basis Accident domain, although it is considered as a Beyond Design Basis Accident according to the usual rules. Thus, it must considered for the design of important safety related equipment such as containment buildings, walls of the pools, and post accident heat removal systems [12]. Up to now, French research reactors with aluminium plate-type fuel and water moderator have been designed to account for the consequences of such a core disruptive RIA, based on the following conditions: (1) an envelope bounding thermal energy of 135 MJ during the power transient, (2) 100% fuel melting and (3) 9% conversion of thermal energy to mechanical energy by FCI phenomena.

In the framework of the JHR safety assessment, the Institut de Radioprotection et de Sûreté Nucléaire (IRSN, France) recognized that these assumptions should have been revised, as two main features restrict the possibility of a direct extrapolation of the results obtained from the BORAX-I and SPERT-I tests to the Jules Horowitz Reactor case [12]:

- the fuel of those reactors was highly enriched (93 wt% U^{235}), which is not the case for many current research reactors, including JHR;
- no absolute limit seems to exist on the thermal energy release and on the efficiency of conversion of thermal to mechanical energy. This parameter is strongly dependent on the introduced reactivity, the fuel kinetics, and the FCI processes.

As a result, IRSN found that another approach for the BORAX accident based on the analysis of an accident scenario was needed. To accomplish this, IRSN launched a research program with two main goals: the analysis of the BORAX and SPERT experiments using the existing codes for the simulation of the whole transient and the evaluation of the consequences of the steam explosion on the pool and the hall of the reactor [12, 13].

Most computer codes for transient analyses in water-cooled reactors are tailored to commercial power reactors. System codes such as RELAP [14] and RETRAN [15] are devoted mainly to the modelling of the coolant loops and their components and treat the reactor core with less detail. The neutronics model coupled to the thermal-hydraulics of RELAP and similar codes usually describe the core by means of a few channels representing the whole core. The transient analyses are usually performed by employing point kinetics methods, the reactivity coefficients and the axial power shapes for each channel being provided by input. When the spatial kinetics approach is employed, the reactivity feedbacks are computed by interpolation of data from pre-calculated tables of macroscopic cross-sections (XSs) depending upon a number of parameters such as fuel temperature and coolant density for specified sub-assembly geometries. The reason lies in the significant amount of time needed to compute the effective XSs for a heterogeneous thermal reactor cell. In fact, in order to accurately compute the core reactivity and reaction rates, the fine spatial neutron flux distribution within the sub-assembly should be taken into account. The preparation of these tables and the use of interpolation procedures,

however, often pose a non-trivial problem, especially if large deviations from steady-state conditions need to be considered as accident scenarios.

For the analyses of transients for research test reactors including Design Basis Analysis, more refined neutronics and thermal-hydraulics models are necessary. Material testing reactors, such as JHR, show a complex and very heterogeneous arrangement for fuel sub-assemblies and irradiation devices that may change during a hypothetical accident. For these reactors, the neutronics models should be as close as possible to the actual core so that the point kinetics approach might not be sufficient in simulating the neutronics transients. Moreover, a relatively large number of energy groups should be employed in the XS processing in order to more accurately take into account the shift of neutron spectra at different spatial positions under different perturbation conditions, e.g for the coolant void. As materials are also tested under severe conditions, the neutron XSs should be recalculated more often than the near nominal as larger variations in reactivity and power should be taken into account. Moreover, sophisticated mechanical and thermal-hydraulic models should be used to predict the behaviour of the different fuel sub-assemblies under these accident conditions.

Analyses of experiments in previous test reactors were mainly performed by *ad hoc* codes in a mostly non-mechanistic manner, which did not allow the establishment of an automatic procedure which could couple neutronic and thermal-hydraulic phenomena. The conventional approach aimed at the development of empirical models for neutronics and thermal-hydraulics on the basis of available experimental results [16, 17, 18]. Usually, the feedback reactivity effects were derived by fitting measured values of temperature and void coefficients near nominal conditions. The results were employed then for simulating transients with the point kinetics approach, usually using the diffusion approximation.

Conventional codes show a reasonable performance when employed for analyses of non-destructive experiments in material test reactors [19, 20]. Nevertheless, since this is not their main mission, such codes may not be able to perform core destruction analyses after the core geometry is distorted. When an accidental scenario is analysed, dedicated codes are usually employed to simulate specific phenomena separately, e.g. the MC3D code [21] for the steam explosion simulation. There are also some ongoing attempts to assess

very complex platforms of codes for these situations, however, the neutronics and the thermal-hydraulics are not yet coupled in a tightly manner [22].

For such complex cases the SIMMER–III (2D) and SIMMER–IV (3D) two/three-dimensional codes [23, 24, 25] were originally developed for application for liquid metal-cooled fast reactors to mechanistically analyse accident scenarios from initiation up to core disruption [25]. Complex phenomena can be simulated, e.g. coolant voiding, fuel and clad melting, pin break-up, fuel redistribution, fission gas release, and already defined FCI. In particular, as a fast reactor core loaded with MOX fuel is reactivity-wise not in its most reactive configuration, fuel compaction or sloshing phenomena could lead to a reactivity transient and power excursion. Therefore the complete code framework, including neutronics, was developed to describe material interactions, material redistributions, and other related phenomena.

The thermal-hydraulics part of SIMMER uses a three-velocity-fields, multi-phase, multi-component, Eulerian fluid dynamics model coupled with a structure model (fuel pins etc.). The model employs an elaborate set of equation of state functions for fuel, steel, coolant (light and heavy liquid metals, water, and gas), absorber, and special alloys used in experiments [26]. The thermal-hydraulics module is coupled to the neutronics part of the code, which includes a model for generating XSs from CCCC multigroup libraries [27, 28] and space-, time-, angle-, and energy-dependent neutron transport models. The neutron flux distribution during the transient is calculated using the improved quasi-static method [29] and the time-dependent flux shape is evaluated by the improved deterministic TWODANT and THREEDANT codes [30], which are essential sub-packages of DANTSYS [31].

With these coupling capabilities, SIMMER is a powerful deterministic tool to be used in safety analyses for advanced test reactors. IRSN and KIT (Karlsruhe Institute of Technology) initiated a collaboration with the intention of extending the range of application of the SIMMER code for the analysis of SPERT experiments [12, 13].

Even if the SIMMER code is tailored to meet analysis of metal-cooled fast reactors, water as coolant has been tested in the thermal-hydraulics models. Many basic experiments (e.g. multi-phase, steam explosion) were recalculated during the SIMMER code validation [32] and, in recent years, SIMMER thermal-hydraulics models have been

extended to simulate specific phenomena for analyses of light water-cooled research reactors [33, 34]. Further improvements are foreseen in the future.

The extension of the code to transient analyses of water-cooled systems requires upgrading of the SIMMER XS processing scheme to take account of the effect of heterogeneities. Since the influence of this effect is not so large, at least compared to the uncertainties in reactivity effects in fast reactors, the heterogeneity treatment is not deployed in the neutron XSs processing scheme. On the contrary, this effect is significant in water-cooled systems, both in steady state and during transients. Therefore, the application of the original SIMMER XS model to transient analyses of these systems would provide non-conservative reactivity feedbacks and would compute inaccurate kinetics parameters. This is shown in Figure 2, where the Doppler and void effects evaluated by SIMMER and MCNP [35] (here used as a reference neutronics code) are compared for the low-enriched MTR core model proposed in the IRSN/KIT collaboration assuming different moderator void fractions (0%, 10% and 20%) in the central fuel sub-assembly.

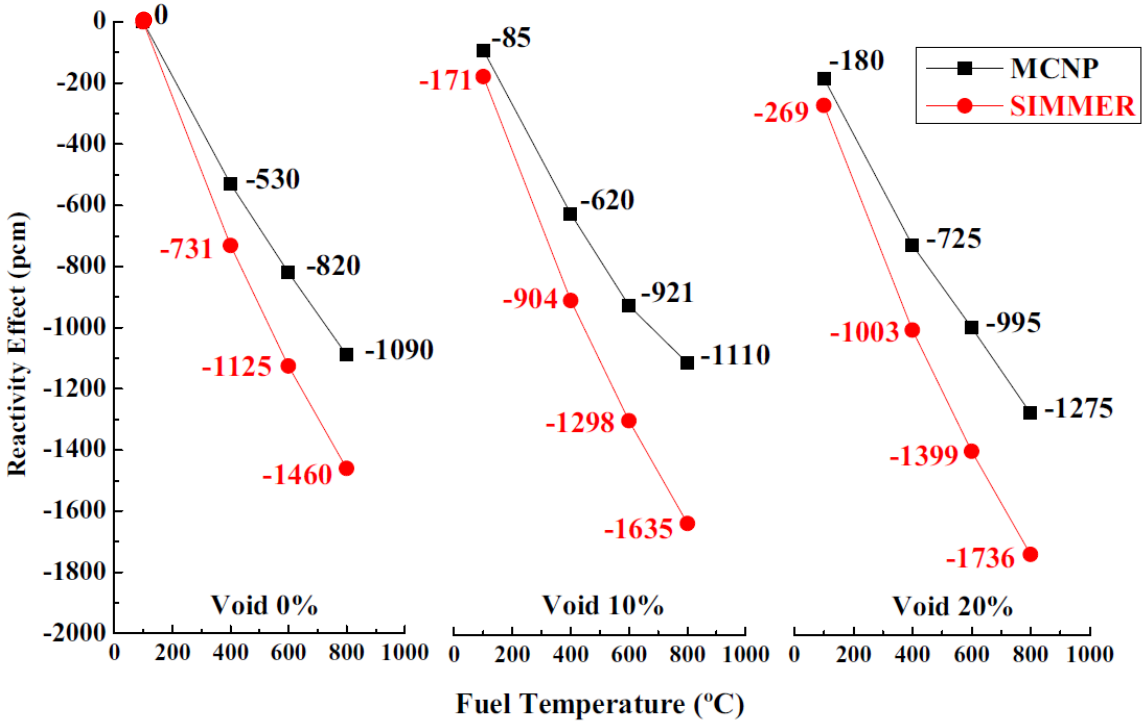

Figure 2. Fuel Doppler and moderator void effect in a low enriched MTR core computed by the SIMMER and MCNP codes

1.3 Improving the SIMMER approach

In coupled neutronics and thermal-hydraulics transient calculations based on the spatial kinetics approach, effective multigroup neutron XSs should be recalculated from time to time to evaluate the reactivity feedbacks and change in power distribution due to variations in the reactor material and temperature distributions. As the SIMMER neutronics module was initially developed for mechanistic safety analyses of liquid metal-cooled fast reactors, the usual XS processing-scheme for fast reactors is employed. Since the heterogeneity effects are not large in fast metal-cooled systems compared to existing uncertainties in reactivity effects, the XSs can be computed reasonably accurately by assuming that each particular reactor region can be approximated – for the purpose of XS processing – by a bulk of a homogeneous mixture of reactor materials. Furthermore, the spatial neutron flux distribution may be considered as a flat or a "smooth" function within a fuel sub-assembly. The XSs for a homogeneous model can usually be computed in a relatively simple and fast manner, compared at least to neutron transport calculations.

During the transient, the multigroup XSs of each nuclide are processed in SIMMER using a basic multigroup data library, while taking account of resonance self-shielding effects employing f-factors, i.e. by using the Bondarenko method [36, 37, 38]. This method is very attractive due to the fact that a relatively simple interpolation scheme is pursued to evaluate the microscopic XSs during the transient simulation.

The aim of this work is to upgrade the original SIMMER XSs processing scheme to properly compute the reactivity feedbacks and kinetic parameters while taking into account heterogeneity effects during the transient analyses for thermal-water-cooled systems. In order to properly treat the heterogeneity, the following points should be considered:

1) the neutron flux is not the same in fuel and non-fuel regions (structure, coolant) within the same energy group;
2) when computing the background XSs to be used for determining the f-factors of fuel isotopes, the non-fuel nuclides should contribute with a smaller weight than the unity weight which is assumed in the standard treatment.

The new method [39, 40, 41, 42] implemented in the SIMMER code can successfully represent core sub-regions by simplified cell models consisting of three components: fuel, structure, and coolant. Control rod material can be added optionally.

The technique employs a set of pre-calculated, energy-dependent, non-unity factors which are applied to the macroscopic XSs for the non-fuel components to take account of the intra-cell neutron flux distribution in space group-wise.

Moreover, the formulation of the background cross-section (σ_0) in the original SIMMER code has been upgraded. The new formulation is based on the original developed by Wigner and Bell [37, 43] to take account of the effect of heterogeneity. In the original formulation, an escape term is added to the fuel lump XS. This term accounts for the effect of the non-fuel region which is composed by homogeneously mixing coolant and cladding.

In the present work, this approximated formulation has been extended to improve accuracy. This is accomplished by applying energy dependent reduction factors to the escape term to properly account for the self-shielding effect. These factors are pre-calculated by reference codes. The advantage of this approach is that the computation of σ_0 is accomplished in the same way as the original SIMMER code for homogeneous media. Since the f-factor Bondarenko method is employed [36, 37, 38], it can be easily checked and fitted in advance using reference tools.

Pre-calculated parameters are evaluated for the fuel sub-assembly by means of sophisticated neutronics codes, such as the deterministic European Cell Code (ECCO) [44] and the Monte Carlo Neutral Particle Transport code (MCNP [35]/MCNPX^{TM} [45]).

Results show that these pre-calculated parameters exhibit a weak sensitivity to the moderator void fraction and even less to the moderator and fuel temperatures. Thus, these parameters can be evaluated for a few representative sets of reactor states (e.g. nominal and voided conditions) and a relatively simple interpolation scheme can be used during transient simulation, as long as the geometry of the sub-assembly does not change appreciably. Moreover, as the f-factor method is used, no significant increase in computation time occurs for SIMMER XS processing during the transient compared to the original SIMMER scheme.

For validation, the extended SIMMER code has been benchmarked against reference neutronics codes (ECCO/ERANOS [46] and MCNP) and experiments for reactivity coefficients and kinetics parameters, for a MTR core model proposed in the frame of the IRSN/KIT cooperation and SPERT core. Results show a decisive improvement of the code performance when the new extensions are deployed.

Chapter 2. Multigroup cross-sections and Resonance Self-Shielding

An advanced cross-section processing technique is necessary in the resonance region in order to properly account for the effect of heterogeneity. In this chapter, the theoretical background of the multigroup XS processing scheme employed in the original SIMMER code is discussed. With this aim, the treatment of resonance self-shielding by use of the f-factor method (Bondarenko method) is described. Since the extended SIMMER model is based on pre-calculated parameters evaluated by the deterministic ECCO or the stochastic MCNP codes, a short description of their features related to the heterogeneity treatment is provided later in the chapter.

2.1 Definition of multigroup cross-sections

The main steps of neutronics analyses during a transient simulation are the XSs processing and the calculation of the neutron flux shape by solving the time-dependent Boltzmann transport equation [49]. XSs are processed in different ways depending on the numerical methods employed in neutron transport simulations. Two numerical methods are available: stochastic (Monte-Carlo) methods and deterministic methods. Most of the codes based on stochastic methods (MCNP and MCNPX) employ basic nuclear data libraries characterized by a continuous-energy representation. The results are usually highly reliable because the original data are based on a very fine energy resolution of the XSs energy dependence. Nevertheless, these simulations may sometimes require very long computation times and may currently have certain restrictions with respect to treatment of the XSs temperature dependence.

The codes based on deterministic methods (such as the neutron transport solver in SIMMER) employ the multigroup XSs where the variable energy is discretized [37, 49]. These XSs are generated under the assumption that the continuous-energy spectrum can be subdivided in energy domains, i.e. energy groups, and that XSs and neutron fluxes are

approximated by their average values: the multigroup effective XSs, $\sigma^g(r,\Omega,t)$, and the multigroup neutron fluxes, $\phi^g(r,\Omega,t)$, respectively.

One of the main difficulties in the evaluation of the multigroup effective XSs is the accurate representation of the continuous-energy information. The criterion used for the proper evaluation of multigroup effective XSs and neutron fluxes is the conservation of the reaction rates in each energy group compared to continuous-energy calculations. If we consider an isotope i and a nuclear reaction x, the reaction rate for the reaction x in the energy group g is given by [37, 49]:

$$R^g_{x,i} = \int_g \sigma^g_{x,i}(\mathbf{r},\mathbf{\Omega})\phi^g(\mathbf{r},\mathbf{\Omega})d\mathbf{\Omega} \tag{2.1}$$

where $\phi^g(\mathbf{r},\mathbf{\Omega}) = \int_{4\pi} \phi^g(\mathbf{r},\mathbf{\Omega})d\mathbf{\Omega}$. The multigroup flux $\phi^g(\mathbf{r},\mathbf{\Omega})$ (n/cm^2·s) in the group g is

$$\phi^g(\mathbf{r},\mathbf{\Omega}) = \int_{E_{g-1}}^{E_g} \phi(\mathbf{r},E,\mathbf{\Omega})dE \tag{2.2}$$

For capture, fission, elastic, and inelastic scattering reactions, the multigroup effective XS in the group g is the XS which, when multiplied by the multigroup flux (Eq. 2.2), provides the reaction rate in Eq. 2.1. Therefore, after combining Eq. 2.1 and Eq. 2.2, the XS of the isotope i in the group g for the reaction x is obtained (for simplicity the spatial and angular dependences are omitted) [37, 49]:

$$\sigma^g_{x,i} = \frac{\int_g \sigma_{x,i}(E)\phi(E)dE}{\int_g \phi(E)dE} \tag{2.3}$$

If the number of energy groups is large enough, $\phi(E)$ can often be considered as representative for the whole reactor, or at least for certain large domains within it. Otherwise, the multigroup XSs and related diffusion coefficient parameters should be computed by employing space-dependent spectra.

The different spectra of the neutron currents require that σ_t used for the transport XS calculation is averaged in a manner different from the other XSs. This XS can be obtained by using Eq. 2.3, employing the neutron current spectrum J(E) as a weighting function. The multigroup total microscopic XS used for computing transport XSs can be evaluated as [37, 49]:

$$\sigma_{t,i}^{g} = \frac{\int_{g} \sigma_{t,i}(E) \frac{\phi(E)}{\Sigma_t(E)} dE}{\int_{g} \frac{\phi(E)}{\Sigma_t(E)} dE} \tag{2.4}$$

Effective multigroup XSs can be calculated rigorously by means of Eq. 2.3, if the energy dependence of $\phi(E)$ is known exactly. Eq. 2.4 gives approximate results even if $\phi(E)$ is known, since the approximation $J(E) \cong \phi(E)/\Sigma_t(E)$ is employed.

For practical applications, the evaluation of $\phi(E)$ for averaging the XSs for a particular isotope is a non-trivial problem when the isotopic composition within the medium is not known in advance. The reason lies in the resonances of other isotopes influencing the neutron spectrum. In more detail, let us consider the U^{238} total XS (see Figure 3).

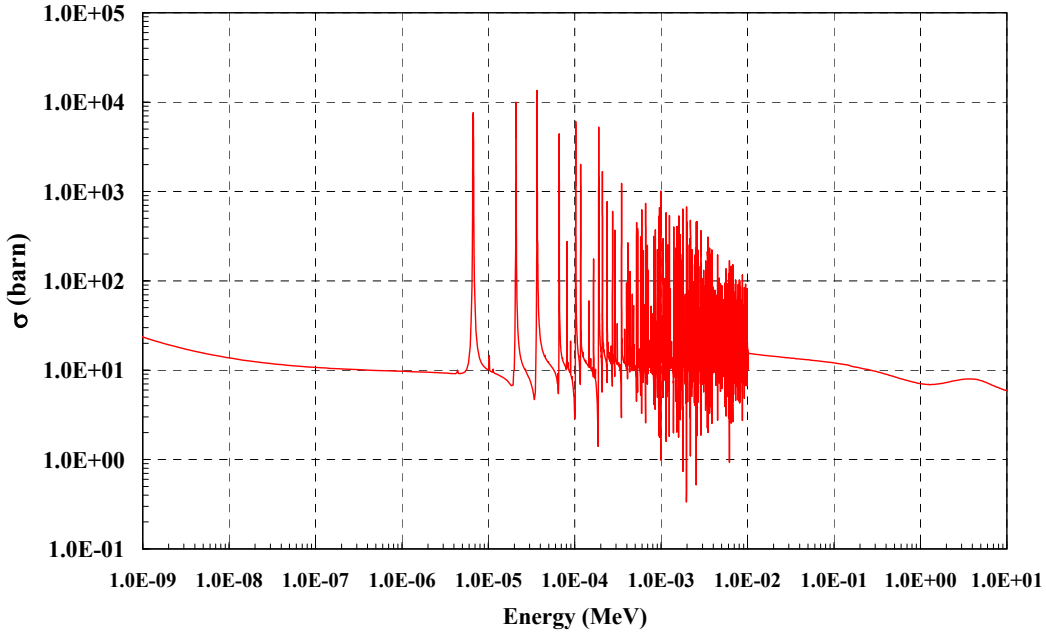

Figure 3. U^{238} neutron total cross-section at room temperature

Figure 3 shows that the U^{238} total XS has numerous resonances in the energy region relevant for nuclear reactors (5 eV – 20 keV).

Apart from the resonance region, the multigroup XSs for a particular isotope can be reasonably easily and accurately determined by means of Eqs. 2.3 and 2.4 provided that the number of energy groups is not too small. In contrast, several calculation methods have been developed to process the multigroup effective XSs in the resonance region [47].

2.2 Resonance self-shielding

In the vicinity of a resonance energy of an isotope with appreciable concentration in a material mixture, the total XS Σ_t varies appreciably. This has the effect of locally influencing the neutron flux and therefore the corresponding reaction rates. For example, let us consider the resonance of the U^{238} total cross section between 6.16 eV and 7.52 eV in a UO_2 mixture (see Figure 4).

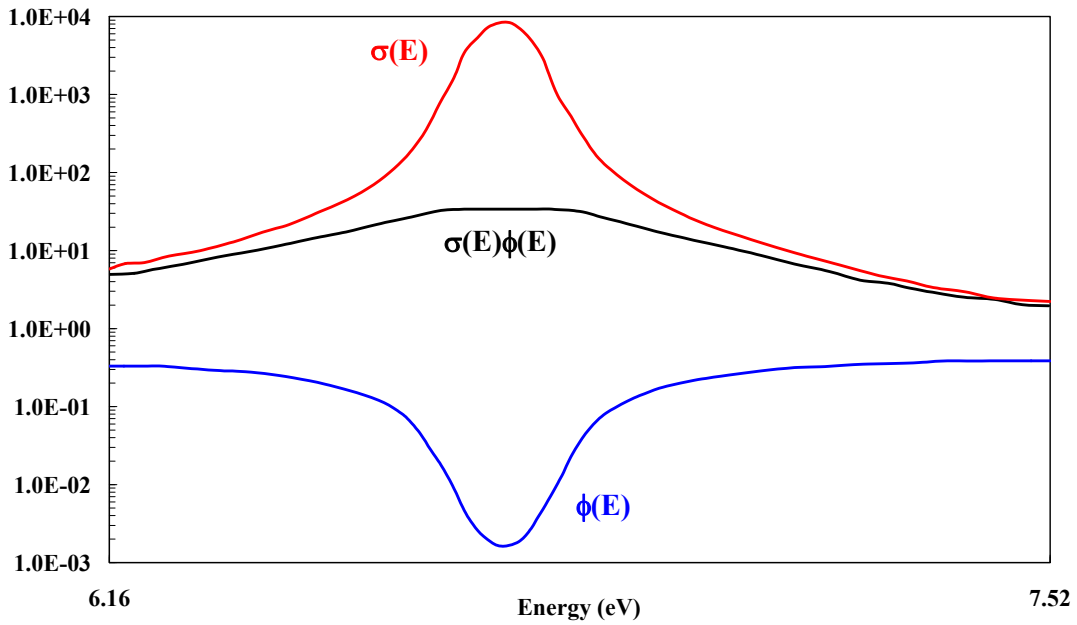

Figure 4. Self-shielding at the U^{238} total cross-section resonance in UO_2 in the 6.16- to 7.52 eV energy range

The effect of the resonance depresses the neutron flux $\phi(E)$. As a result, the average value of the reaction rate $\sigma(E)\phi(E)$ is smaller than the product of the average neutron flux and the average value of the XS (see Figure 4). This effect is known as resonance self-shielding, and the corresponding multigroup XSs are known as resonance self-shielded XSs [48, 50, 51].

The crucial point in the calculation of the multigroup XSs is the accurate determination of the energy dependence of the neutron flux caused by large variations of XSs.

Two different neutron flux spectra are employed to evaluate the effective XSs: a 'global' spectrum which approximates the flux in the absence of resonances, and a 'fine' spectrum which takes account of the local resonance structure of XSs. The former is a combination of three different average neutron energy distributions. At energies well below 1 MeV the flux spectrum is determined by neutron moderation and approaches the Fermi spectrum ($1/E$) above the thermal region and the Maxwellian distribution within the thermal region (below about 0.5 eV). A cutoff energy is usually defined between the Fermi- and higher-energy regions, with typical value at about 2MeV. Above this value, the neutron population is governed by the fission spectrum, which is often specified for a fissile isotope i in the following manner [49]:

$$\phi(E) = C\sqrt{\frac{E}{(kT_x)^3}}e^{-E/kT_x} \tag{2.5}$$

where T_x is a characteristic nuclear temperature for the fissile isotope i and k is the Boltzmann constant, $8.617 \cdot 10^{-5}$ eV/K. For Pu^{239}, kT_x is equal to about 1.4 MeV. The constant C provides the proper dimensional units and must have a numerical value such that the transition from $1/E$ region to the fission spectrum is continuous.

In the resonance region a finer neutron spectrum has to be considered due to the self-shielding effect. Let us consider, as an example, the neutron spectrum in a PWR and in a fast reactor sub-assembly (see Figure 5). A more accurate approach has to be used to properly evaluate the effective XSs in the vicinity of the resonances (see Figure 3).

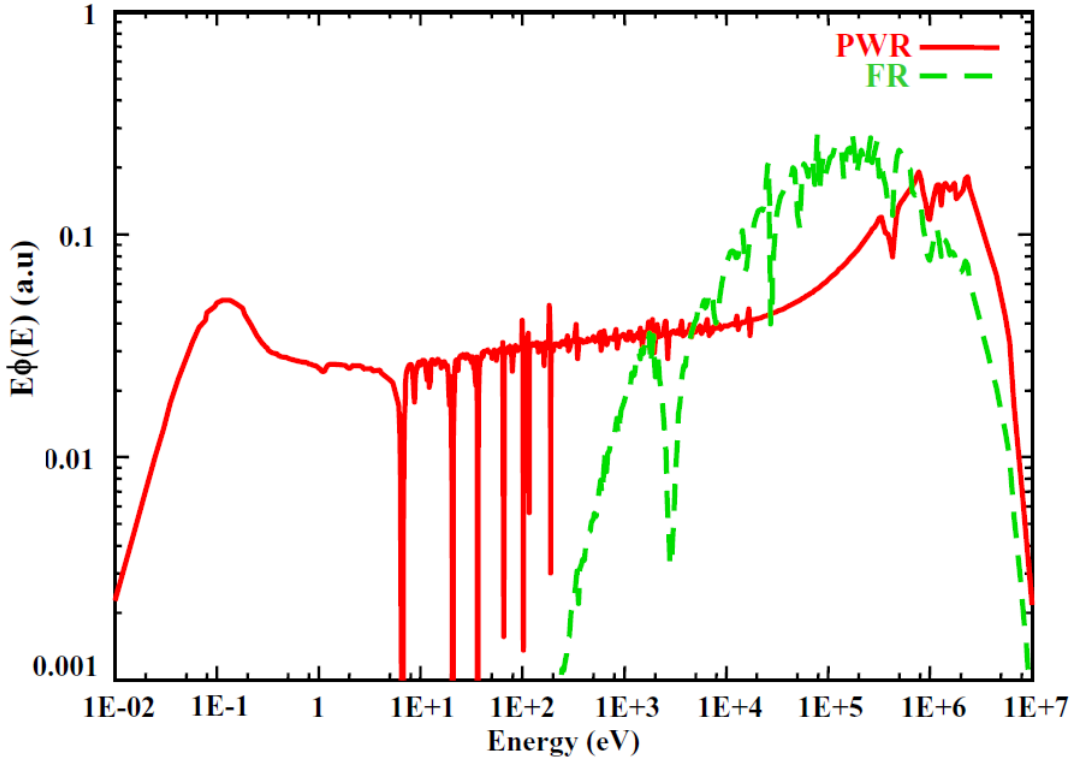

Figure 5. Neutron spectrum in PWR and fast reactor sub-assemblies

The evaluation of the 'fine' structure of the neutron flux is based on the narrow resonance (NR) approximation [48]. This means that the collision density, $\Sigma(E)\phi(E)$, is a smooth function of energy and the total XS corresponding to a resonance at energy E is substituted by the constant potential scattering XS σ_p (see Figure 6) [48, 50, 52].

The applicability of this evaluation is confirmed by analytic and numerical solutions in the energy region where neutron capture, fission, and elastic scattering phenomena are dominant due to the fact that inelastic processes are practically absent at these energies.

When applying the NR approximation to evaluate the fine flux spectra, it is also often assumed that the resonances are well separated and that the resonance widths are narrow enough that scattered neutrons come into the resonance from energy regions where the neutron spectra are not significantly influenced by the resonance [48, 50].

Even if such conditions are not fulfilled (with respect to scattering, isolated resonances, etc.), the NR approximation has been proven as reasonable.

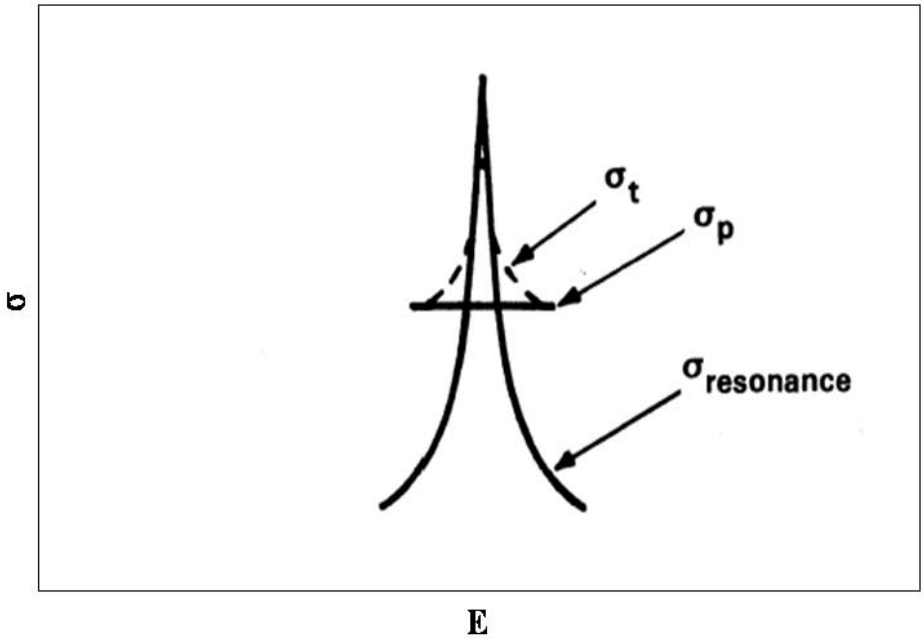

Figure 6. Schematic illustration of XS behaviour in a resonance [37]

As discussed above, we define the collision density, F(E), as the product of the total macroscopic XS and the neutron flux [49]:

$$F(E) = \Sigma_t(E)\phi(E) \tag{2.6}$$

Under the assumption that the neutron scattering is elastic and isotropic and that the scattering macroscopic XS, Σ_s, dominates and does not vary appreciably with energy, the asymptotic flux per unit energy may be evaluated as [48, 50]:

$$\phi_0(E) = \frac{C_1}{E} \tag{2.7}$$

In the absence of resonances at the energy E the collision density is:

$$F(E) = \Sigma_s(E)\phi_0(E) \tag{2.8}$$

However, if there is a resonance at the energy E, $\Sigma_t(E)\phi(E)$ is constant as a consequence of the narrow resonance approximation. Thus, the actual flux and the asymptotic flux (see Figure 7) are related by [48, 50]:

$$\phi(E) \approx \frac{1}{\Sigma_t(E)}\phi_0(E) \tag{2.9}$$

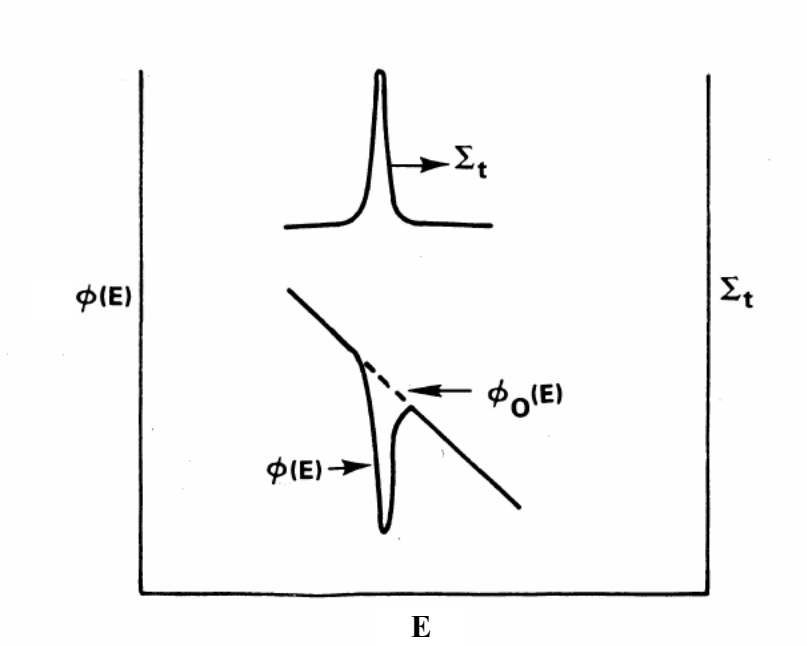

Figure 7. Effect of the resonance self-shielding: cross-section, asymptotic and actual flux in a resonance [37]

Thus, there is a sharp decrease in the actual flux, $\phi(E)$, at the energy of the resonance relative to the flux without a resonance, $\phi_0(E)$. Schematically the neutron flux will appear as shown in Figure 7. The effect of the resonance is to depress the flux in vicinity of the resonance as $1/\Sigma_t$. Therefore, the following effective multigroup XS can be evaluated from Eq. 2.3 [37]:

$$\sigma_{x,i}^{g} \approx \frac{\int_g \frac{\sigma_{x,i}(E)\phi_0(E)}{\Sigma_t(E)}dE}{\int_g \frac{\phi_0(E)}{\Sigma_t(E)}dE} \tag{2.10}$$

This is the simplest approximation to take the resonance self-shielding into account. Additional details on the weighting function for determining group constant and, in particular, the adjoint and bilinear weighting and correlated group collapsing can be found in References 53 and 54.

2.3 Bondarenko method

The SIMMER multi-physics code system employs the Bondarenko self-shielding f-factor approach [36, 38] to treat resonance self-shielding in XS processing. This iterative method, named in honour of the lead scientist who developed it in the USSR, is one of the main approaches used worldwide to compute multigroup XSs for design purposes of fast reactors.

New models developed in this work for the treatment of heterogeneous material arrangements, e.g. lattices of fuel pins embedded in water- or metal- coolant, are based on this method. In addition, these models employ a new combination of techniques to adjust the parameters used in XSs processing, which will be described in the next chapter.

The Bondarenko method takes into account two problems [36, 38]. The first is how to generate average XSs and parameters for later application in computing self-shielded multigroup XSs. These XSs and parameters are obtained for a given isotope i in a medium as a function of a background XS, $\sigma_{0,i}$, in every resonance energy group. These parameters, called f-factors, are generally obtained for a wide range of σ_0 values at several temperatures. The second problem addressed by the Bondarenko method consists of the evaluation of a set of self-shielded XSs obtained from the average XSs and tabulated f-factors for a particular composition at a given temperature.

Following the Bondarenko approach, Eq. 2.10 is augmented. If a bulk mixture of isotopes is considered, as is usually done in fast reactors analyses, the total macroscopic XS, Σ_t, employed in Eq. 2.10 for a particular isotope i is assumed to be the sum of the total XS for isotope i and effective or self-shielded XSs for all other isotopes k≠i [52], so that

$$\Sigma_{t,i}(\mathbf{r},E,\mathbf{\Omega}) = N_i(\mathbf{r})\sigma_{t,i}(\mathbf{r},E,\mathbf{\Omega}) + \sum_{k\neq i} N_k(\mathbf{r})\sigma^g_{t,k}(\mathbf{r},\mathbf{\Omega}), \qquad E_g \le E \le E_{g+1} \tag{2.11}$$

As a result, Eq. 2.10 can be approximated as [52]:

$$\sigma^g_{x,i} = \frac{\int_g \frac{\sigma^g_{x,i}(E)\phi_0(E)}{\sigma^g_{t,i}(E)+\sigma^g_{0,i}}dE}{\int_g \frac{\phi_0(E)}{\sigma^g_{t,i}(E)+\sigma^g_{0,i}}dE} \tag{2.12}$$

where the background XS for the isotope i in the energy group g is [52]:

$$\sigma_{0,i}^{g} = \frac{1}{N_i}\sum_{k\neq i} N_k \sigma_{t,k}^{g} \tag{2.13}$$

As an illustration, a mixture of UO_2 is considered in an energy group g, where U^{235} has two resonances (see Figure 8) which are clearly separated from those of U^{238}.

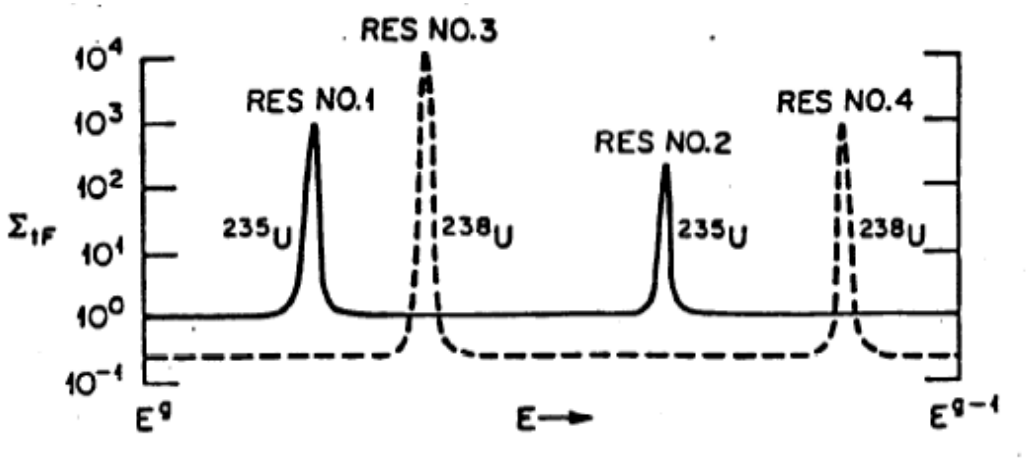

Figure 8. Clearly separated resonances of U^{235} and U^{238} XS in UO_2 [52]

The background XSs for U^{235} and U^{238} are then:

$$\sigma_{0,U235}^{g} = \frac{1}{N_{U235}}\left(\Sigma_{t,U238}^{g} + \Sigma_{t,O16}^{g}\right), \qquad \sigma_{0,U238}^{g} = \frac{1}{N_{U238}}\left(\Sigma_{t,U235}^{g} + \Sigma_{t,O16}^{g}\right) \tag{2.14}$$

Thus, the effect of $\Sigma_t(E)$ in the resonance region at the energy E is taken into account, including both influences, the dip in the neutron flux for each XS peak and the effects of σ_0 which controls the magnitude of the dip. The effect of $\Sigma_t(E)$ depends on the fuel enrichment.

In codes using the Bondarenko approach, the microscopic XS for the reaction x and for the isotope i, $\sigma_{x,i}^{g}$, is computed by employing average infinitely-diluted XSs, $\sigma_{x,i}^{g}(\infty)$, and f-factors, $f(\sigma_0)$ (or Bondarenko factors), for each nuclide, i, and for each XS, for which the resonance self-shielding effect is important [37, 55]. The infinitely-diluted XS is defined as the XS of the nuclide i present in the mixture in such small quantities that its resonances do not affect either its own effective XS or that of other nuclides.

Until now, the temperature dependence of the XSs has not been included. To take this dependence into account, f-factors are evaluated as a function of temperature, $f^{g}_{x,i}(\sigma^{g}_{0,i}, T)$, while the infinitely-diluted XSs are usually computed only at room temperature T_0. The microscopic XS for the reaction x and for the isotope i is usually expressed as the infinitely-diluted value times the f-factor [36, 38, 52]:

$$\sigma^{g}_{x,i}(\sigma^{g}_{0,i}, T) = f^{g}_{x,i}(\sigma^{g}_{0,i}, T)\sigma^{g}_{x,i}(\infty, T_0) \tag{2.15}$$

The explicit appearance of temperature in the f-factor recognises the Doppler broadening of the XS at the specified temperature. An additional point to be noted is that the Bondarenko approach generally improves the accuracy compared to using only average XSs, in the presence of overlapping resonances [52]. Figure 9 shows an example of the resonance overlap of total XS for various isotopes at 300 K in the energy range 4 eV - 10 eV.

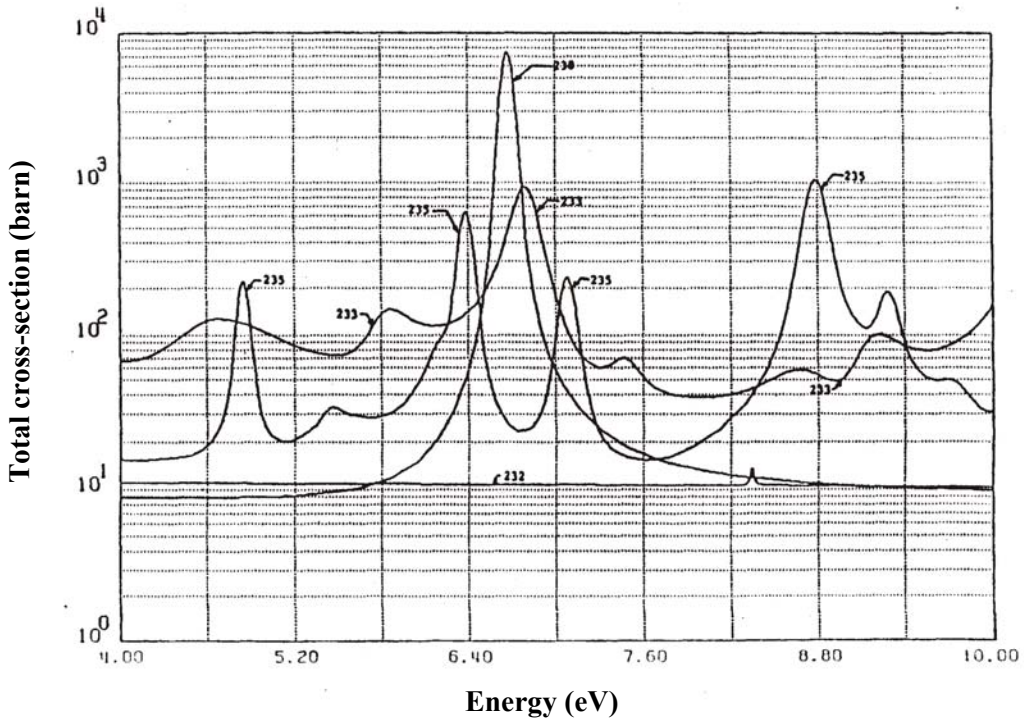

Figure 9. Resonance overlap for Th^{232}, U^{233}, and U^{238} in the 4eV - 10 eV energy range

The Bondarenko method is very attractive for fast rector safety codes as a sufficiently simple interpolation scheme is necessary to evaluate the microscopic XSs during the

transient simulation [52]. As an example, Figure 10 shows the f-factors for the U^{238} capture XS in two energy groups (5.04 eV - 9.9 eV and 1.01 eV - 2.1 keV) and at three different temperatures (300 K, 900 K, and 2100 K). The results show the typical 'S-shape' of the background XS σ_0 variation of the Bondarenko factors [52].

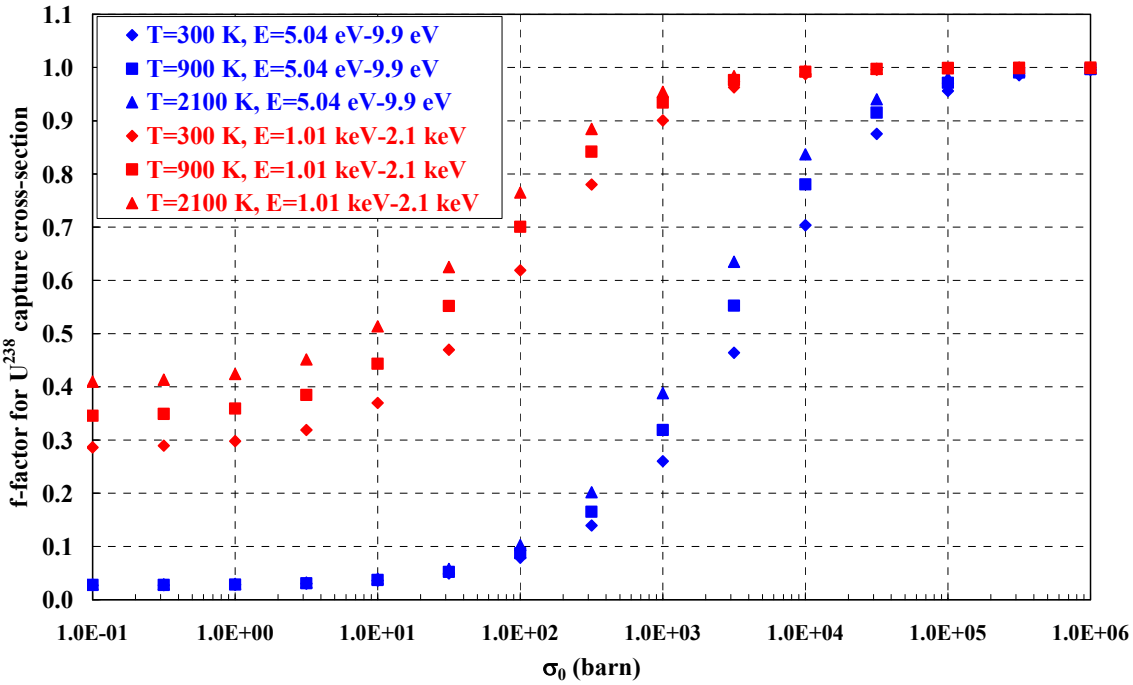

Figure 10. F-factors for U^{238} capture XS in two energy groups

2.4 The ECCO/ERANOS cross-section processing scheme

Multigroup reactor calculations using deterministic codes consist of solving the multigroup direct and adjoint transport equations [49, 73] by discretizing the independent variables E, r and Ω (the latter by discrete ordinates, S_n approximation, or P_n methods). The multigroup XSs are computed from data libraries containing average XSs and finally transferred to the modules which perform core calculations (VARIANT [64] or DANTSYS/THREEDANT [30, 31]). After the multigroup direct and adjoint equations [49, 73] are solved, several parameters characterizing the system can be obtained, such as k_{eff} or α eigenvalues with the corresponding eigenfunctions and the kinetics parameters (β_{eff} and prompt neutron generation time, Λ) [49, 73].

In the European Reactor Analysis Optimized System (ERANOS) [46], effective microscopic and macroscopic XSs are computed by the European Cell Code (ECCO) [44]. This code generates multigroup self-shielded XSs and elastic, inelastic, and (n,xn) group-to-group transfer XSs (or matrices) for use in the reactor core or shielding calculations which are performed by ERANOS. ECCO solves the integral transport equation [49] in an infinite lattice, using multigroup XSs with a fine energy-group structure (1968 energy groups up to 20 MeV) and accurate geometrical representation. Multigroup XSs with broad energy structure are obtained in ECCO by collapsing data from fine energy-group libraries. Several libraries are available based on the evaluated nuclear data files (JEFF [56], JENDL [57], ENDF [58]).

2.4.1 The subgroup method

The ECCO cell code [44] enables XSs processing for almost any type of a reactor sub-assembly (PWR, BWR, or hexagonal subassemblies of fast reactors) by employing the subgroup (or probability table) method [59]. The subgroup method is an extension of the f-factor method, used to treat resonance self-shielding effects in heterogeneous systems. The method can be derived from f-factor using integrals similar to those employed for f-factor computation [37, 55].

The subgroup method is particularly suitable for calculations involving complex heterogeneous structures. It brings the XS accuracy to the level required for current reactor designs and deals with numerous different geometries, e.g. hexagonal and rectangular sub-assemblies.

The subgroup parameters (probability tables) are stored in the XSs libraries for ECCO in the resolved and unresolved resonance regions in a more compact way than f-factors [59]. The probability tables describe the XS fluctuations within one energy group by employing discrete values. This philosophy can be explained as follows. The variation of the total effective XS $\sigma(E)$ as a function of neutron energy, E, in the group G (see Figure 11a) can be represented as a distribution of probability $P(\sigma)$ in the domain $[0, \max(\sigma)]$ (see Figure 11b). The product $P(\sigma)d\sigma$ is the probability that the value of the effective XS $\sigma(E)$ lies within σ and $\sigma+d\sigma$. The probability table is then obtained by discretizing the

P(σ) values using weights p_i and corresponding representative XS, σ_i (see Figure 11c). As a result, the total and partial XSs in each energy group g are described at each temperature by means of a set of N values (p_i, $\sigma_{t,i}$, $\sigma_{x,i}$, i=1, N). In this way, resonances are effectively described in a detailed and compact manner without the need to significantly increase the number of energy groups.

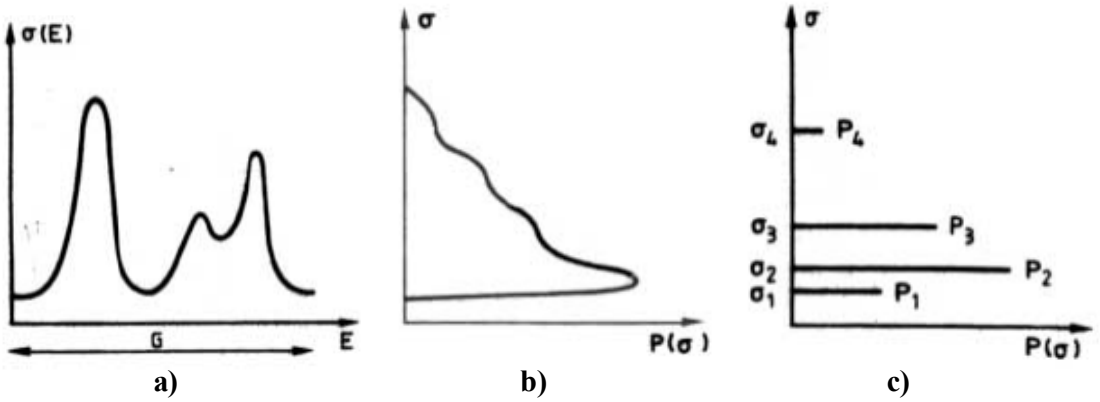

Figure 11. Qualitative description of the probability tables

For core calculations using ECCO/ERANOS, the 1968 energy-group probability tables are condensed through refined algorithms which enable the preservation of the reactivity balance. As a result, calculations can be performed with reasonable accuracy even if XSs with a broad energy-structure are employed.

As heterogeneous sub-assembly models cannot be directly employed in the ERANOS core calculations, homogenization is performed in the ECCO code. If one considers a cell composed of n different regions, the multigroup neutron flux and the macroscopic XSs for the reaction, x, in each energy group, g, in the homogenized cell are given by:

$$\phi^g_{hom} = \frac{\sum_n V_n \phi^g_n}{\sum_n V_n} \qquad \Sigma^g_{x,hom} = \frac{\sum_n V_n \phi^g_n \Sigma^g_{x,n}}{V_{cell} \sum_n \phi^g_n} \tag{2.16}$$

where V_n is the volume of the region and x the reaction. In this way each reaction rate is conserved. XSs derived from Eq. 2.16 are known as homogeneous equivalent XSs.

2.5 The Monte-Carlo method

The Monte-Carlo method can simulate sequentially all events involving in each particle in a system (such as interactions with nuclei) from the birth up to disappearance and compute the required parameters by means of statistical procedures [35, 45].

The codes based on this method, such as MCNP and MCNPX, do not explicitly solve the neutron transport equation, but simulate the behaviour of individual particles to obtain statistically averaged results using the central limit theorem. Calculating k_{eff} consists of estimating in the phase-space the mean number of fission neutrons produced in one generation per fission neutron started. A generation is the life of a neutron from birth in fission to death by escape, parasitic capture, or absorption leading to fission. The computational equivalent of a fission generation is a k_{eff} cycle, which is an estimate of an actual fission generation. As fission neutrons are terminated in each cycle to provide the fission source for the next cycle, a single history can be viewed as continuing from cycle to cycle [35, 45].

The final k_{eff} is the statistical combination of three estimated values for k_{eff} which take account of several physical phenomena (fission, capture, scattering, and absorption) that occur when a neutron collides with the nuclei of the medium, where each reaction has a characteristic weight [60]. It is extremely important to emphasize that the result from a criticality calculation is a confidence interval for k_{eff} that is computed using the final estimated k_{eff} and the estimated standard deviation.

MCNP can easily employ continuous-energy data using several basic data libraries (JEFF, JENDL, ENDF) in very complicated geometries. Due to these features, this code is capable to treat the effect of heterogeneity more accurately than the deterministic codes, which are limited by the maximum number of energy groups, the moments of the scattering matrix, and the choice of the geometrical models.

Nevertheless, deterministic codes do have some advantages over MCNP. First, MCNP calculations are usually much more expensive than deterministic calculations, in term of CPU time. Second, the reliability of deterministic codes with respect to the MCNP codes can be increased by employing several techniques such as the subgroup method in the ECCO/ERANOS code as well as the new method developed here for the SIMMER code.

Chapter 3. Extension of the SIMMER code for safety studies of thermal reactors

This chapter describes a new technique for the incorporation of the heterogeneity treatment in the original SIMMER cross-section processing scheme. The purpose is the accurate evaluation of the reactivity feedbacks during transient analyses in water-cooled systems. The new features, in conjunction with the capability of the SIMMER code to analyse in a mechanistic way an accident scenario from accident initiation up to core disruption, provide a powerful tool for analyses of transients in material testing reactors. In this chapter the SIMMER-III code extension is presented, and benchmarked against the original SIMMER scheme, the ECCO [44], and the MCNP/MCNPX^{TM} [35, 45] reference neutronics codes for the main reactivity feedbacks. Before its application to reactor cores, the fuel Doppler and the moderator void reactivity effects are computed for typical PWR and MTR fuel sub-assemblies.

3.1 The original SIMMER cross-section processing scheme

The original XS processing scheme of the SIMMER code is based on the assumption that all materials (fuel, coolant, clad, etc.) are mixed homogeneously in every reactor region [23, 24, 25]. As a result, in a sub-assembly where each material occupies a particular volume fraction (V_f, V_{cool}, V_{clad}) the corresponding multigroup macroscopic XS for the reaction x is given by:

$$\Sigma_x^g = \sum_k \sum_i N_{i,k} \sigma_{x,i,k}^g \frac{V_k}{V_{total}} \tag{3.1}$$

where $\sigma_{x,i,k}^g$ is the infinitely-diluted multigroup microscopic XS for the neutron reaction x of the isotope i present in the material k. Infinitely-diluted multigroup XS libraries can

be computed for SIMMER for example by using the C[4]P code and data system, developed at the Karlsruhe Institute of Technology [27].

This system (see Figure 12) includes several fine-groups "master" libraries (560 neutron energy-groups below 20 MeV) based on recently evaluated nuclear data files. The fine-group data are stored in the Committee of Computer Code Coordination (CCCC) format [28], which was extended to properly take account of thermal scattering effects.

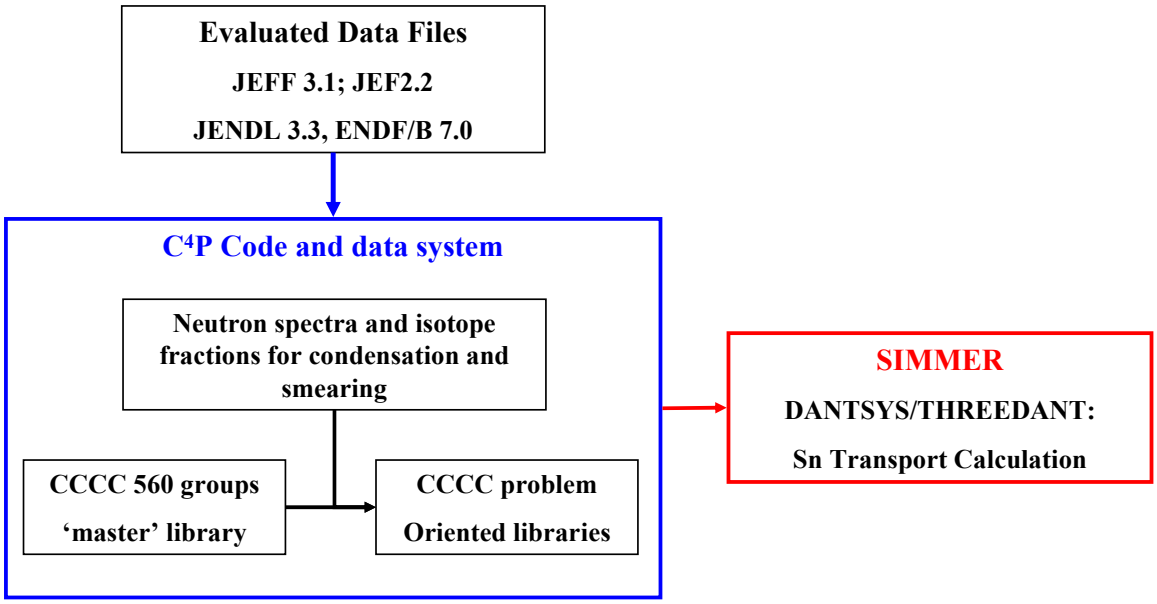

Figure 12. Flow chart of the SIMMER XS processing scheme

It was shown [27] that deviations among the results (criticality and major reactivity effects) computed with the 560-group and corresponding "point-wise" nuclear data are quite small (about 200 pcm or lower) for a set of simplified models for water-cooled, liquid metal-cooled, and molten-salt reactors [27, 38] and the corresponding critical assemblies.

Moreover the C[4]P system offers the capability to generate a library (in the extended CCCC format, including f-factors) with less than 560 energy-groups by employing a "master" library and an appropriate weighting function (see Figure 12). This capability is used to generate problem-oriented XSs for SIMMER.

Extensive tables of various self-shielding f-factors, $f^{g}_{x,i}(\sigma^{g}_{0,i}, T)$, are processed for various nuclear reactions x: fission, capture, elastic scattering, total and absorption. Therefore,

given a library of pre-tabulated data, one needs only to apply the various f-factors (evaluated at the appropriate $\sigma_{0,i}^{g}$ value) to obtain the necessary self-shielded XS data [36, 38]. By using a unique set of infinitely-diluted (homogeneous) microscopic XSs for different nuclear reactions and pre-tabulated self-shielding factors, the SIMMER XS processing scheme evaluates the background XS at the onset and during the transient by taking account of temperature and density perturbations through the isotope densities N_i and N_j [23, 24, 25]:

$$\sigma_{0,j}^{g} = \frac{1}{N_j} \sum_{i \neq j} \sum_{x} N_i f_{x,i}^{g}(\sigma_{0,i}^{g}, T) \sigma_{x,k}^{g} \tag{3.2}$$

When the composition of a given mixture is known, the code calculates $\sigma_{0,i}^{g}$ then goes to an appropriate table to find the self-shielded group-dependent factor of $\sigma_{0,i}^{g}$ for that particular mixture by a suitable interpolation. The use of pre-calculated self-shielded XS data tabulated as a function of $\sigma_{0,i}^{g}$ has proved to be an attractive alternative compared to other methods when performing space-time depletion analyses for certain types of reactors.

3.2 The new approach for heterogeneity treatment during transient simulations

In conventional light water reactors, water is not used only as coolant but also as moderating medium. Neutrons are therefore thermalized in order to maintain the fission chain in a nuclear power plant with low enriched fuel. As a result, the neutron spectrum in a thermal system considerably differs from that of a fast reactor, which requires higher fuel enrichment because the neutron spectrum peaked at high energies (about 0.1 MeV - 1 MeV). In this energy range the cross-section ratio $\sigma_{f,U235}/\sigma_{c,U238}$ is less favourable for maintaining the fission chain than in the thermal energy range. The difference in neutron

spectra is shown in Figure 13, where the multigroup neutron spectra in a thermal water-cooled (40-energy-groups) and a fast sodium-cooled system (26 energy groups) are compared.

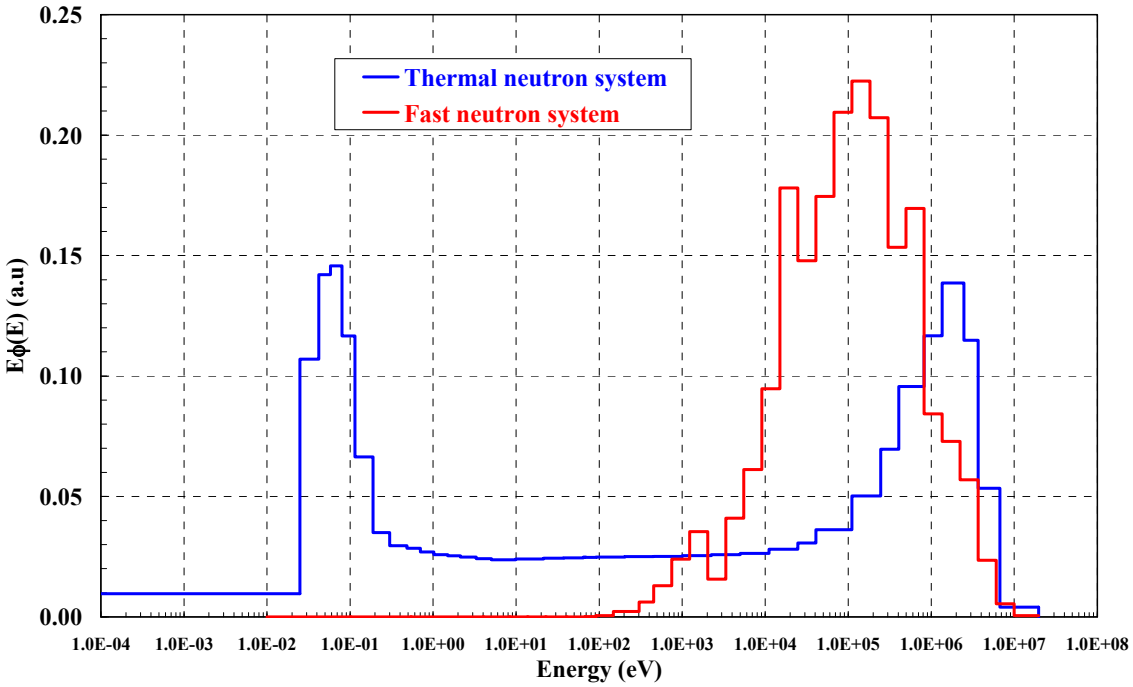

Figure 13. Multigroup neutron spectra for a typical thermal water-cooled and fast sodium-cooled reactor

No effective moderator material is available to slow down neutrons in a fast breeder reactor (liquid metal cooled); therefore, an insignificant number of neutrons exist in the thermal range. In the thermal reactor, the neutron flux in the intermediate energy region (1 eV to 0.1 MeV) has a dependence of approximately 1/E, i.e. Eϕ(E) is almost constant.

In addition, as the XSs generally decrease with energy, the neutron mean free path (the average distance travelled by a neutron before interaction) in a fast neutron reactor is large relative to the fuel-rod and coolant-channel dimensions.

In contrast, this distance is short in a thermal neutron system. In the resonance region, the neutrons mean free path decreases in the energy domain where a resonance occurs because resonance XSs are much higher. Thus, the effect of heterogeneity will have a marked influence in the resonance region and will therefore be much more important in thermal neutron than in fast neutron systems.

The effect of heterogeneity appears in the resonance region through the resonance absorption by heavy isotopes, leading to pronounced dips in the flux spectra in the fuel, and less pronounced dips in the flux spectra in the moderator and clad regions. To take account of heterogeneity effects, the following points should be considered:

1) the neutron flux is not the same (particularly in thermal systems) in the fuel and non-fuel regions (structure, coolant) within the same energy group, i.e. it is not constant within a sub-assembly;
2) when the background XSs for the fuel isotopes are computed (taking into account the resonance self-shielding effect by means of f-factor method), the non-fuel nuclides should contribute with a smaller weight than the unity weight which is assumed in the original SIMMER scheme.

In addition, a particular requirement to treat thermal systems is the consideration of a sufficient number of energy groups below 1 eV to take account of the neutron population in this part of the energy spectrum.

To address these issues, the original SIMMER XS processing scheme has been extended to properly take account of the heterogeneity effects in thermal reactor safety studies. This has been accomplished by introducing the ability to represent core sub-regions by simplified cell models consisting of several components such as fuel, structure, and coolant. The heterogeneity treatment makes use of three techniques [39, 40, 41]:

- application of pre-calculated non-unity "weights" to XSs for non-fuel cell components, e.g. structure and coolant, while computing the macroscopic cell XSs in order to accurately take account of the intra-cell flux distribution in space group-wise;
- upgrading the formulation of the background XS for the fuel isotopes (Eq. 3.2) and applying pre-calculated reduction factors to non-fuel XSs in order to properly take account of resonance self-shielding effects;
- employment of a multigroup XS library with a fine energy description of the thermal spectrum region.

The corrective parameters may be computed by any neutronics code. In this work, the multigroup ECCO code is mainly used because it has shown a high level of reliability

when computing safety parameters in water-cooled fuel sub-assemblies [39, 40]. Moreover, the ECCO code is faster than MCNP in terms of both CPU time and data post-processing.

3.2.1 Model for accounting for the intra-cell neutron flux behaviour

Let us consider a typical PWR fuel pin composed of a UO_2 fuel (4.5 wt% U^{235}), surrounded by clad and water (see Figure 14). Each component (fuel, clad, and water) is characterized by its isotopic composition (N_i), the set of microscopic XSs for each reaction x and each isotope i ($\sigma_{x,i}$), the volume V, and the local neutron flux (ϕ).

Homogenizing the heterogeneous cell (see Figure 14, left) requires the evaluation of a set of macroscopic XSs for each neutron reaction x, $\Sigma_{x,Mcell}$, for the bulk (Eq. 3.1).

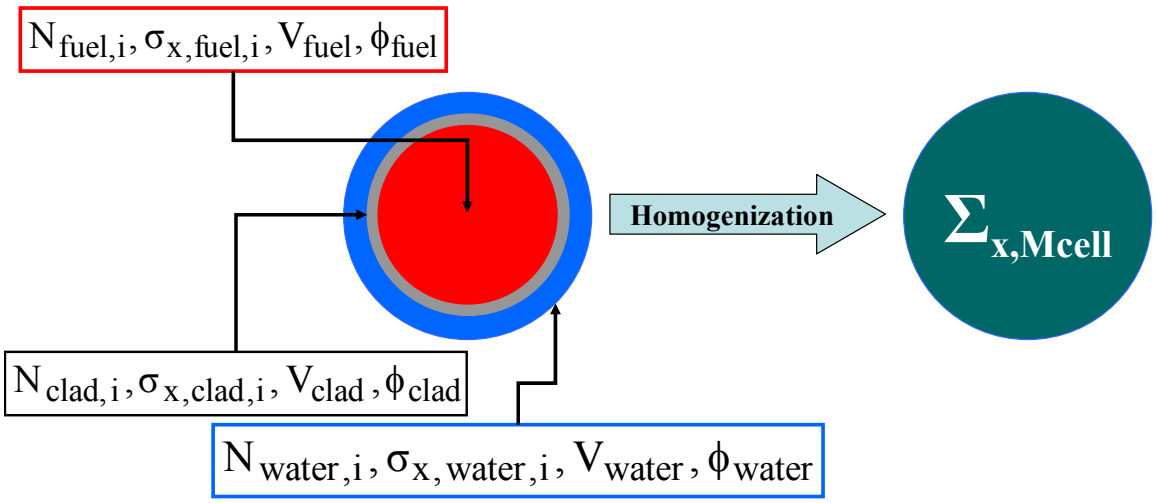

Figure 14. Cross-section homogenization

To take account of the fine geometric structure of the pin, the real weights of the different sub-regions (structures, coolant) should be considered in the original SIMMER XSs processing.

Therefore, Eq. 3.1 is upgraded by multiplying the microscopic XSs of each isotope i of the structure and of the moderator by the ratio of the neutron flux in these components to

the neutron flux in the fuel [39, 40]. As a result, a so called heterogeneous equivalent XS, $\Sigma_{x,Mcell}$, is evaluated for the reaction x:

$$\Sigma^{g}_{x,Mcell} = \sum_{i} N_{k,i}\sigma^{g}_{x,k,i}\left(\frac{\phi^{g}_{k}}{\phi^{g}_{fuel}}\right)\left(\frac{V_{k}}{V_{Mcell}}\right) \qquad (3.3)$$

where k stands for the different media (fuel, clad, and coolant). These weights are computed by means of reference codes (ECCO) for the fine geometric model for the analyzed case [39, 40].

Figure 15 shows the unity weight assumed in the original SIMMER model (Eq. 3.1) and the new non-unity weights (clad-to-fuel flux ratio and coolant-to-fuel flux ratio) for the heterogeneous PWR pin in Figure 14. Calculations have been performed in this case by means of MCNP and averaged within 172 energy groups.

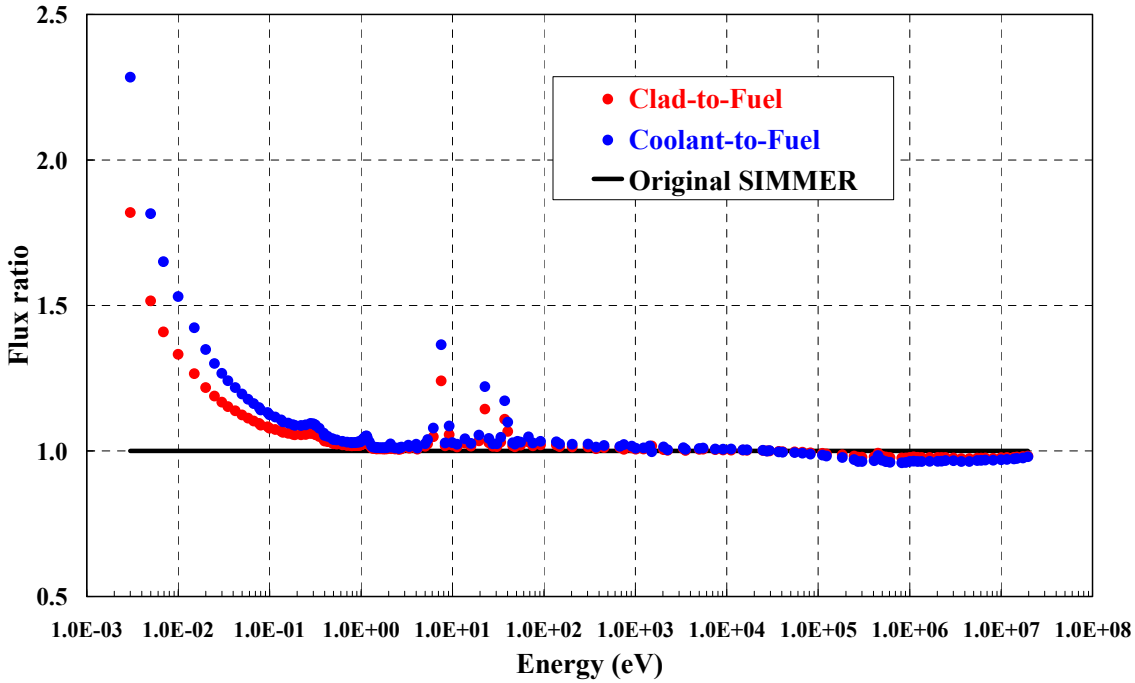

Figure 15. Comparison of the weights applied to the microscopic XSs in the original (flat flux) and in the extended SIMMER XS processing scheme

The results show that application of the non-unity weights accounts for two effects at the same time: the neutron flux pile-up in the energy region below 1 eV (see Figure 15) and the effect on the flux of the ^{238}U resonances in the 1 eV – 100 eV energy range where a

strong deviation from unity can be observed. In addition, the results in Figure 13 confirm that the unity weight approximation is reasonable for fast reactors, where the energy range below 100 eV is not very important.

3.2.2 Model to consider the influence of heterogeneity on resonance self-shielding effect

The accuracy of the XS processing scheme employed in the SIMMER code can be improved by using some special formulae developed in the past to take account of the heterogeneity effect in the background XSs calculation.

The formulae used for computing the self-shielding-correction parameters for fuel XSs are based on the so-called rational approximation modified by Bell [37, 43, 61]. It is an upgrade for a heterogeneous fuel-lattice of the so called rational approximation (sometimes also referred to as Wigner approximation or canonical approximation) [43, 61], which is based on an approximation of the neutron leakage probability from a single fuel rod embedded in region where moderator and clad are homogenously mixed.

The Bell approximation follows from the 'Second Equivalence Theorem of resonance escape', which states that a heterogeneous lattice characterized by an escape XS, σ_e, has the same resonance integral as a homogeneous mixture with a background XS equal to $\sigma_0+\sigma_e$. Therefore, the effect of the non-fuel region in the heterogeneous geometrical arrangement is converted into an escape XS, σ_e, for the equivalent homogenized mixture.

As a result, it can be demonstrated that the heterogeneity-corrected background XS for the fuel isotope i in a homogenized cell composed of fuel (region 1), clad and moderator (homogenously mixed in the region 2) is given by the following formula [37, 52]:

$$\sigma_{0,het,i} = \sigma_{0,hom,i} + \frac{\tau_1}{N_i}\frac{V_1}{V_{cell}} \qquad \tau_1 = \frac{\tilde{\Sigma}_2 \frac{S}{4V_1}}{\tilde{\Sigma}_2 + \frac{S}{4V_1}\frac{V_1}{V_2}} \tag{3.4}$$

where N_i is the atomic number density of the fuel isotope i, S is the surface between regions 1 and 2, $\tilde{\Sigma}_2$ is the region 2 total macroscopic XS, and V_1 and V_2 are the volumes

of each region. In Eq. 3.4, $\sigma_{0,hom,i}$ is the background XS for the fuel isotope i in the homogenized cell where the f-factor is omitted for simplicity, so that:

$$N_i\sigma_{0,hom,i} = \Sigma_{fuel} - \Sigma_{fuel,i} \tag{3.5}$$

Eq. 3.4 can be rewritten in the following form [37], where the XS of the region 2 is smeared over the cell volume V_{cell}:

$$N_i\sigma_{0,het,i} = N_i\sigma_{0,hom,i} + \sigma_e = N_i\sigma_{0,hom,i} + \Sigma_2 \frac{1}{1+\left(\frac{4V_{cell}}{S}\right)\Sigma_2} \tag{3.6}$$

Thus the correction term depends upon the so called mean chord length (MCL), $4V_{cell}/S$, where V_{cell} is the cell volume and S is the fuel cell surface [37, 52]. If $4V_{cell}/S$ is near zero the formulation employed in the original SIMMER code is obtained (Eq. 3.2) and the f-factors are similar to those in the homogeneous media. If not, the clad and coolant XSs will have a lower weight.

The escape XS has the same form as the background XS for the homogeneous medium (Eq. 3.2), but $\sigma_{0,hom,i}$ includes other elements in the fuel, e.g. Oxygen in UO_2-PuO_2 fuel. Clad and coolant XSs enter into the homogeneous equivalent background XS $\sigma_{0,het,i}$ through the escape XS.

Bell's formulation of the background XS has been adopted instead of the 'homogeneous' concept employed in the original SIMMER code (Eq. 3.2). The accuracy of the escape term in Eq. 3.6 has been further improved in order to account for the strong spatial and spectral effects typical of water-cooled reactor systems.

It should be noted that by incorporating the escape XS, the effective XSs in heterogeneous geometry can be approximately evaluated by tabulated self-shielded XSs based on calculation results in the homogeneous geometry with various background XSs. As a result, the effect of heterogeneity is taken into account, but no additional time is required in the XS processing during the transient.

This new technique consists of upgrading the escape XS term of Eq. 3.6 in order to simultaneously take into account:

1) the effect of cladding and moderator independently;

2) the effect of resonances and the different neutron spectra in fuel, clad, and coolant.

Having this in mind, a new formulation of the background XS is developed [40, 41]:

$$N_i\sigma_{0,het,i} = N_i\sigma_{0,hom,i} + (\Sigma_{clad} + \Sigma_{mod})\frac{1}{1 + L(\Sigma_{clad} + \Sigma_{mod})} \tag{3.7}$$

With respect to Bell's formulation (Eq. 3.6), the mean chord length coefficient ($4V_{cell}/S$) is substituted by an energy and moderator-void dependent term (L). This parameter is called effective mean chord length (EMCL) and takes account of the detailed energy-dependence of the XSs and the neutron flux distribution in the heterogeneous sub-assembly model. Σ_{clad} and Σ_{mod} are computed using this new technique (Eq. 3.3) to account for the effect of the different spectra in the clad and moderator regions.

3.2.3 Evaluation of the Effective Mean Chord Length

The effective mean chord lengths (EMCLs) are computed by processing results obtained with reference cell codes, which take account of the actual model of the fuel sub-assembly geometry. These parameters are evaluated for each energy group by means of the following relationship [40]:

$$\Sigma_{clad} \cdot \frac{V_{clad}}{V_{total}} + \Sigma_{mod} \cdot \frac{V_{mod}}{V_{total}} \cdot h = \left(\Sigma_{clad} \cdot \frac{V_{clad}}{V_{total}} + \Sigma_{mod} \cdot \frac{V_{mod}}{V_{total}} \right) \cdot \frac{1}{1 + L \cdot \left(\Sigma_{clad} \cdot \frac{V_{clad}}{V_{total}} + \Sigma_{mod} \cdot \frac{V_{mod}}{V_{total}} \right)} \tag{3.8}$$

where Σ_{mod} and Σ_{clad} are the moderator and structure macroscopic XSs computed using a reference code and V_{mod} ,V_{clad}, and V_{total} are the moderator, cladding, and total volumes, respectively.

The EMCLs are determined from Eq. 3.8 for each energy-group in such a manner that the fuel XSs fit those computed by reference cell codes. EMCLs can be pre-calculated for a representative set of different reactor states so that application of Eq. 3.8 leads to more

accurate results for each particular state that might be encountered during a transient, e.g. steam ingress in a voided fast reactor. If L is equal zero, the conventional definition of the background XS is used (Eq. 3.2).

In Eq. 3.8, the parameter h is the moderator fraction which yields the capture XS of the main resonant isotope in a homogeneous cell (where fuel, clad, and coolant are smeared) equal to the XS in the refined model at the moderator density condition in the reactor state we are considering.

As an example, let us consider a typical PWR fuel pin (UO_2, 4.5 wt% U^{235}), where U^{238} is the main resonant isotope. Figure 16 shows the ratio of the U^{238} capture self-shielded XSs (evaluated by means of ECCO) computed in the refined cell to those computed in the corresponding homogeneous model at room temperature and zero moderator void condition.

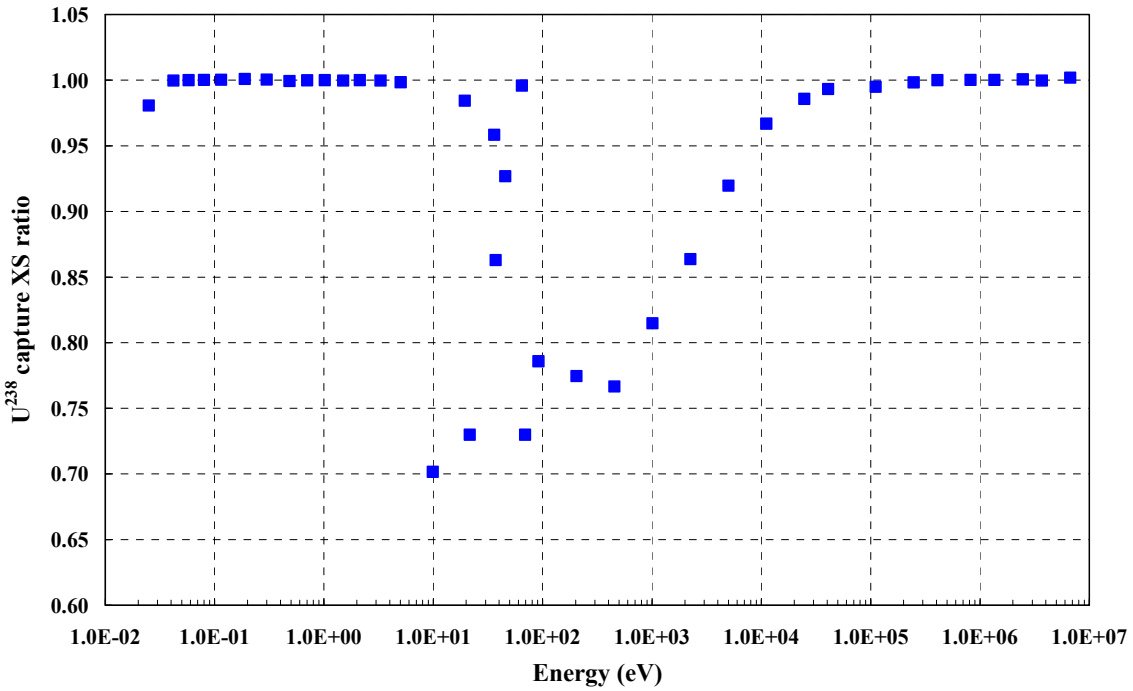

Figure 16. Ratio of the ^{238}U capture self-shielded XS at 40-energy-groups in the heterogeneous cell to that in the corresponding homogeneous cell at room temperature and zero moderator void condition

Results show that discrepancies in the 10 eV –10 keV energy-range reach about 30 %.

Therefore, in accordance with Eq. 3.8, the EMCLs will take account of the change of the neutron spectra during the perturbation induced by a change in the moderator/coolant density via the parameter h [39, 40].

3.2.4 SIMMER cross-section library for thermal system analyses

SIMMER multi-physics code systems can employ XSs libraries with different numbers of energy groups. As the XSs are recalculated during a transient simulation, a large effort was mounted in the past to identify XS libraries with the lowest number of groups.
With this aim, an 11-group library which shows very good performance for fast reactor studies has been developed since the 90's at KIT [62].
In order to extend the application of SIMMER to thermal systems, a new XS library necessary for the description of the thermal region of the neutron spectrum was produced. Then, a 40-energy-groups XS library with 10 groups below 1 eV in the extended CCCC format [28] and including f-factors has been processed by means of the C^4P code and data system [27]. The upper limits of each energy group are shown in Table 2.

g	Upper limit (eV)	g	Upper limit (eV)	g	Upper limit (eV)	g	Upper limit (eV)
1	1.9640E+07	11	2.4788E+04	21	4.5517E+01	31	1.0200E+00
2	6.7032E+06	12	1.1138E+04	22	3.7267E+01	32	7.0500E-01
3	3.6788E+06	13	5.0045E+03	23	3.6045E+01	33	4.8500E-01
4	2.4660E+06	14	2.2487E+03	24	2.1501E+01	34	3.0000E-01
5	1.3534E+06	15	1.0104E+03	25	1.9455E+01	35	1.8900E-01
6	8.2085E+05	16	4.5400E+02	26	9.9056E+00	36	1.1500E-01
7	4.0762E+05	17	2.0400E+02	27	5.0435E+00	37	8.0000E-02
8	2.4724E+05	18	9.1661E+01	28	3.3000E+00	38	5.8000E-02
9	1.1109E+05	19	6.9045E+01	29	2.1300E+00	39	4.2000E-02
10	4.0868E+04	20	6.4592E+01	30	1.5000E+00	40	2.5000E-02

Table 2. 40-energy-group structure used for the application of SIMMER to thermal systems

3.3 Effect of the new approach on the treatment of the resonance self-shielding

The effect of the implementation of this new technique on the original SIMMER XS processing scheme can be explained in Figure 17. The U^{238} background XSs computed by the original scheme (Eq. 3.2) and by the new technique (Eq. 3.7), taking into account the heterogeneity treatment, are compared for a typical PWR fuel sub-assembly. In Figure 17, the 0.1 eV – 1 MeV energy range where the U^{238} XS resonances occur has been considered.

The background XS σ_0 for U^{238} is computed by the extended SIMMER code by employing the EMCLs and the geometrical mean chord length ($MCL=4V_{cell}/S$).

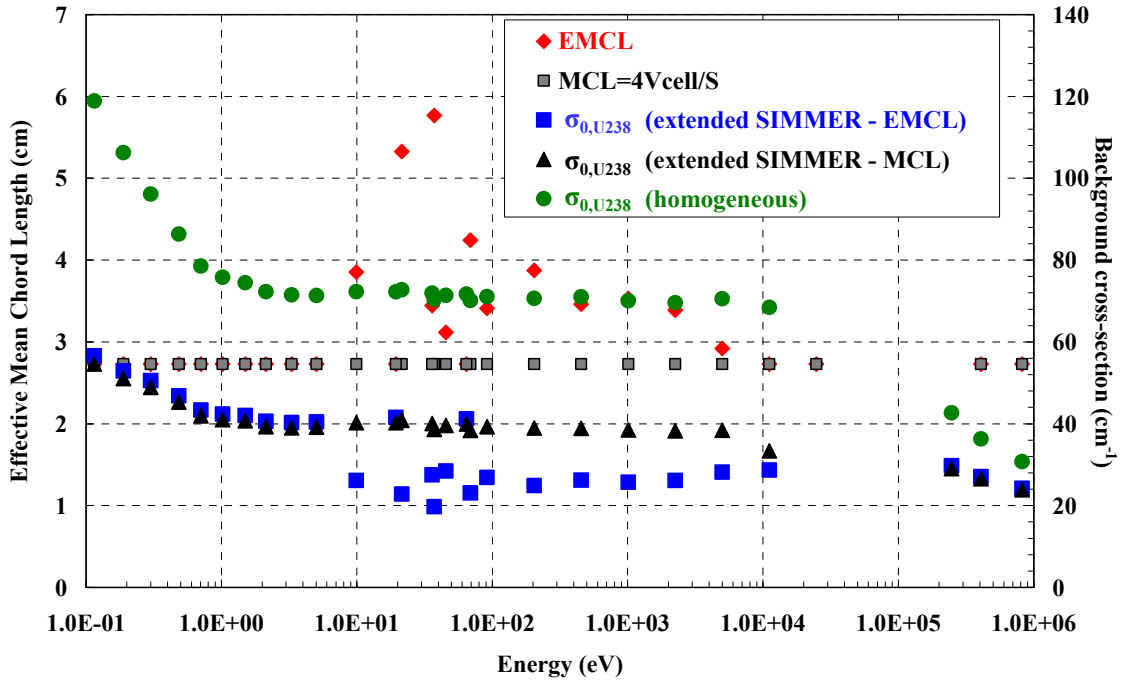

Figure 17. 40-energy-groups U^{238} background XS in the original and in the extended SIMMER code by using the MCL and the EMCL values

Figure 17 shows that:

- in the new technique employing the EMCL parameters (red diamonds), the influence of fuel XS resonance structure on the effective σ_0 (blue squares) is taken into account. Its influence is neglected in the homogeneous case (green bullets). On the contrary, it

appears in the heterogeneous case, due to the space-dependence of the neutron flux structure. In this case, the σ_0 (blue squares) shows some deviations in the region of the ^{238}U resonances corresponding to peaks in the EMCLs plot. The deviations of σ_0 are absent when the original SIMMER scheme is employed (green bullets);

- as expected, σ_0 in the new technique using the EMCLs (blue squares) is lower than σ_0 computed in the original model (green bullets) due to the escape XS term in Eq. 3.7. Thus, according to the theory, the contribution of non-fuel isotopes is less than the contribution of fuel nuclides;
- if the geometrical MCL (black squares) is employed in the extended SIMMER model, the corresponding σ_0 (black triangles) is close to the σ_0 which employs the EMCLs (blue squares), but remains unaffected by the resonances. The application of the new method will show that this feature achieves a significant improvement in the performance of the new SIMMER code.

3.4 Sensitivity of the pre-calculated parameters to perturbations

During the transient simulations, the XSs are processed from time to time to take account of the variations of the temperature and density in different regions. Therefore, different sets of pre-calculated correction factors should be computed depending on these parameters to perform a proper treatment for heterogeneity.

With this aim, a parametric study has been performed to evaluate the sensitivity of the EMCLs and of the flux ratios (clad-to-fuel and coolant-to-fuel) to fuel, clad, and water temperature and to moderator density variations. For these calculations the PWR and the MTR fuel sub-assemblies proposed as a calculation benchmark in the frame of the IRSN/KIT collaboration on JHR have been considered.

The PWR fuel sub-assembly is a standard 17 x 17 (264 fuel rods with 25 water gaps). Figure 18 shows the layout of the fuel sub-assembly. The fuel pellet radius is 4.1266 mm and the clad outer radius 4.7436 mm. The pin pitch is 12.621 mm and the inter-assembly water gap is 0.779 mm. The fuel is UO_2 (4.5 wt% U^{235}), the coolant is borated water (0.701 g/cm^3, 600 ppm of Boron) and the clad is Zircaloy.

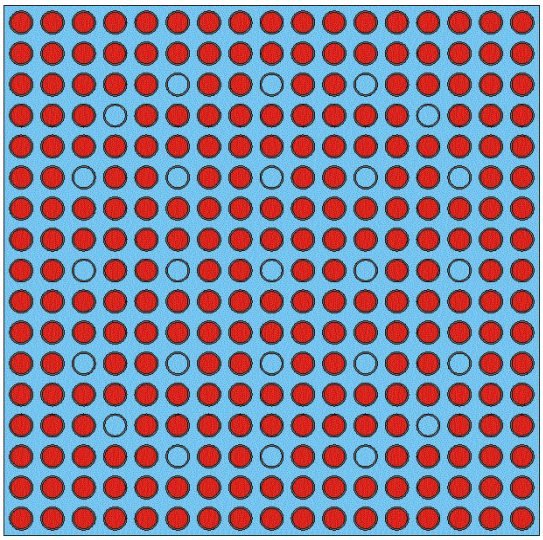

Figure 18. PWR fuel sub-assembly layout

The MTR fuel sub-assembly model (see Figure 19) is similar to that deployed in the SPERT experiments [10]. The fuel sub-assembly is loaded with 22 symmetric slab cells in an aluminium box (8.206 x 8.22 x 63 cm^3) with two grooved aluminium side plates for supporting the removable fuel plates. The dimensions of each fuel plate are 0.127 x 7.27 x 63 cm^3, with the active dimensions of 0.051 x 6.84 x 63 cm^3. The thickness of each water channel is 0.246 cm.

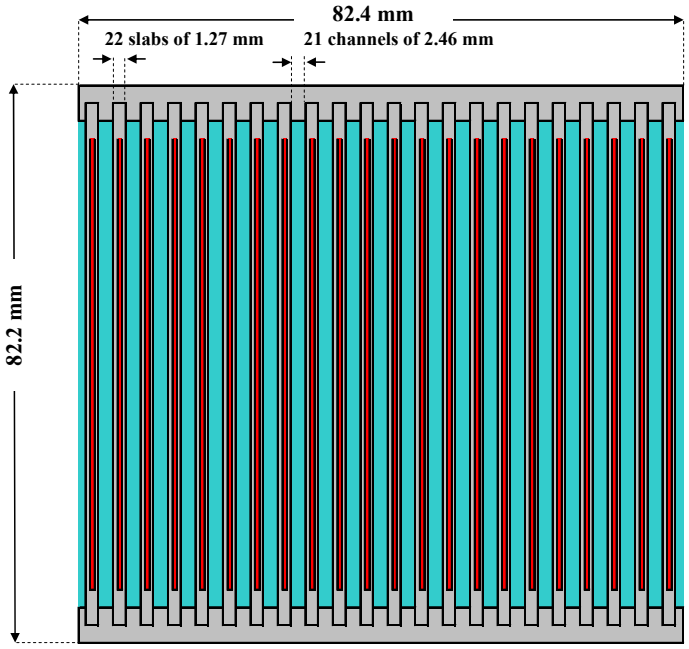

Figure 19. MTR fuel sub-assembly layout

The fuel is an alloy composed of aluminium and uranium silicide (U_3Si_2) (19.75 wt% U^{235}). Cladding is aluminium (density 2.7 g/cm^3) and coolant is water (density 0.9982 g/cm^3). The isotopic composition of each medium is presented in Table 3.

Fuel		**Moderator**		**Clad**	
Isotope	Atoms/barn-cm	Isotope	Atoms/barn-cm	Isotope	Atoms/barn-cm
^{235}U	2.4295E-03	H	3.3385E-02	Al	6.0221E-02
^{238}U	9.7474E-03	^{16}O	6.6770E-02		
Si	8.2256E-03				
Al	3.1910E-02				

Table 3. Fuel, moderator, and clad composition in the MTR fuel sub-assembly

3.4.1 Dependence of the neutron flux ratios on the temperature

Figure 20 and Figure 21 show the dependence of the clad-to-fuel and the water-to-fuel neutron flux ratios on fuel, clad, and water temperature perturbation in the MTR fuel sub-assembly model. In the legend of the figures, the first number refers to the fuel and clad temperature and the second to the water temperature [39, 40, 41]. Temperatures are in Kelvin.

For calculations, the density and the dimensions of the different components have been assumed to be independent on the temperature. In this manner, the effect of the temperature on the neutron XSs has been taken into account only.

The results show that the flux ratios are almost insensitive to temperature variations of the components for MTR fuel sub-assembly. The same conclusion was also found to be valid for the PWR sub-assembly.

The important result is that no interpolation of these parameters is necessary.

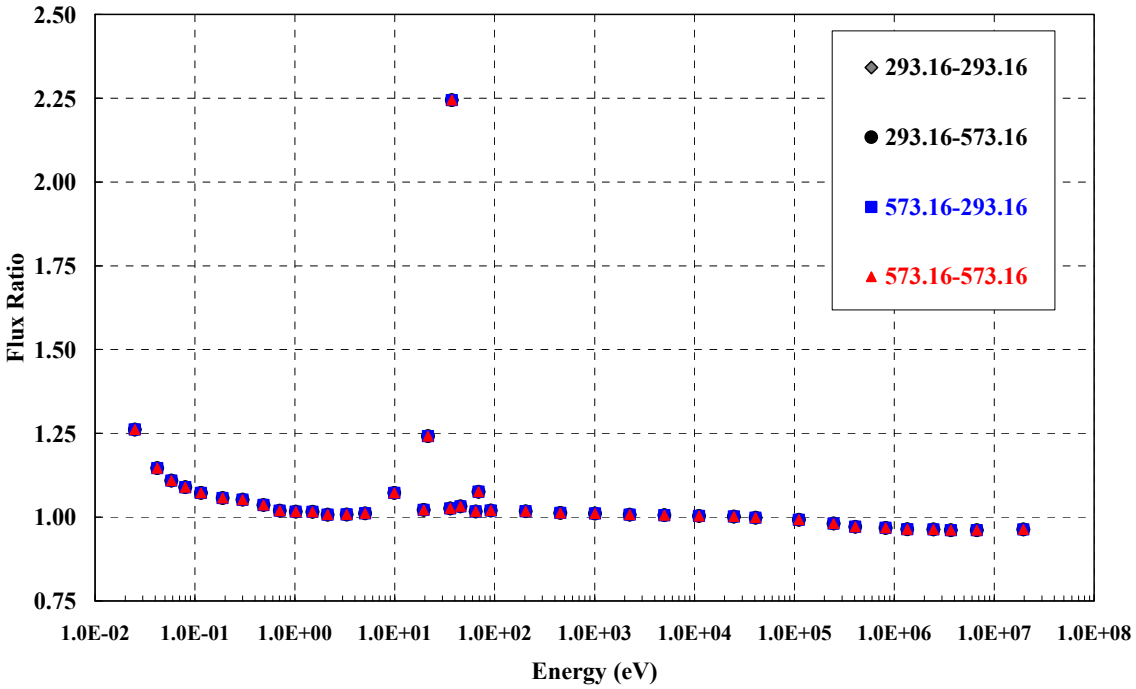

Figure 20. 40-energy-groups clad-to-fuel flux ratios at different fuel, clad, and water temperatures (K)

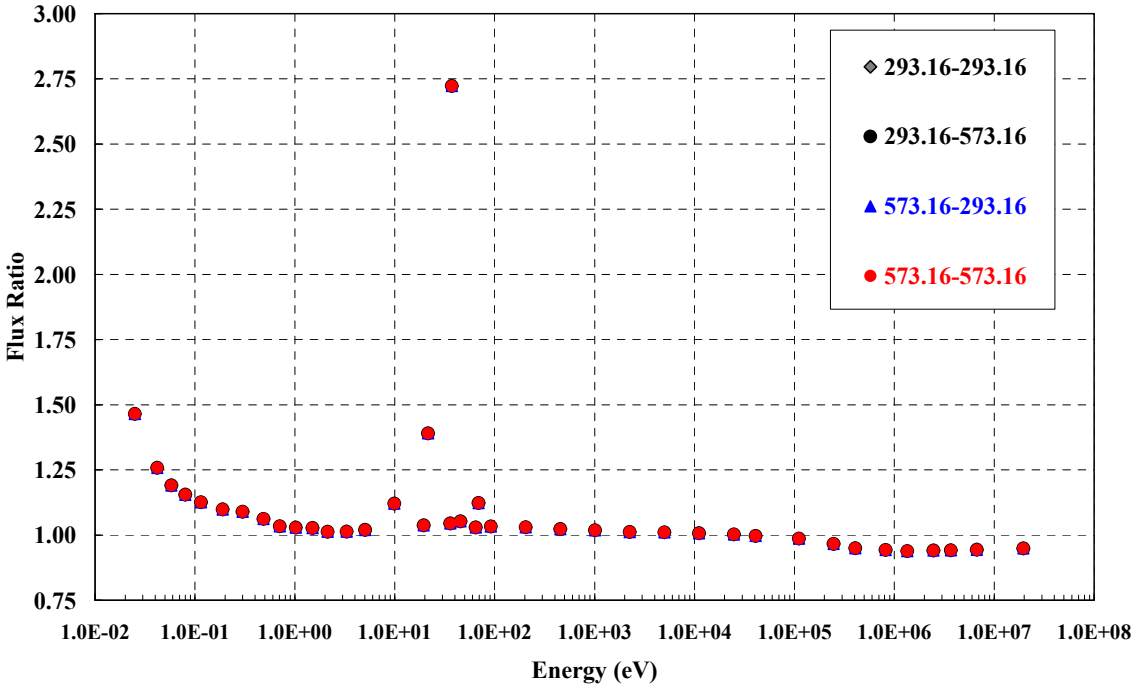

Figure 21. 40-energy-groups water-to-fuel flux ratios at different fuel, clad, and water temperatures (K)

3.4.2 Dependence of the neutron flux ratios on the moderator density

Coolant-to-fuel and clad-to-fuel flux ratios have been evaluated for different coolant void fractions. Figure 22 and Figure 23 show the coolant-to-fuel flux ratios for the PWR and the MTR fuel sub-assemblies, respectively [39, 40, 41].

The results show a strong deviation from unity localized in particular energy-groups corresponding to the resonances of U^{238} total XS. It should be also noted that the coolant-to-fuel neutron flux ratios are almost insensitive to the perturbation up to about 50% moderator void fraction. In contrast, appreciable variations are observed when 50% or more coolant is removed. In such conditions, the behaviour of these parameters is in general less regular, and reflects variations in the neutron spectra that have a quite complex influence in the vicinity of strong resonance peaks. Nevertheless, deviations from unity lead to smaller inaccuracies as the coolant-to-fuel flux ratio plays no role in the calculation of the homogenized XSs when there is almost no coolant in the system. The same considerations are valid for clad-to-fuel neutron flux ratios (see Figure 24 and Figure 25) which show a similar behaviour [39, 40, 41].

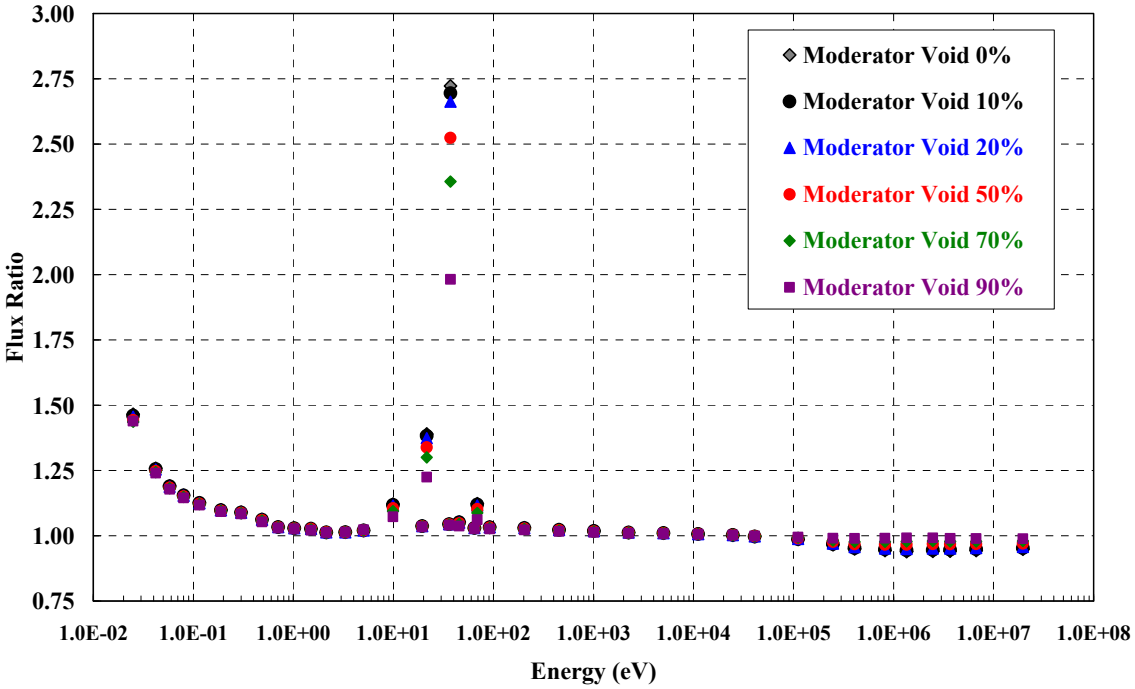

Figure 22. 40-energy-groups coolant-to-fuel flux ratios at different coolant void fractions in the PWR sub-assembly

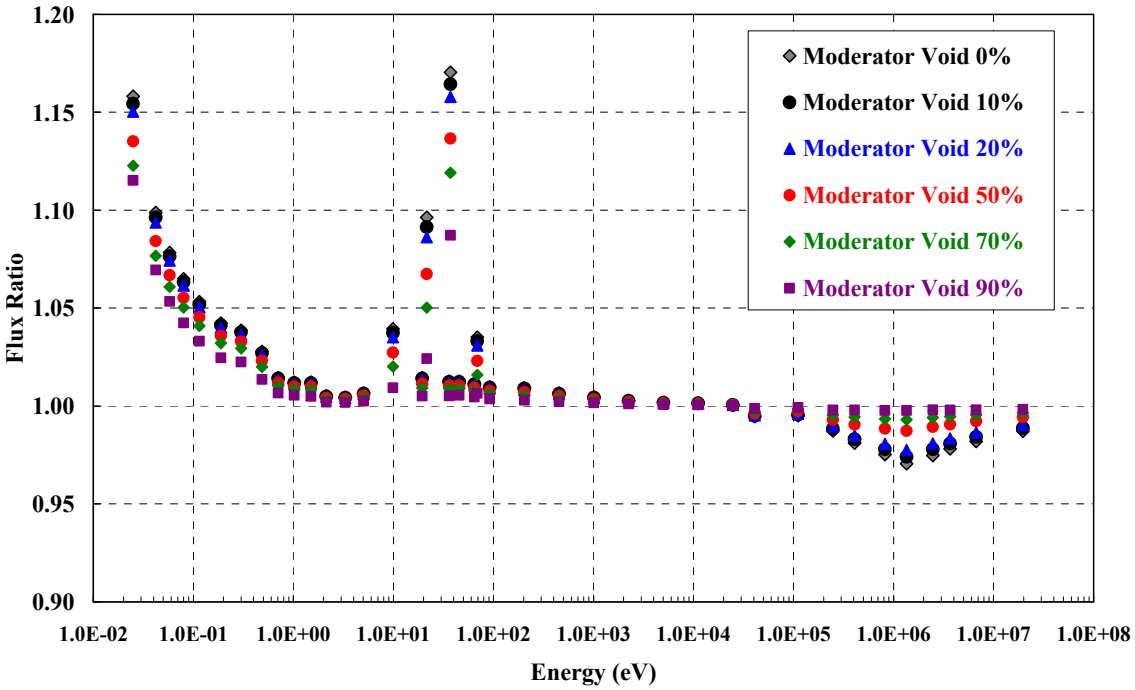

Figure 23. 40-energy-groups coolant-to-fuel flux ratios at different coolant void fractions in the MTR sub-assembly

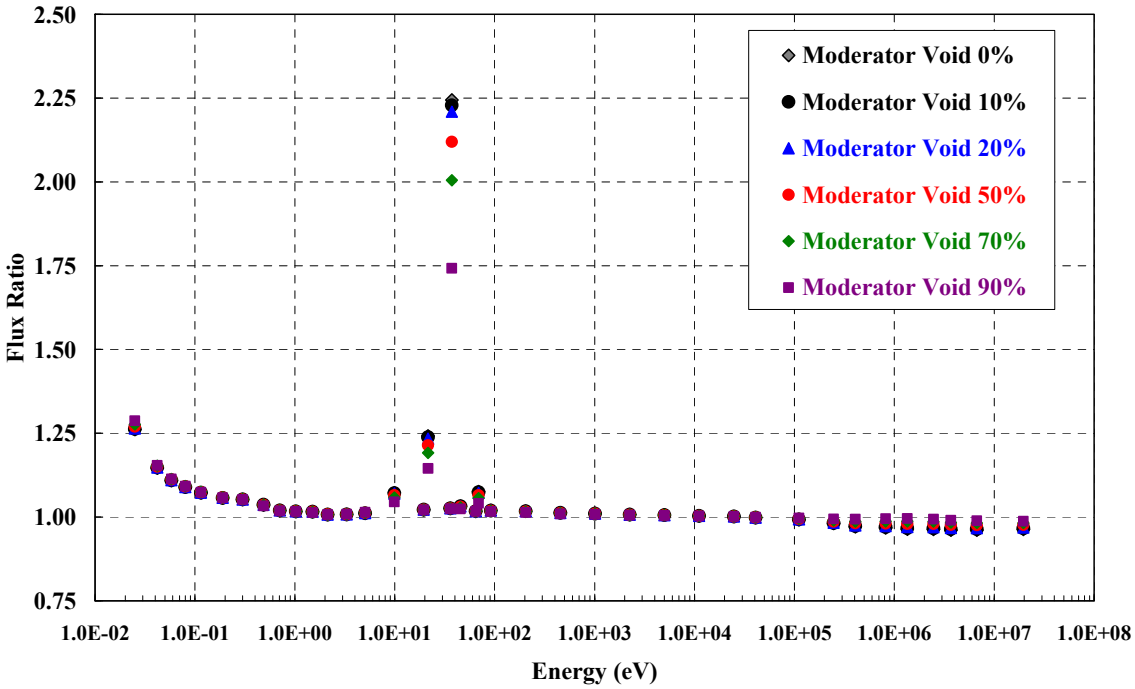

Figure 24. 40-energy-groups clad-to-fuel flux ratios at different coolant void fractions in the PWR sub-assembly

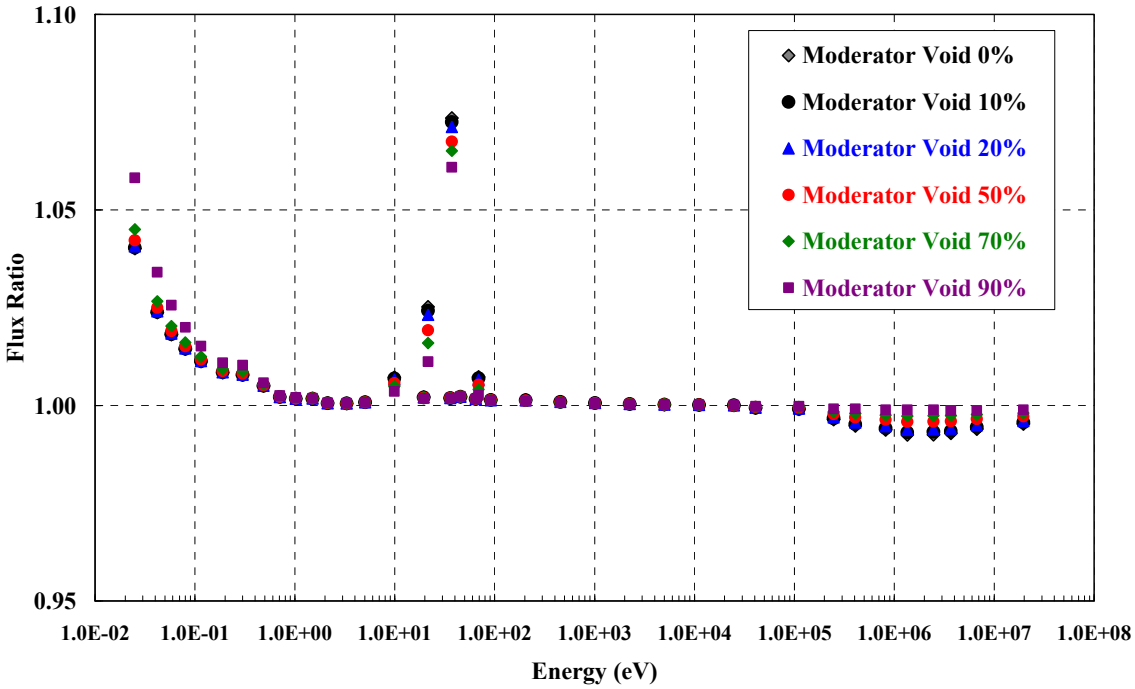

Figure 25. 40-energy-groups clad-to-fuel flux ratios at different coolant void fractions in the MTR sub-assembly

3.4.3 Effective mean chord lengths for unperturbed and perturbed configurations

The dependence of EMCLs in PWR and MTR fuel sub-assemblies on coolant density has been evaluated for different coolant void fraction in the unperturbed state, where all components are assumed to be at room temperature [39, 40, 41, 42].

Figure 26 and Figure 27 show the 40-energy groups EMCLs values computed by the ECCO code for 0%, 10 %, 25 %, 50%, 75 % and 95 % coolant void fraction in the PWR and MTR fuel sub-assembly, respectively.

In the Figures, EMCLs for both models are compared to the geometrical mean chord length (MCL=$4V_{cell}/S$) which is equal to 2.73 cm and 0.74 cm for the PWR and MTR fuel sub-assembly, respectively.

For calculations, EMCLs are assumed to be equal to the geometrical values in those energy groups where the resonance self-shielding effects are small.

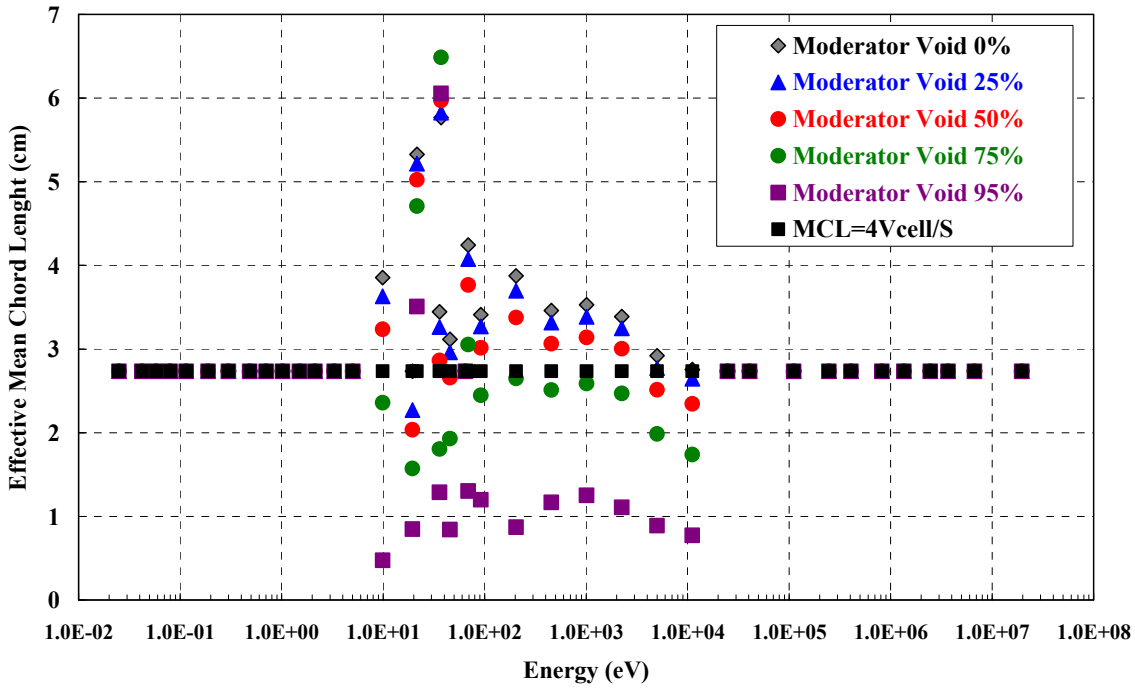

Figure 26. 40-energy-groups EMCLs at different coolant void fractions in the PWR sub-assembly

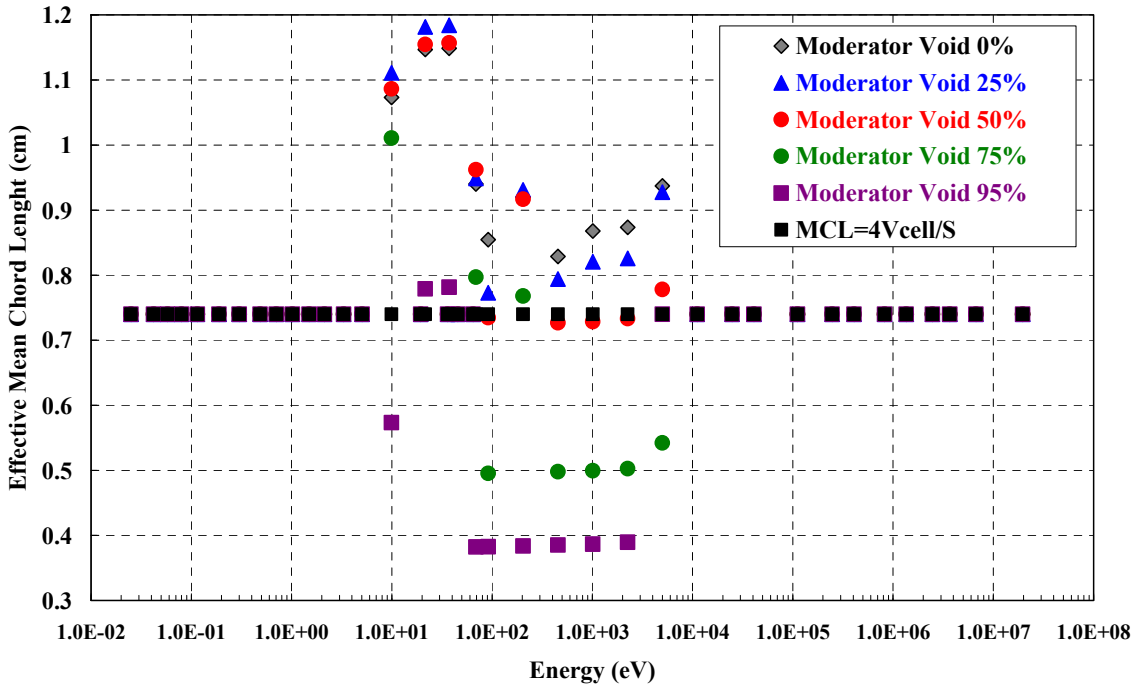

Figure 27. 40-energy-groups EMCLs at different coolant void fractions in the MTR sub-assembly

As expected, the EMCLs deviate significantly from the geometrical MCL ($4V_{cell}/S$) in the energy region of the major U resonance peaks [39, 40, 41, 42].

The most important result is that the sensitivity to perturbations is relatively small, in particular with respect to fuel and moderator temperature. In fact, when assuming constant materials densities and no change in the geometry, the macroscopic XSs in coolant and cladding do not vary significantly. Therefore, the application of Eq. 3.8 to evaluate EMCLs leads to almost temperature independent values.

Consequently, a relatively simple interpolation scheme can be employed during transient simulations as long as the geometry of the assembly does not change appreciably [39, 41].

As for the neutron flux ratios, significant variations of EMCLs are observed when 50% or more coolant is removed.

Nevertheless, under such conditions, deviations from MCLs lead to smaller inaccuracies because the contribution of the resonance energy region to a reaction rate is smaller if the void fraction is higher.

3.5 Application of the new methods to fuel sub-assembly models

For validation, the fuel Doppler effect has been computed in the unperturbed state and at different coolant void conditions for the PWR and MTR fuel sub-assembly models described above. With this aim, the extended SIMMER XS processing scheme has been benchmarked against the original SIMMER scheme and the ECCO code. Two ECCO models are assessed for the fuel sub-assembly: a homogeneous and a heterogeneous, the latter of which is assumed as reference.

For these calculations, the extended SIMMER code employs the pre-calculated neutron flux ratios and EMCLs computed under unperturbed condition, i.e. all materials are assumed to be at room temperature and no moderator is removed.

In the benchmark exercise, the densities of the materials are taken as constant and no thermal expansion is taken into account. As a result, the macroscopic XSs in coolant and cladding do not show meaningful variations.

3.5.1 MTR fuel sub-assembly

Table 4 shows the k_∞ values obtained from the ECCO heterogeneous model, MCNP, and extended SIMMER with fuel and water at room temperature. The results show a reasonable agreement with respect to k_∞.

	MCNP	ECCO@40 groups	SIMMER@40 groups
k_∞	1.68984 ± 0.00067	1.69004	1.70691

Table 4. MTR sub-assembly k_∞ values computed by MCNP,ECCO, and SIMMER

The fuel Doppler effect has been computed for different fuel temperatures (100 ºC, 400 ºC and 600 ºC) at different moderator void fractions (0%, 10% and 20%) and the coolant is assumed to be at room temperature (see Figure 28) [39, 42].

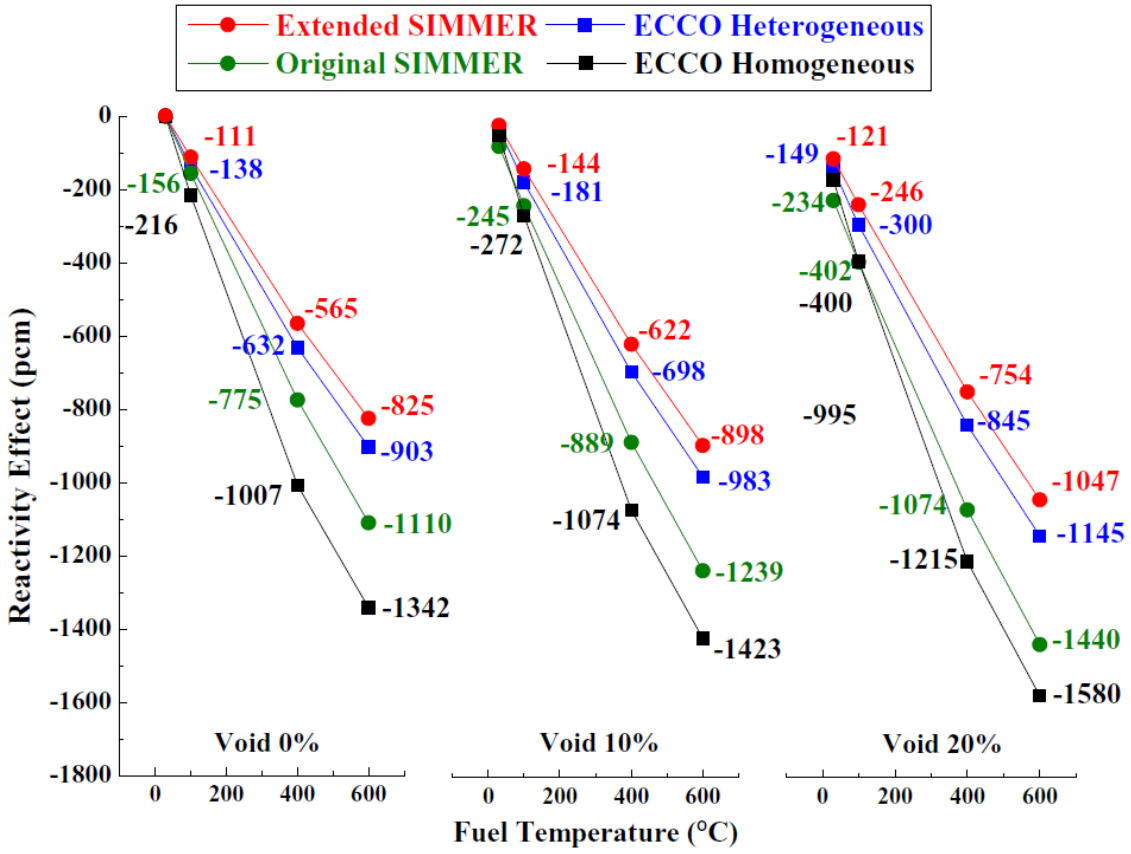

Figure 28. MTR fuel sub-assembly: comparison between the fuel Doppler effect computed by SIMMER and ECCO at different moderator void fractions

The results demonstrate that the use of the extended SIMMER XS generation scheme clearly improves the agreement with ECCO heterogeneous results as compared to the original SIMMER scheme. The reactivity difference between the SIMMER extended version and the ECCO heterogeneous model is always below 100 pcm. However, this difference increases up to about 300 pcm when the original SIMMER model is used. The results also show that:

- the original SIMMER model overestimates the fuel Doppler effect when compared to ECCO heterogeneous results, however it is underestimated by the extended SIMMER scheme of about 10%;
- similar or smaller deviations are observed concerning the moderator void effect.

The results also show that the heterogeneity effects evaluated by means of the ECCO and SIMMER codes are similar, even if some discrepancies are observed. Figure 29 shows the comparison between the effect of heterogeneity computed by using the two codes.

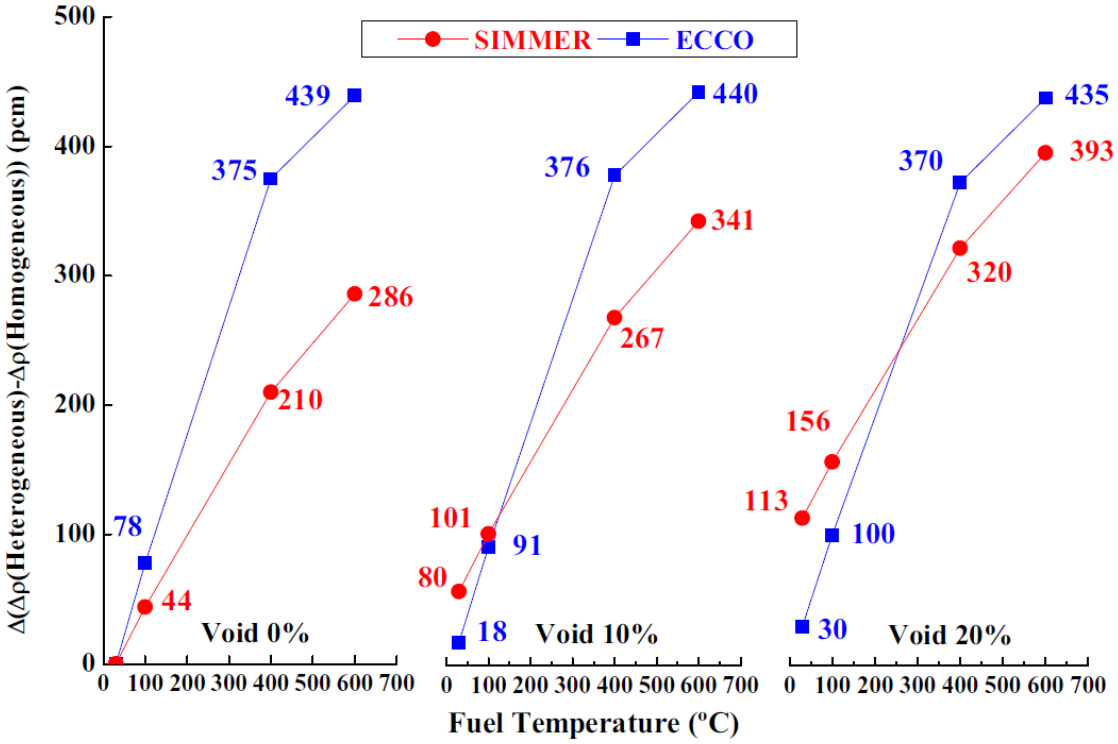

Figure 29. Effect of heterogeneity evaluated by the SIMMER and ECCO codes

One may note that SIMMER takes into account the major part of the heterogeneous effect computed by ECCO. Discrepancies are mainly due to different performance of the homogeneous models in the ECCO (1968 groups) and the SIMMER (40 groups) models.
As already evident from Figure 29, Table 5 shows that the results for the Doppler effect reactivity are much closer between SIMMER and ECCO for the heterogeneous than for the homogenous model, i.e. the differences between the results of both codes become smaller if the heterogeneous model is used instead of the homogeneous model.

	Δρ(SIMMER) – Δρ(ECCO)	
Fuel Temperature increase (°C)	Homogeneous model	Heterogeneous model
70	60	27
370	232	67
570	231	78

Table 5. Reactivity difference between the fuel Doppler effect computed by homogeneous and heterogeneous models at zero moderator void fraction

One important finding from Figure 28 and Figure 29 is the following: if the extended model for the treatment of heterogeneities is not employed in the SIMMER code, larger discrepancies are observed in the fuel Doppler effect [39, 41]. As a result, the new techniques employed in the SIMMER code allow a more accurate accounting for the effect of heterogeneities.
Moreover, a reasonable agreement can be obtained even by employing pre-calculated parameters corresponding to the unperturbed conditions, as the maximum moderator void fraction is rather low (20%). This is an important result because it confirms that it is not necessary to compute a large set of pre-calculated parameters in order to take account of the effect of heterogeneity in the XSs processing during the transient simulation.

3.5.2 PWR fuel sub-assembly

Concerning the PWR fuel sub-assembly, the extended SIMMER code shows reasonable agreement with MCNP and ECCO with respect to k_∞ (Table 6) [41].

	MCNP	ECCO@40 groups	SIMMER@40 groups
k_∞	1.35209 ± 0.00063	1.34593	1.36648

Table 6. PWR sub-assembly k_∞ values computed by MCNP, ECCO, and SIMMER

Doppler effect values have been calculated for different fuel temperatures (100 ºC, 300 ºC, 500 ºC and 700 ºC) at different moderator void fractions (0 %, 10 % and 20 %) and the is coolant assumed to be at 30 ºC (see Figure 30) [40, 42].

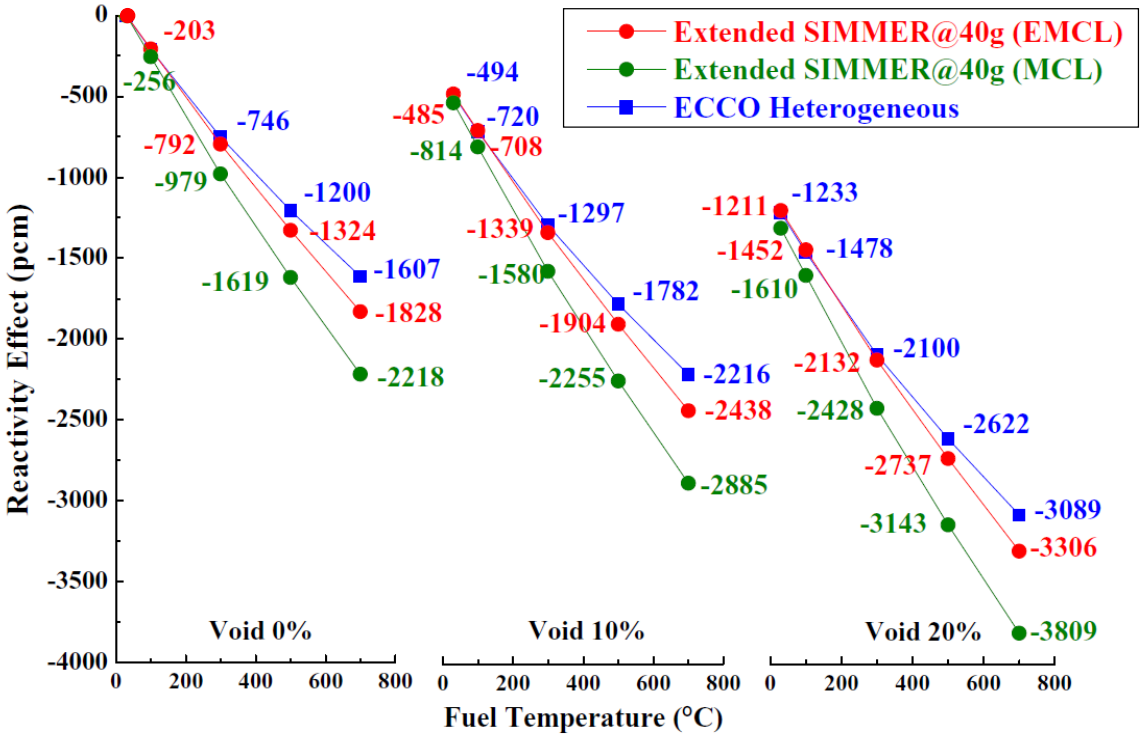

Figure 30. PWR fuel sub-assembly: comparison between the fuel Doppler effect computed by SIMMER and ECCO at different moderator void fractions

The reactivity effects have been computed by using the extended SIMMER code employing the EMCL parameters and the geometrical MCL.

The extended SIMMER results show a reasonable agreement with those computed using the ECCO heterogeneous model when the EMCL parameters are employed. In this case the maximum deviations are about 200 pcm.

Figure 30 also shows that employment of the EMCL instead of the MCL parameters leads to an appreciable improvement in the accuracy of the extended SIMMER code.

This is due to the ability of the new method to more accurately compute the U^{238} background XS in the resonance region.

The good agreement of the extended SIMMER code in the highest void condition with the reference results confirms that the heterogeneity parameters in the unperturbed state may be employed also in different perturbed conditions in a reliable way in the PWR fuel sub-assembly case. Similar to the MTR fuel sub-assembly case, the results also show that:

- the use of the extended SIMMER model for heterogeneities treatment allows a better agreement with the ECCO code than the original SIMMER model [40, 42];
- the extended SIMMER model underestimates the fuel Doppler effect when compared to ECCO of about 10%;
- similar or smaller deviation are observed concerning the effect of the water density.

Chapter 4. Application of the new method to material test thermal reactors

In this chapter, the extended SIMMER neutronics model is applied to the MTR core model proposed in the frame of the IRSN/KIT collaboration and to the SPERT-I D-12/25 experimental core configuration. The aim is to confirm the improvement of the accuracy of the SIMMER code when the new methods for heterogeneity treatment are employed. Neutronics models have been first assessed for each reactor core by means of the MCNP and ECCO/ERANOS reference codes. Then the extended SIMMER code is tested by benchmarking against the reference codes for the criticality and major reactivity effects, e.g. fuel Doppler and coolant void. The new method is applied for the analysis of a transient test case for the MTR core model and results are compared with the original SIMMER code. Concerning the SPERT core, the availability of a large amount of experimental data represents an important step for the final validation of the new SIMMER model. Having this in mind, reference neutronics codes and experiments are benchmarked with respect to criticality, the control rod worth, and neutron flux profiles. Due to their importance in simulating the behaviour of the system, the main kinetic parameters (Λ and β_{eff}) are computed and compared to experimental data.

4.1 Investigation of the MTR thermal reactor core

The MTR core model investigated in this work (see Figure 31) has a diameter of 68.8 cm and is surrounded by an aluminium vessel (2 cm thick) permitting 34 fuel sub-assemblies and 3 aluminium sub-assemblies as material irradiation positions. The vessel is surrounded by an aluminium shield (4 cm thick), a beryllium reflector with an external diameter of 143.8 cm, and a water pool with external diameter 226 cm. The active core length is 600 mm, bounded by 100 mm of water (above and below).

The fuel sub-assembly (see Figure 32) has an external diameter of 9.47 cm. It is an arrangement of 8 fuel circular blades, supported by means of 3 aluminium blades, around

a central aluminium circle with a diameter of 4 cm. Each fuel blade is composed of an alloy of aluminium and uranium silicide (U_3Si_2) (19.75 wt% U^{235}) 0.06 cm thick with a 0.137 cm thick clad separated by a 0.184 cm thick coolant channel. The isotopic composition of each component is shown in Table 7.

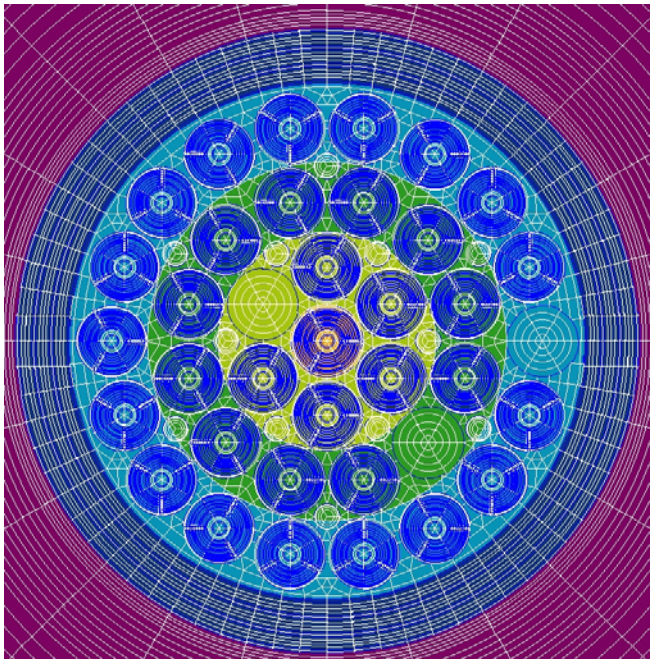

Figure 31. MTR core layout

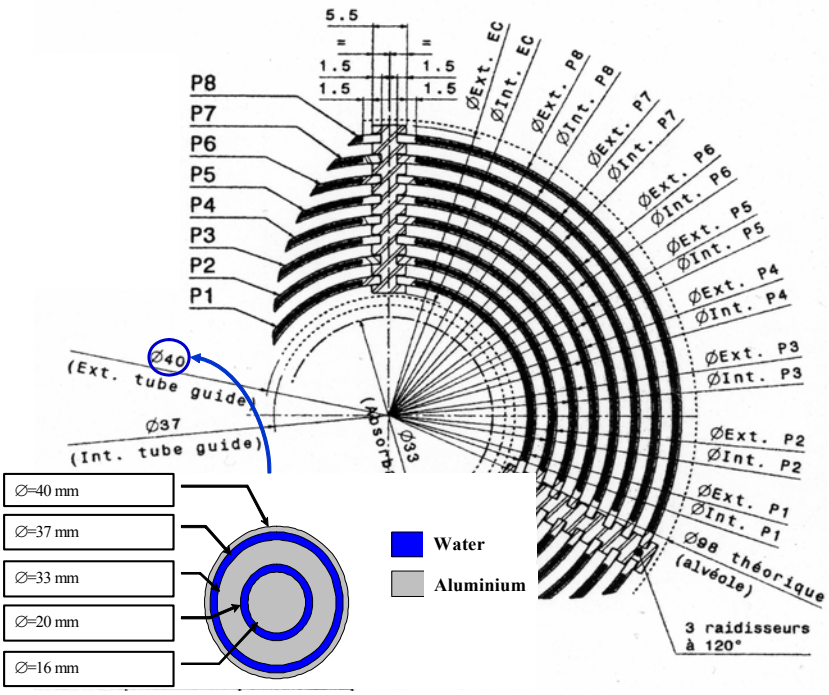

Figure 32. Layout of fuel sub-assembly in the MTR core

Fuel		Moderator		Clad	
Isotope	Atoms/barn-cm	Isotope	Atoms/barn-cm	Isotope	Atoms/barn-cm
Al	2.9791E-02	H	3.3366E-02	Al	5.8969E-02
^{234}U	9.2631E-07	^{16}O	6.6732E-02	^{54}Fe	1.7167E-05
^{235}U	3.3205E-03			^{56}Fe	2.6949E-04
^{236}U	1.8002E-05			^{57}Fe	6.2238E-06
^{238}U	8.8455E-03			^{58}Fe	8.2827E-07
Si-nat	8.1233E-03			^{58}Ni	1.9027E-04
				^{60}Ni	7.3291E-05
				^{61}Ni	3.1862E-06
				^{62}Ni	1.0157E-05
				^{64}Ni	2.5881E-06
				Mg-nat	6.7487E-04

Table 7. Fuel, moderator, and clad composition in the fuel sub-assembly

4.1.1 Pre-calculated parameters for the MTR core analysis

A fuel sub-assembly model of the MTR core has been assessed by ECCO in order to compute the coefficients employed for the heterogeneity treatment for use in SIMMER. As the ECCO code cannot model the actual MTR core fuel sub-assembly (see Figure 33a), a simplified model without stiffeners has been assessed (see Figure 33b).

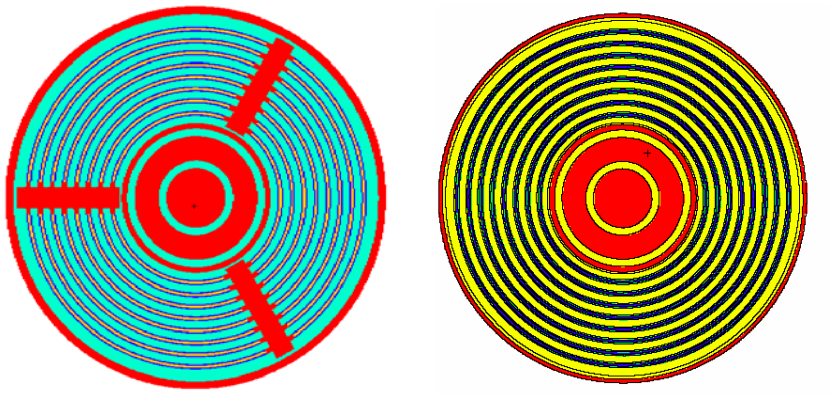

(a) **(b)**

Figure 33. Layout of actual (a) and simplified (b) fuel sub-assembly models

In this model, the aluminium in the stiffeners has been smeared into the fuel and into the cladding, while the total amount is kept constant.

MCNP results in Table 8 show that the simplified model may reasonably represent the actual model in the reference state, where all components are assumed to be at room temperature and the moderator void is zero. In fact, the k_∞ eigenvalues computed for the two assessments are in a good agreement. Moreover, Table 8 shows that ECCO results for the simplified model are in good agreement with MCNP results.

Fuel sub-assembly model	MCNP	ECCO@1968g	ECCO@40g
Actual	1.67059 ± 0.00054	-	-
Simplified	1.67217 ± 0.00071	1.67414	1.67401

Table 8. k_∞ computed by ECCO and MCNP for the fuel sub-assembly models loaded in the MTR core in the reference state

The performance of the ECCO sub-assembly model has been evaluated by benchmarking against the corresponding MCNP model. MCNP and ECCO results for the moderator void effect ell agree (Table 9), as does for the fuel Doppler (Table 10). Reactivity effects are evaluated with respect to the reference state assuming that the density of each component does not change with temperature.

Water Void (%)	MCNP (pcm)	ECCO@1968g (pcm)	ECCO@40g (pcm)
10	-99 ± 33	-146	-146
30	-629 ± 34	-718	-718
50	-1839 ± 35	-1925	-1924
90	-10433 ± 44	-10608	-10607

Table 9. Comparison of the coolant void effect computed by ECCO and MCNP4C

ΔT Fuel (K)	MCNP (pcm)	ECCO@1968g (pcm)	ECCO@40g (pcm)
500	-304 ± 36	-360	-360
800	-699 ± 33	-782	-782
1000	-961 ± 34	-1018	-1019

Table 10. Comparison of the fuel Doppler effect computed by ECCO and MCNP4C

As a result, ECCO has been used to determine the EMCLs and the clad-to-fuel and water-to-fuel neutron flux ratios for the heterogeneity treatment in the extended SIMMER code (see Figure 34). The parameters were evaluated at zero coolant void condition and with the components at room temperature.

It should be remind here that EMCL factors and neutron flux ratios show a weak dependence on the fuel and water temperature. Major deviations versus coolant density have been observed only when more than about 40 % of coolant is removed.

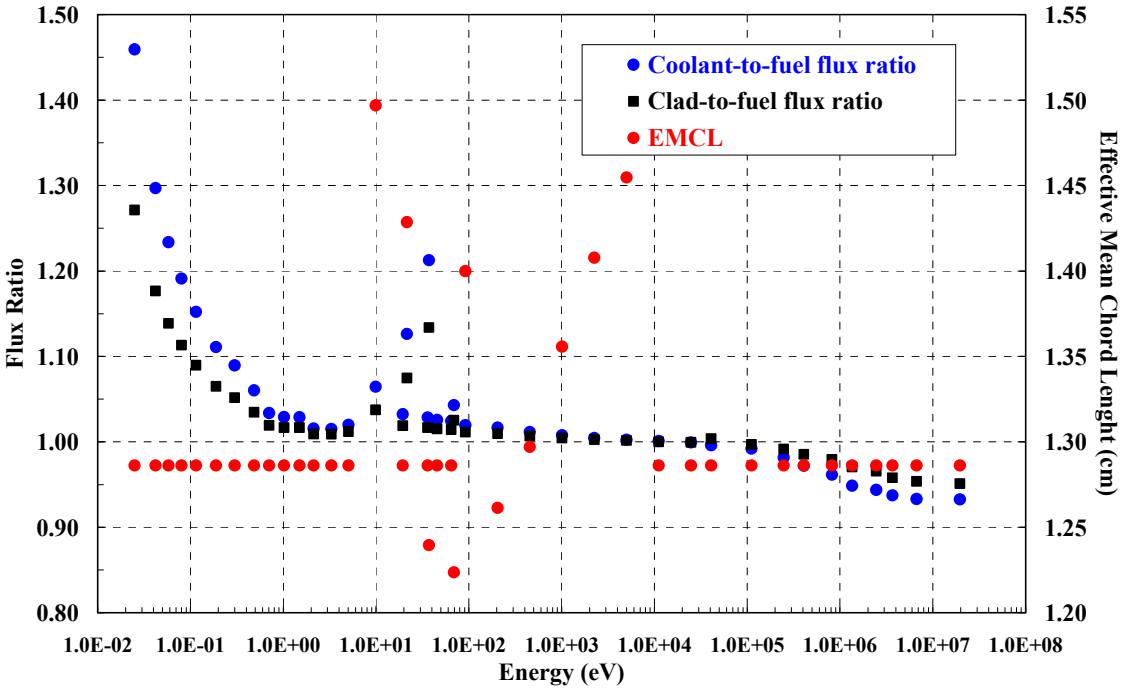

Figure 34. Pre-calculated parameters for heterogeneity treatment in the SIMMER code for the analysis of the MTR core

4.1.2 2D model assessment for the MTR core

In order to perform the investigations by means of the SIMMER code, a 2D model for the MTR core has to be assessed. The actual 3D model cannot be directly assessed by ERANOS, thus making the validation of the 2D model difficult, because the sub-assemblies pitch is not constant in the MTR core (see Figure 35a).

With this aim, a similar but regular 3D (HEX-Z) model with a constant pitch of 10.7 cm has been studied (Figure 35b). As a result, the 3D hexagonal model (HEX-Z) and the corresponding 2D (RZ) model can be easily assessed (Table 11).

The 3D (HEX-Z) model is then used by the ERANOS code in the frame of the validation of the new SIMMER XS processing scheme.

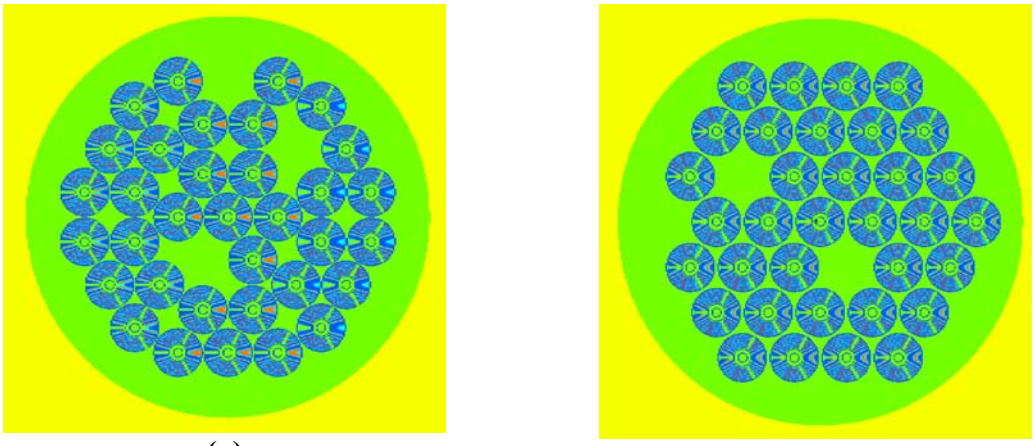

(a) **(b)**

Figure 35. Actual (a) and regular (b) MTR core model

Ring	External Radius (mm)	Ring Composition
1	56.55	1 FA
2	149.6	5 FA + 1 Al assembly
3	246.5	11 FA + 1 Al assembly
4	334	17 FA + 1 Al assembly
5	404	Vessel
6	719	Beryllium Reflector
7	1130	Water Pool

Table 11. Geometrical data of the 2D (RZ) MTR core model

4.1.3 Performance of the new SIMMER model for the MTR core

Using the 2D model for the MTR core, the extended SIMMER code has been benchmarked against the original SIMMER code, the MCNP (3D and 2D), and the

ERANOS (3D HEX-Z and 2D) codes. The criticality level, the fuel Doppler effect, and the coolant void effect have been computed. For calculations, the JEF 2.2 evaluated nuclear data has been used.

For multigroup SIMMER [23, 24] calculations, the 40-energy-groups XS library described in the previous chapter has been used. ECCO/ERANOS calculations have been performed with the equivalent 40-groups XSs obtained by collapsing the 1968 fine-group XSs. ERANOS transport calculations have been carried out using the two-dimensional S_n transport optimized code (BISTRO) [63] and Variational Anisotropic (VARIANT) [64] codes. BISTRO is a code for solving neutron transport problems by the S_n method (in angle) and the finite difference method in space for two-dimensional geometries. The VARIANT code solves the diffusion and transport equations by using the variational nodal method [64].

The calculated k_{eff} eigenvalues at room temperature and the reactivity variations with respect to the actual 3D MCNP model for the MTR core, here assumed as reference, are shown in Table 12 where:

- '*homogeneous*' means that a 'bulk' model for the fuel regions has been employed. Concerning the ERANOS calculations, this condition also means that the neutron XSs have been processed in ECCO for a homogeneous mixture;
- '*heterogeneous*' means that the XSs for ERANOS calculations have been processed in ECCO by using a fine geometry description of the fuel sub-assembly.

	k_{eff}	**Δρ(pcm)**
Actual MTR core - MCNP	1.26801 ± 0.00031	-
3D 'Regular' - MCNP	1.26833 ± 0.00035	20 ± 29
RZ - MCNP (Homogeneous)	1.26336 ± 0.00031	-290 ± 27
RZ - ERANOS (Homogeneous)	1.25873	-581 ± 19
3D - ERANOS (Heterogeneous)	1.26245	-347 ± 19
RZ - ERANOS (Heterogeneous)	1.27050	155 ± 19
RZ- SIMMER (Original model)	1.26865	40 ± 19
RZ – SIMMER (Extended model)	1.26796	-3 ± 19

Table 12. MCNP, ERANOS, and SIMMER benchmark results at room temperature

The results for k_{eff} are in general in good agreement. In particular, results for the 2D models show a reasonable agreement with those for actual 3D MCNP model. Moreover, no meaningful discrepancy is observed if 'homogeneous' XSs are employed instead of 'heterogeneous' XSs. This effect only becomes evident when reactivity effects are evaluated. The fuel Doppler effect has been computed by increasing the fuel temperature from 300 K to 1000 K (Table 13).

	Δρ(pcm)
Actual MTR core – MCNP	-1186 ± 52
3D 'Regular' – MCNP	-1227 ± 49
RZ - MCNP (Homogeneous)	-1651 ± 69
RZ - ERANOS (Homogeneous)	-2166
3D - ERANOS (Heterogeneous)	-1171
RZ - ERANOS (Heterogeneous)	-1180
RZ- SIMMER (Original model)	-1535
RZ – SIMMER (Extended model)	-1243

Table 13. Fuel Doppler effect in the MTR core computed by SIMMER, MCNP, and ERANOS

The results show that application of the new methods in the SIMMER XS processing scheme leads to a significant improvement compared to the results obtained using the original SIMMER scheme. In particular:

1. in the extended SIMMER version, the results show a good agreement with respect to the 3D and 2D ERANOS calculations, when heterogeneous XSs employed;
2. 2D and 3D ECCO/ERANOS models show a good agreement with 3D MCNP models, when the XSs are processed for a fine description of the fuel sub-assemblies;
3. with respect to the MCNP calculation for the actual 3D core model, fuel Doppler computed by the SIMMER and ERANOS heterogeneous models show a deviation from -1% to 3.5 %;
4. homogeneous calculations are not conservative. Compared to the extended SIMMER code, the fuel Doppler effect is overestimated by homogeneous models about 33% (2D MCNP), 74% (ECCO/ERANOS), and 23% (original SIMMER model).

The coolant void effect has been computed by removing 50% of water in the central fuel sub-assembly (in 3D models) or in the central ring (in 2D models).

The results (Table 14) are in excellent agreement. The extended SIMMER model shows a slightly better performance than the original SIMMER version, but a discrepancy of about 20% remains with respect to the MCNP reference. This result is in agreement with the observations of the sensitivity of the pre-calculated parameters for heterogeneity treatment to perturbations (Par. 3.4.2 and 3.4.3). As previously mentioned, the parameters show only a weak dependence on the coolant voiding up to about 50%. Thus, it may be concluded that employing additional sets of void-dependent parameters could improve the results.

	Δρ(pcm)
Actual MTR core – MCNP	-434 ± 15
3D 'Regular' – MCNP	-483 ± 17
RZ - MCNP (Homogeneous)	-526 ± 24
RZ - ERANOS (Homogeneous)	-590
3D - ERANOS (Heterogeneous)	-582
RZ - ERANOS (Heterogeneous)	-460
RZ- SIMMER (Original model)	-527
RZ – SIMMER (Extended model)	-516

Table 14. Coolant void effect after removing 50% of coolant in the central sub-assembly in the MTR core computed by SIMMER, MCNP, and ERANOS

The results also show that the 'heterogeneous' ERANOS model agrees well with the MCNP reference. Thus, the ERANOS results can be considered as reference for the SIMMER code in the following investigations.

The extended SIMMER code is benchmarked against the original version and ERANOS for the fuel Doppler effect at 0%, 10% and 20% coolant void fractions (see Figure 36). Reactivity effects are computed with respect to the initial state where the components are assumed to be at room temperature and the moderator void is zero.

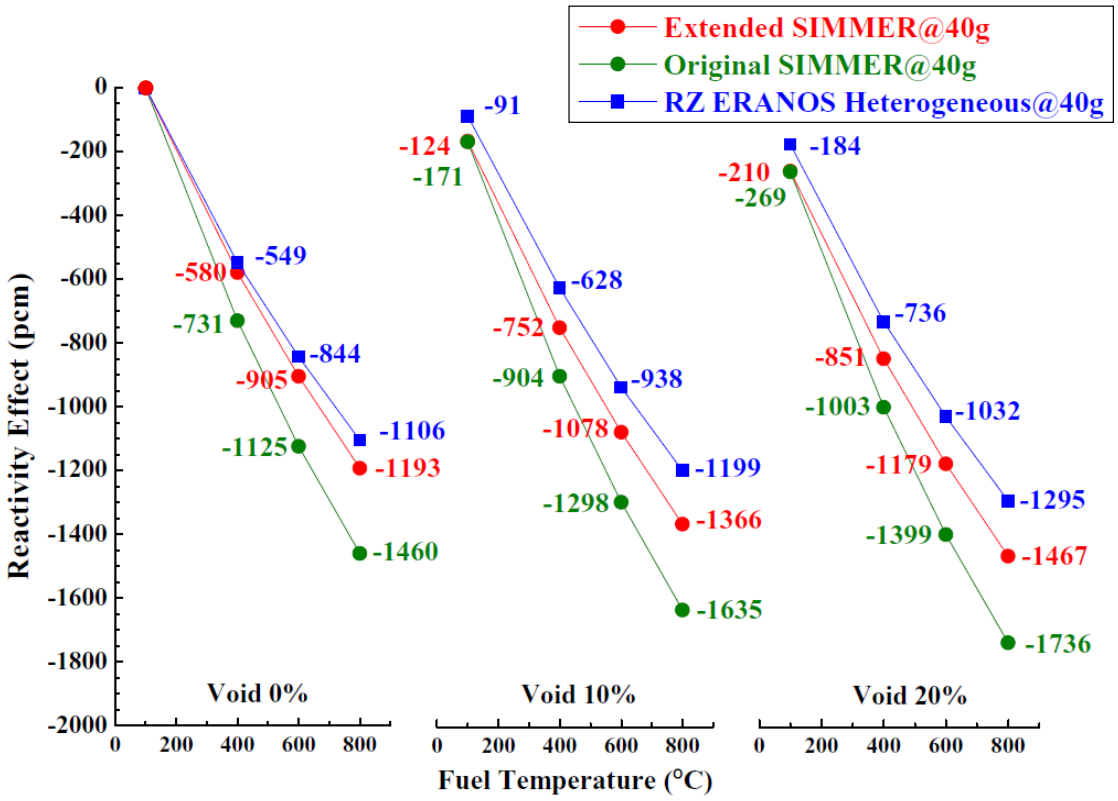

Figure 36. Fuel Doppler and void reactivity effect for MTR core: comparison of the results from the extended SIMMER, the original SIMMER, and the ERANOS codes

The results in Figure 36 clearly show a significant improvement of the accuracy of the SIMMER results when the extensions for heterogeneity treatment are employed:

- at the zero void condition, the original SIMMER calculations overestimates the fuel Doppler effect of about 30% with respect to ERANOS. This discrepancy is reduced to about 6% when the new extended SIMMER model is employed;
- at higher coolant void conditions, this new development reduces the deviation between the original SIMMER and ERANOS by a factor of 2 to 3.

4.1.4 Analysis of a short transient

The effect of using the new approach for a transient has been investigated for a test case using the RZ model established for MTR core (Table 11). A transient induced by the

linear insertion of 2.2 $ within 0.05 s has been simulated and results from the extended and the original SIMMER models have been compared.

The results concerning the reactor power (see Figure 37) show significantly different behaviour due to the alternative computation of the reactivity feedbacks (see Figure 36) in the transient. The original SIMMER results (black line) are not conservative. The peak power (14.7 MW) computed by using the extended SIMMER version (red line) is about 30% higher than that calculated by the original SIMMER code (11.4 MW).

As a result, the total energy release (147 MW-s) and the energy release at the peak power (63.5 MW-s) computed by employing the new method (blue line) are about 35% and 32% higher than that evaluated by using the original SIMMER code (green line).

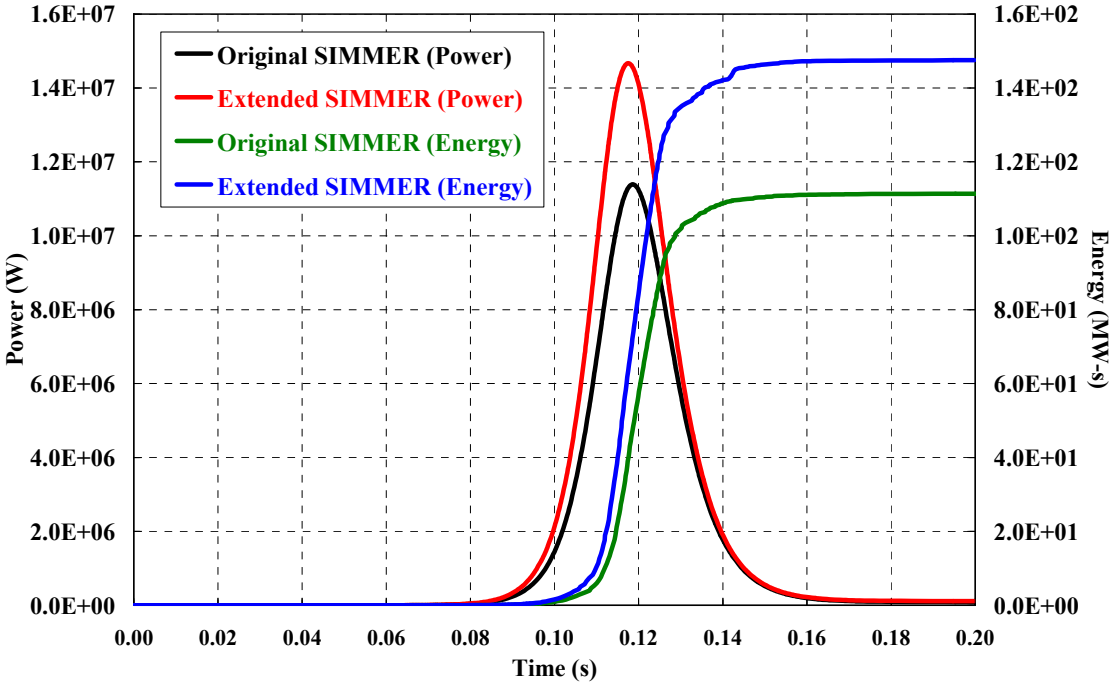

Figure 37. Reactor power and energy release during the transient

Another important result shown in Figure 37 is that the heterogeneity treatment affects both the kinetic parameters (see Figure 38) and the fuel temperature feedbacks (see Figure 39) during the transient. The results in Figure 38 show that the power increases exponentially with a different slope due to the evaluation of different mean neutron generation times, Λ.

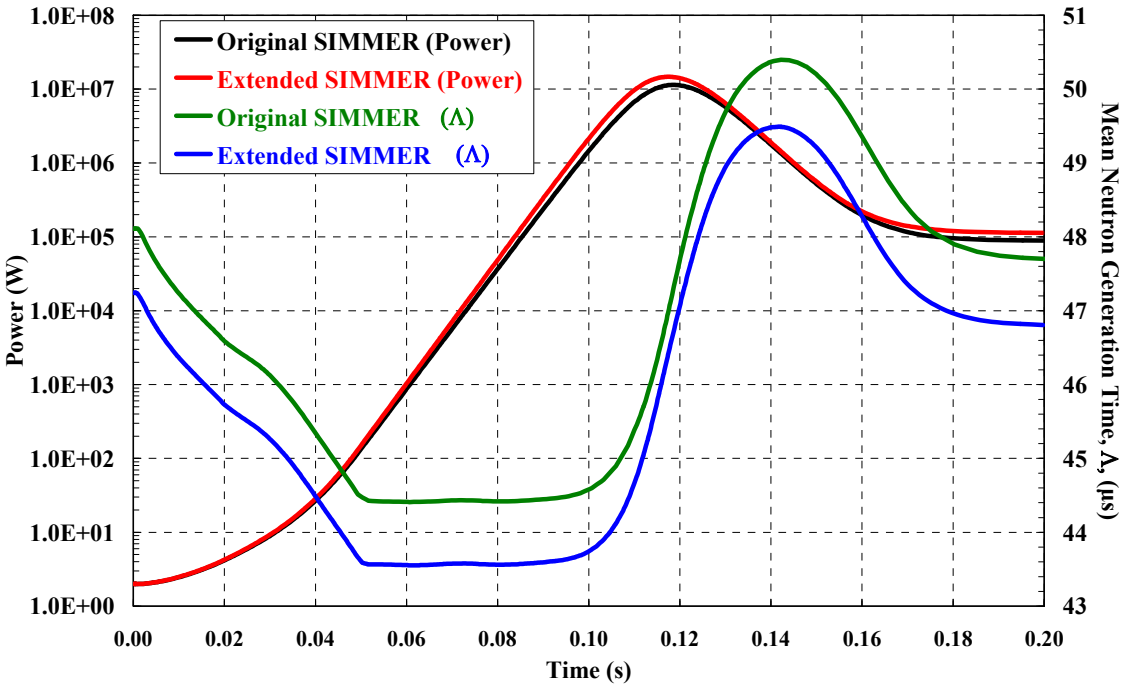

Figure 38. Reactor power and mean neutron generation time during the transient

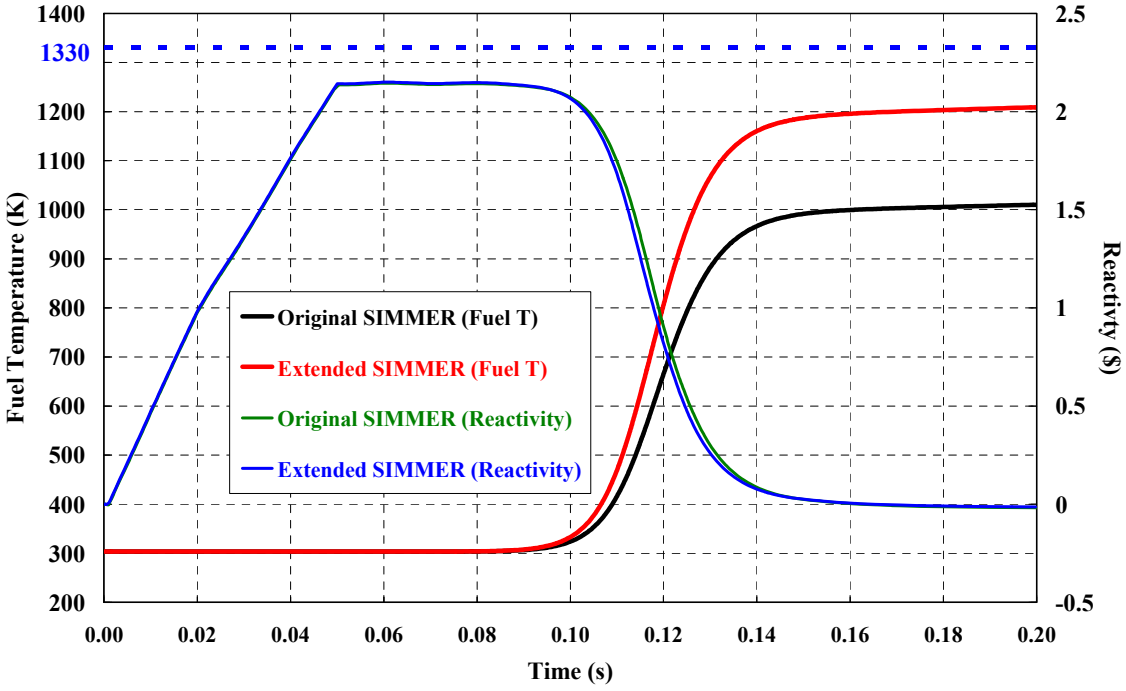

Figure 39. Fuel temperature at the reactor centre and reactivity during the transient

When the power increases by a factor of about 10^4 between 50 ms and 100 ms, Figure 39 show significant changes in fuel temperature at the reactor centre and concerning feedback effects begin around 110 ms.

The results in Figure 39 also provide additional support for the significant improvement of the new modified SIMMER approach in safety analyses. In fact, the fuel temperature at the reactor centre remains below the melting point (dashed blue line) for this transient (see Figure 40). If a larger reactivity (2.6 $) is introduced, the extended SIMMER code predicts that the fuel will melt at 106 ms (blue line), while no fuel melting is predicted if the original SIMMER version (green line) is employed.

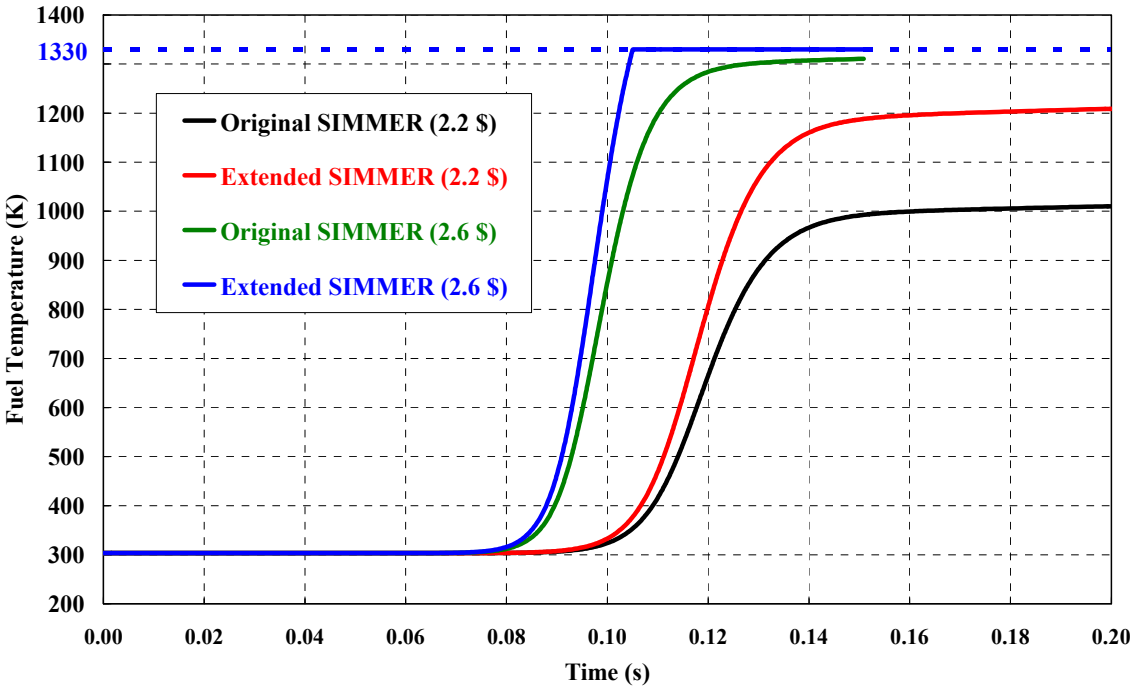

Figure 40. Fuel temperature at the reactor centre from the extended and the original SIMMER code in the transients induced by 2.2 $ and 2.6 $ insertion

4.2 Investigation of the SPERT-I D-12/25 core

The BORAX accident has been historically taken for evaluation of energetic release for the design of the French water-cooled research reactors using Aluminium plate-type fuel [12, 22]. According to the French Security Authority (IRSN), both BORAX-I [8] and

SPERT-I destructive tests [10, 65], as well as the SL-I accident [66], do not show restrictive phenomena on the thermal energy release, which is mainly dependent on the reactivity insertion and on the core features [12, 13]. Therefore, in the frame of the safety design of the JHR, IRSN proposed a different approach based on the study of scenarios representative of large reactivity insertion sequences using the SIMMER code. With this aim, the IRSN launched a research program in collaboration with KIT to simulate some selected transients in the SPERT-I D-12/25 configuration.

A neutronics model for extended SIMMER version for the SPERT-I D-12/25 configuration has been assessed in this work to provide a valid basis to define the SIMMER model for application to SPERT analysis [13, 67, 68].

The experimental data provide uncertainties for some parameters, such as composition of the control rods, positions of both the neutron flux detectors and the thermocouples, and the procedures used for the evaluation of the kinetic parameters, particularly the reduced prompt neutron generation time (Λ/β_{eff}). On the other hand, simulation results also include approximations associated with the neutronic and thermal-hydraulics models.

As different neutronic modelling schemes can appreciably influence the transient simulations, the extended SIMMER model for SPERT-I D-12/25 core has been assessed by benchmarking its performance against both experimental results and calculations using the ERANOS deterministic code and the MCNP code. The focus was given in the evaluation of the criticality, the neutron flux spatial distribution, and the kinetic parameters, namely, Λ and Λ/β_{eff} [69, 70].

4.2.1 Description of the SPERT-I D-12/25 core

The SPERT-I D-12/25 core configuration [10] was an arrangement of 5 x 5 assemblies with 4 symmetrically placed control rod assemblies (CR), one central transient rod (TR), and 20 standard fuel-assemblies loaded in a cylindrical carbon steel vessel 304.8 cm in diameter and 487.68 cm heigh (see Figure 41). The water level in the reactor vessel was 137.2 cm above the top of the fuel plates. There was no forced coolant circulation through the core.

Each standard fuel sub-assembly contain 12 aluminium-clad (Al 6061) fuel plates in a square aluminium box loaded with a highly enriched U-Al alloy (93.17 wt% U^{235}). The dimensions of each fuel plate at room temperature were 0.15 x 6.8 x 63.8 cm^3, and the active component dimensions were 0.05 x 6.23 x 60.96 cm^3 (see Figure 42). The core was loaded with a total of 270 fuel plates, each containing an average of 13.9 g of U^{235}.

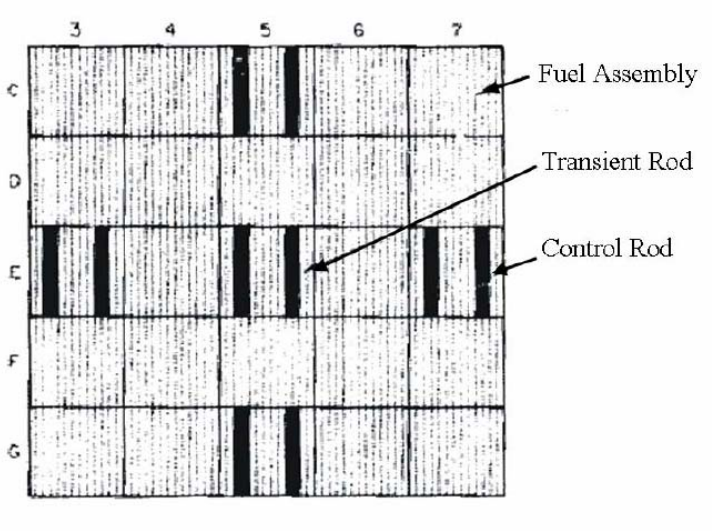

Figure 41. SPERT-I D-12/25 core cross section [10]

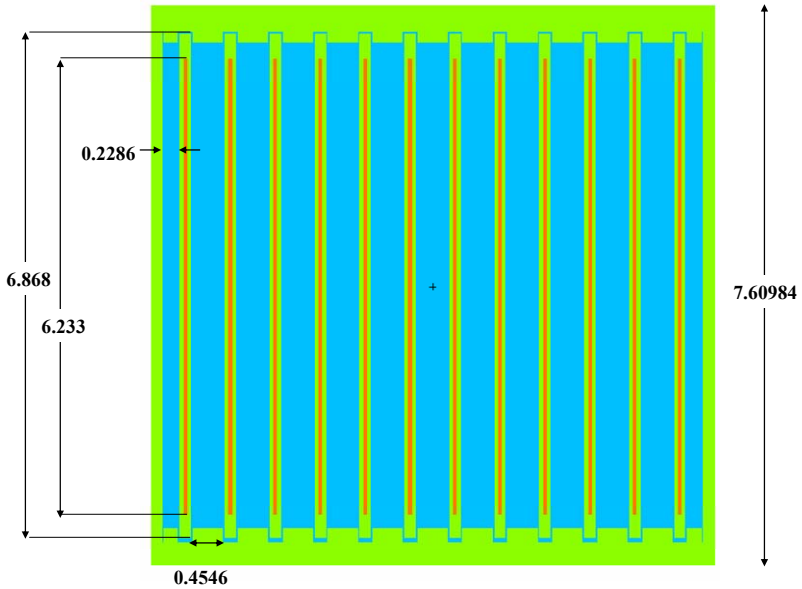

Figure 42. Standard fuel sub-assembly layout [10]

Each control rod sub-assembly was loaded with 6 fuel plates and a pair of control blades with aluminium followers to provide the reactor control (see Figure 43).

The poison material was borated aluminium (BINAL) with a 7 wt% natural boron-aluminium alloy. As no data were found for the SPERT-I configuration under investigation, the poison composition that has been taken into account is the same as in Reference 71.

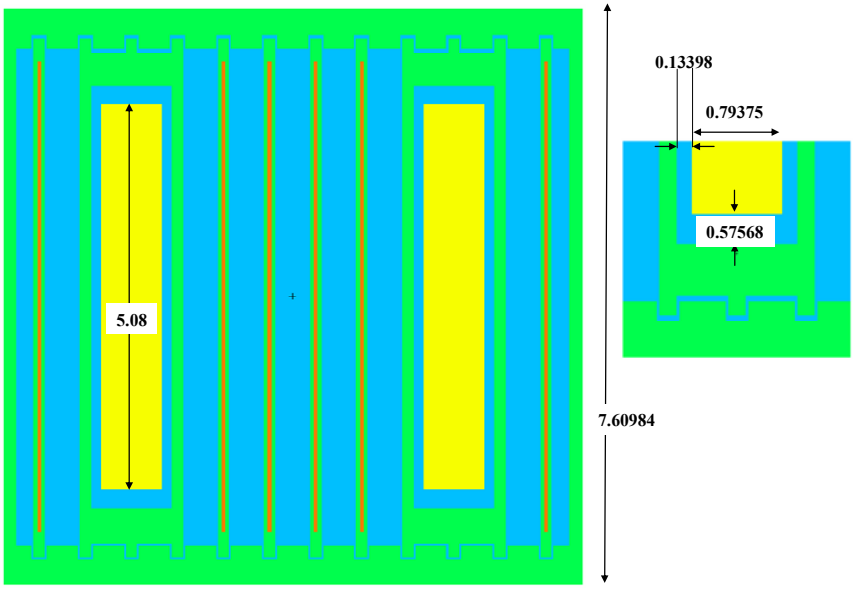

Figure 43. Absorber sub-assembly layout [10]

The central "transient" rod was used to initiate the transients and sudden power rises that this reactor was built to study [10]. In its resting position, the absorbing portion of the rod was below the reactor core. When a transient was to be induced, the four control rods were adjusted to make the reactor just critical, at a power of about 200 W. The central rod was lifted so that its neutron-absorbing portion was brought into the reactor core, making the reactor subcritical. The four control rods were then further withdrawn a particular distance so that a transient with the desired amount of supercriticality would take place. Meanwhile, the reactor power had been decreasing. When it reached a level of a few watts, the central rod was suddenly ejected (travel time varied between 80 and 120 msec), the reactor became supercritical, and the transient occurred. Power rose tremendously and very fast, for example, from initial 2 W to 510 MW in 0.75 s [10]. Excess reactivity additions produced self-limiting power bursts with peaks of up to 1300 MW. During the transient, the steam, generated by the heated fuel plates, ejected moderating water so that the nuclear chain reaction was stopped in another fraction of a second.

4.2.2 Assessment of the reference and SIMMER models

To assess the 2D SIMMER neutronics model, the ECCO/ERANOS and MCNP codes using the JEF 2.2 evaluated nuclear data have been employed as reference models [56].
The ECCO/ERANOS calculations have been performed invoking the TGV/VARIANT [63] and BISTRO [64] codes, for the 3D and 2D models respectively, for which homogeneous equivalent XSs for the fuel sub-assembly have been used (see Figure 42). The XSs for the absorber media and for the fuel in the absorber sub-assemblies have been processed using the fine sub-assembly model of ECCO (see Figure 43).
3D (see Figure 44) and 2D (see Figure 44) MCNP and ERANOS neutronics models for the SPERT-I D-12/25 core have been assessed at room temperature for an experimental critical configuration with the control rods withdrawn 23.37 cm (9.2") and the transient rod out [10]. Considering the 2D model (see Figure 45) will be employed for the SIMMER safety analyses of SPERT, the constraints imposed by thermal-hydraulics have been taken into account. Therefore, fuel volume and fuel mass have been preserved. In the 2D model, absorber media have been modelled by means of 3 rings (see Figure 45, grey regions). Homogenized fuel media in the absorber sub-assembly are indicated with orange in Figure 45.

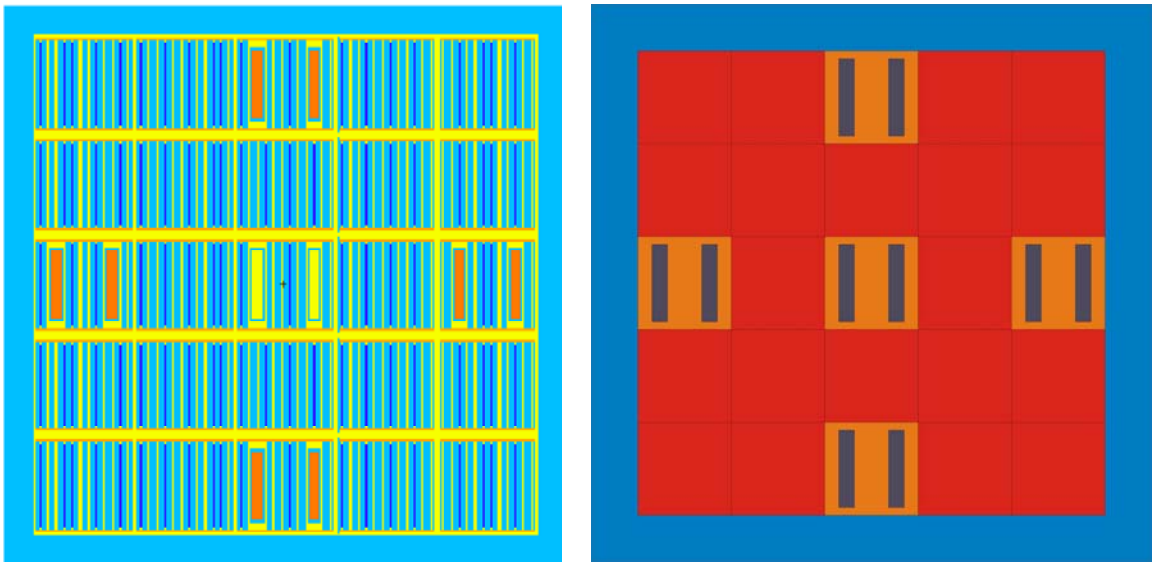

a) **b)**

Figure 44. MCNP (a) and ERANOS (b) 3D neutronics models for SPERT-I D-12/25 core in the experimental critical configuration. Cross-section at half height.

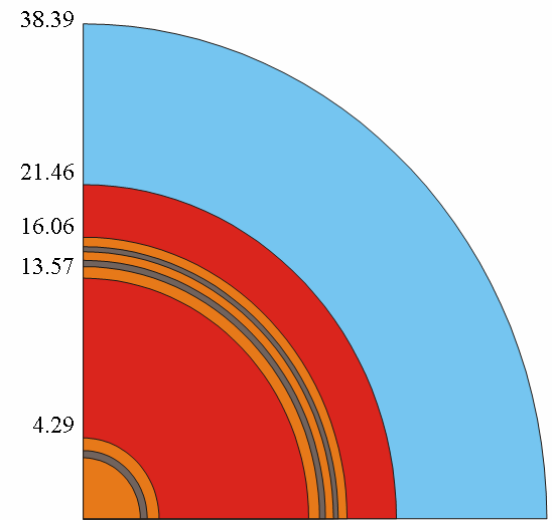

Figure 45. 2D neutronics model for SPERT-I D-12/25 core. Radii in cm of each region are shown

The new method for heterogeneity treatment has been employed for SIMMER calculations in the 2D model. For these calculations, the 40-energy-groups XS library generated by C^4P code and data system [27] was used. The EMCLs, coolant-to-fuel, and clad-to-fuel flux ratios (see Figure 46) have been calculated for the fuel sub-assembly by means of ECCO.

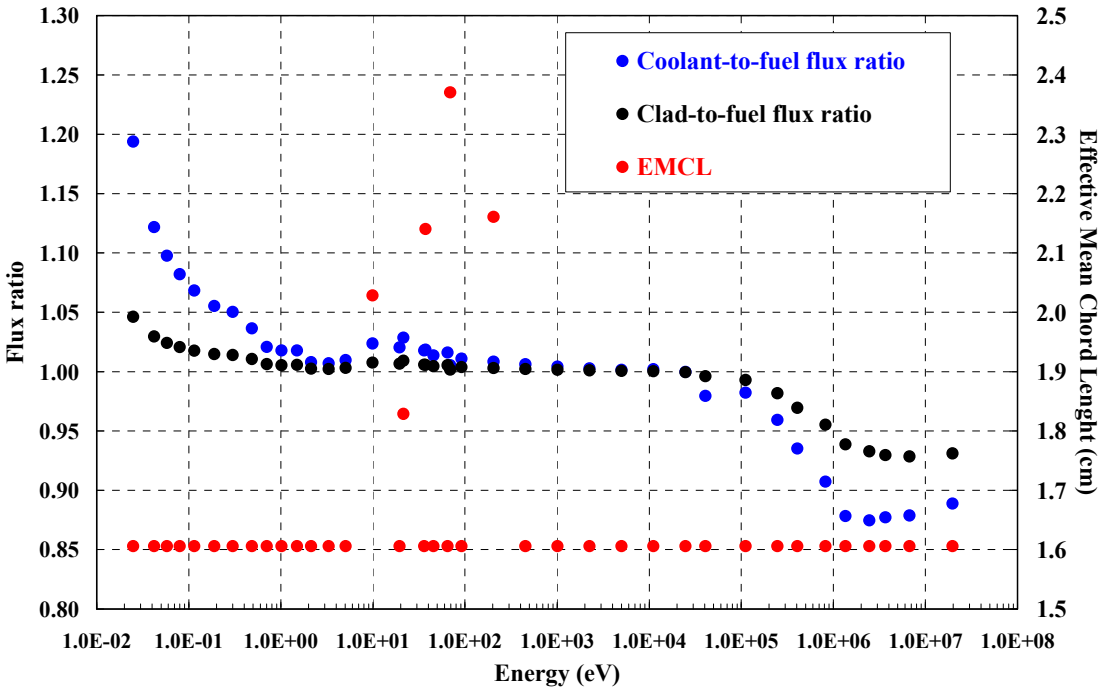

Figure 46. 40-energy-groups pre-calculated parameters for heterogeneity treatment in the SIMMER code for the SPERT-I D-12/25 core analysis

The heterogeneity parameters have been evaluated at room temperature and at zero void coolant conditions. The same set of parameters has been used in each fuel region in the core.

There was no need for the evaluation of heterogeneity parameters for absorber sub-assemblies because a fine description of absorber media has been employed in the 2D model. Nevertheless, a finer heterogeneity treatment should be used when evaluating the heterogeneity parameters for the homogenized fuel in the absorber sub-assemblies. A refined technique for the study of the heterogeneity treatment in absorber sub-assemblies is currently under investigation.

4.2.3 Criticality, neutron flux distribution, and control rod worth

The extended SIMMER model shows good agreement with both the experimental data and the MCNP and ERANOS codes for the criticality level (Table 15).

Model	MCNP	ERANOS	SIMMER
3D	1.00185 ± 0.00078	1.00104	-
2D	0.99881 ± 0.00055	1.00172	1.00026

Table 15. k_{eff} computed by MCNP, ERANOS and SIMMER extended model

The neutron flux spatial distribution has been evaluated and compared to the experimental results. The experimental steady-state flux distribution was determined from activation of Co^{29} wire detectors [10] at different locations in the core (bullets in Figure 47). The total uncertainty in the experimental data is about 20%: 15% due to the detector position and 6% due to the counting error [10].

Uncertainties in calculated results are mainly related to the assessed geometrical model. In fact, when comparing measured and calculated neutron flux traverses, it is necessary to have in mind that the internal structure of the absorber rods is not taken into account in the 2D and 3D ERANOS models.

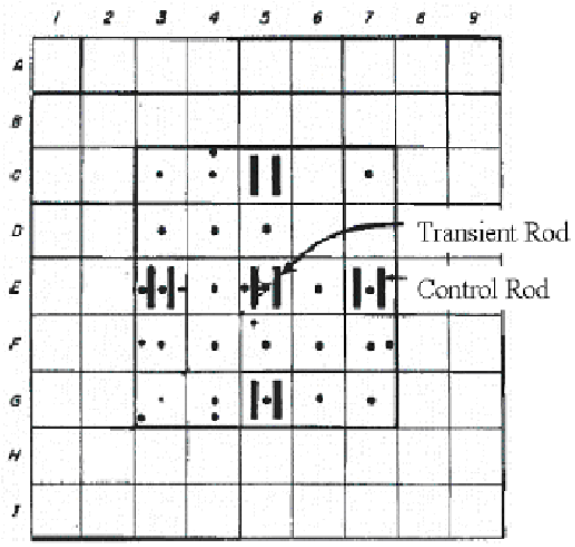

Figure 47. Location of the Co^{29} wire detectors [10]

The results in Figure 48 show good agreement between experiments and 3D and 2D calculations for the axial neutron flux distribution at the centre of the sub-assembly in the position E5. In fact, calculated results lie within the experimental uncertainty range. 3D and 2D models show a maximum deviation of about 8% and SIMMER results agree well with the 2D reference models.

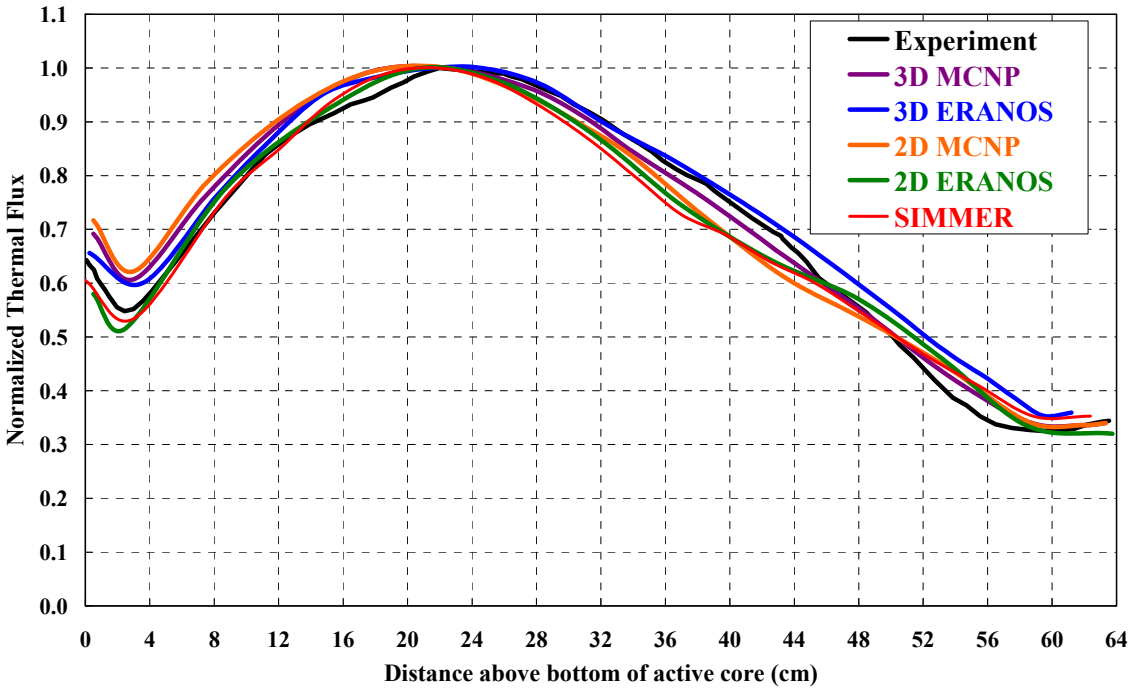

Figure 48. Normalized axial neutron flux profile in the detector position E5

Calculated results have been benchmarked against experimental data with respect to the detector data in the radial traverse E3-E5 (see Figure 47) at 20.32 cm and 30.48 cm above the core bottom. Results are shown in Figure 49 and Figure 50, respectively.

The 3D reference results are in reasonably agreement with the experimental data, while 2D models agree reasonably well with the experimental results up to 15.2 cm from the core centre. At 20.32 cm above the core bottom the follower contains aluminium.

The 2D results (see Figure 49) show a discrepancy of about 20% compared to the 3D models and the experimental data at the core periphery due to the neutron reflection of the water in the pool.

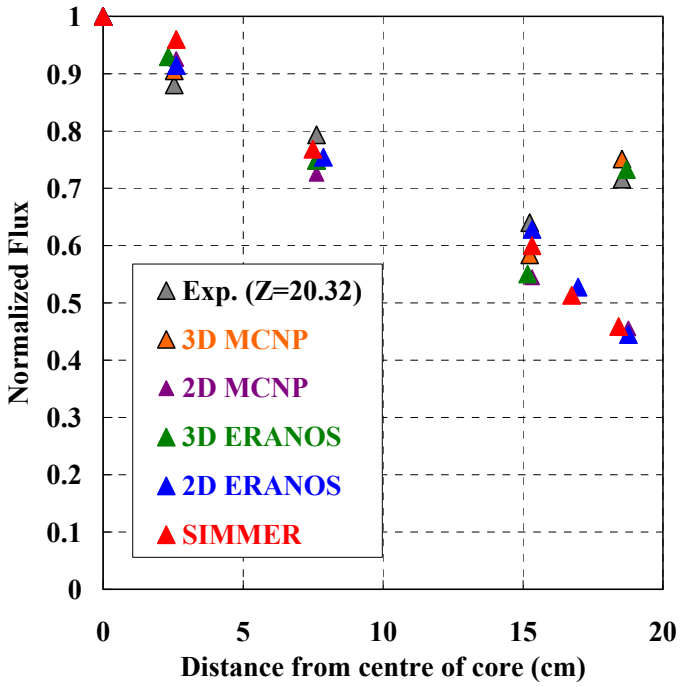

Figure 49. Normalized radial neutron flux profile in the direction E3-E5 at 20.32 cm above the core bottom

Such an effect is not evident at 30.48 cm above the core bottom (see Figure 50) at that position because the follower is replaced by the absorber, whose effect dominates the neutron flux shape.

The different performance between the 3D and 2D models in Figure 49 is expected as it is an intrinsic effect of the geometrical models. In fact, the 3D and 2D models exhibit different neutron leakage from the core [55], which is a direct consequence of having assumed the same volume and fuel mass in the 3D and 2D models. The effect of

geometry is clearly evident when we compare the control rod worth computed by the 3D and 2D models (see Figure 51).

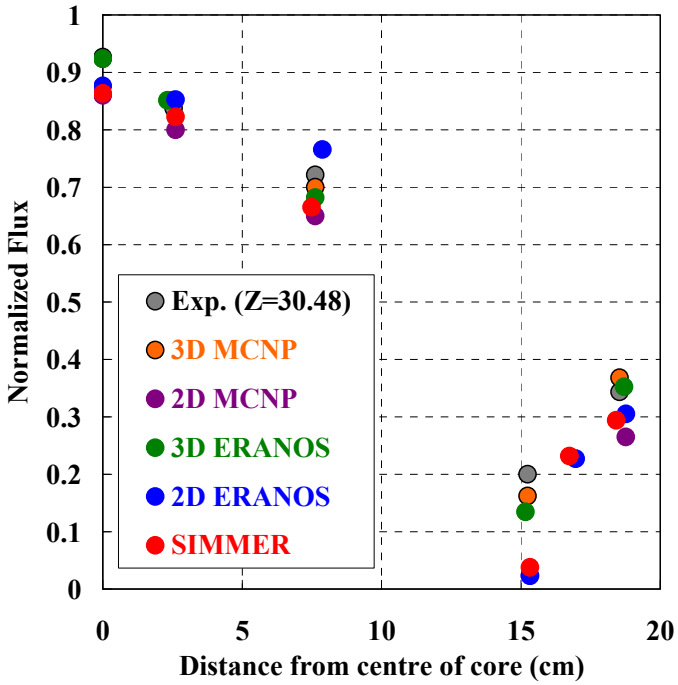

Figure 50. Normalized radial neutron flux profile in the direction E3-E5 at 30.48 cm above the core bottom

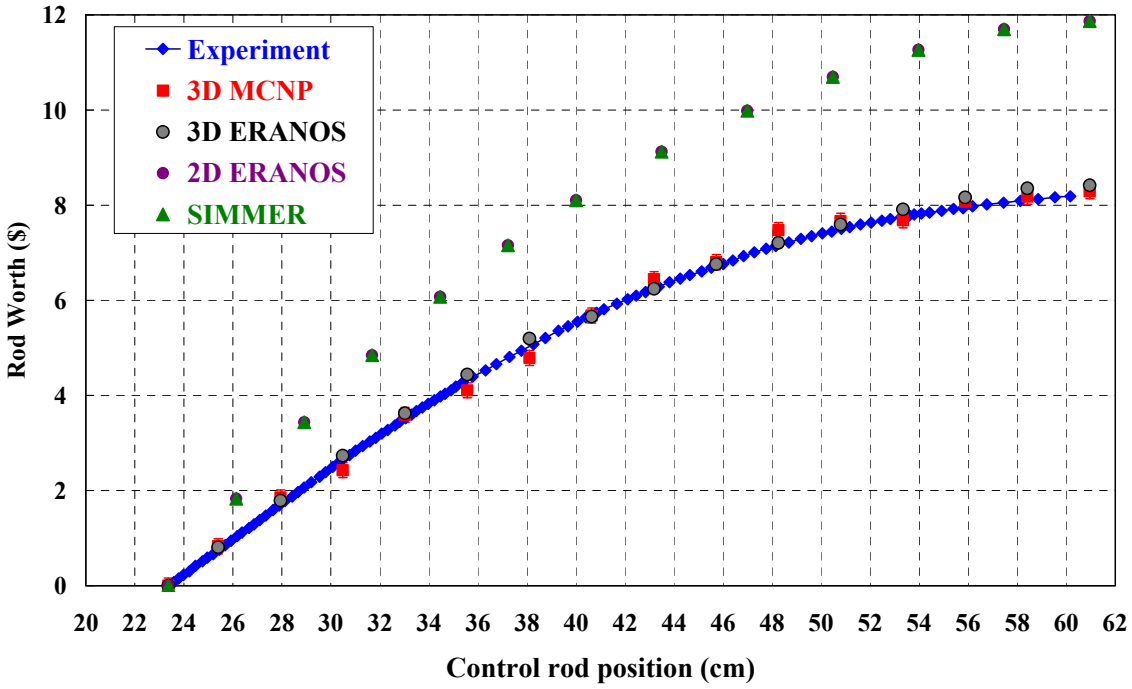

Figure 51. Comparison between the calculated and experimental control rod worth

The results in Figure 51 show a reasonably good agreement between the SIMMER code and the 2D MCNP and ERANOS calculations. On the contrary, a discrepancy of up to 30 % is observed with respect to the 3D models due to the effect of geometry when the control rod bank is completely withdrawn.

Nevertheless the main findings of this study indicate that there is a reasonable agreement between the 3D models and the experimental results and, again, a good agreement between the performance of the 2D ERANOS and SIMMER models [69, 70].

4.2.4 Effect of heterogeneity on criticality and coolant void effect

The effect of heterogeneity on the criticality and coolant void has been evaluated. Fuel Doppler was not considered in these investigations because it is negligible in this system, as the fuel is highly enriched.

Criticality calculations have been performed using the SIMMER model employing the original XS processing scheme, and for the 2D ERANOS model, using the homogeneous effective neutron XSs (these results are labelled as 'Homogen' in Table 16).

The results in Table 16 show that the effect of heterogeneity on k_{eff} is quite large, about 4.4 % and 3.3 % in reactivity in 2D SIMMER and ERANOS, respectively.

The important result from Table 16 is that the extension of the heterogeneity treatment allows SIMMER to recover a larger reactivity effect and the results are closer to those of ERANOS, as observed for the other applications presented in this work.

	k_{eff} (Heterogen.)	**k_{eff} (Homogen.)**	**Δρ (pcm)**
2D ERANOS	1.00172	1.03602	+3305
SIMMER	1.00026	1.04662	+4428

Table 16. Effect of heterogeneity evaluated by ERANOS and SIMMER

The 2D models have been benchmarked against the coolant void (see Figure 52). The results show a reasonable agreement when up to 30% of coolant is removed. ERANOS and MCNP results well agree when the coolant density is reduced of 50%.

The extended SIMMER version with heterogeneity parameters evaluated at zero coolant void condition provides better agreement with the reference results than the original SIMMER version. Nevertheless, a discrepancy of about 3% in reactivity remains when 50% of coolant is removed. The use of void-dependent heterogeneity parameters may further improve the performance of the extended SIMMER model.

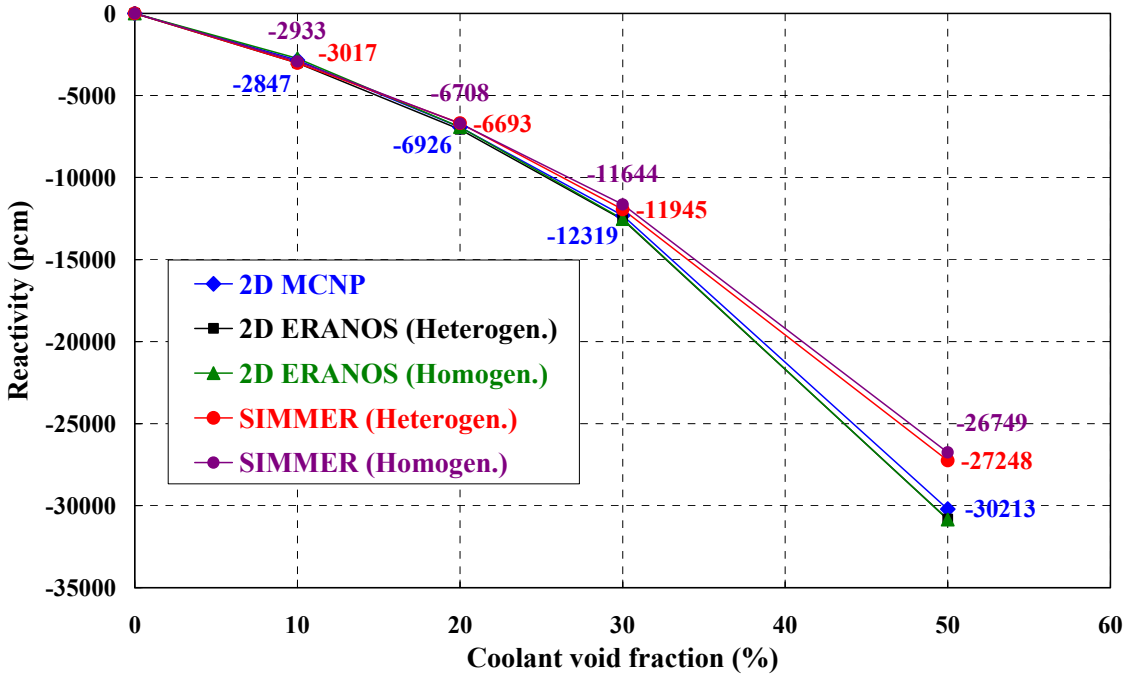

Figure 52. Reactivity effect due to the coolant void computed by the 2D neutronics models for the SPERT core

4.2.5 Evaluation of kinetic parameters

When assessing the extended SIMMER model for transient analyses in the SPERT-I reactor, the main kinetic parameters have been benchmarked against the experimental data and the ERANOS [46], MCNP [35], and KIN3D [74] codes. KIN3D is an extension for the VARIANT code, linked to ECCO/ERANOS, that permits spatial kinetics and perturbation calculations in 3D models, while employing a neutron transport model.

The prompt neutron generation time (Λ) and the effective delayed neutron fraction (β_{eff}) have been computed and the corresponding reduced prompt neutron generation time (Λ/β_{eff}) has been compared with two independent experimental evaluations [10, 72].

Deterministic codes (SIMMER, ERANOS, and KIN3D) can employ the classical formulae derived from nuclear reactor theory [49, 73] for the effective delayed neutron fraction and the prompt neutron generation time. This involves the use of the adjoint neutron flux, ϕ^+, as a weighting function, to improve its effectiveness. The codes may also use a constant value as weighting function. In this case, a so called non-effective delayed neutron fraction, $\bar{\beta}$, is evaluated.

The original MCNP code and calculation options cannot evaluate the adjoint neutron flux. Although some techniques allow adjoint calculations to be performed by means of MCNP [75], the original MCNP code has been employed in this study under the assumption that it is sufficient for the scope and aim of this investigation.

The non-effective Λ is evaluated in MCNP using the removal neutron lifetime [35]. This quantity is computed by default by the code and is associated with the definition of the prompt neutron lifetime ℓ [76, 77]. As a result, Λ can be calculated using the classical formula $k_{eff} = \ell / \Lambda$ [73].

The extended SIMMER, ERANOS, KIN3D, and MCNP results are shown in Table 17 [69, 70] and compared with two independent experimental evaluations of the reduced prompt neutron generation time Λ/β: one for the SPERT-I D-12/25 core [10] and one for SPERT-IV D-12/25 [72].

To determine the uncertainties in the SIMMER modelling, which minimize the discrepancy compared to the experiment, different neutronics options have been used and their influence on the results has been investigated. In order to compare the results of deterministic codes with MCNP, the kinetic parameters have been calculated by using both the adjoint fluxes (labelled as ϕ^+ in Table 17) and a constant function (labelled as 'flat' in Table 17) as weighting functions. Thus, both effective, β_{eff}, and non-effective, $\bar{\beta}$, delayed neutron fractions have been evaluated.

In addition to the 40-energy-group structure, ERANOS calculations have been performed using averaged XSs computed for 172 and 294 energy group structures to analyze the effect of the group structure on the results. These structures were obtained by the 40-energy-group structure by increasing the number of energy groups in the thermal part of the neutron spectrum.

Source	k_{eff}	Λ (μsec)	$\bar{\beta}$ or β_{eff} (pcm)	Λ/β (msec)
Experiment [10]				8.1 ± 0.17
Experiment [72]				7.93 ± 0.12
KIN3D@40g (ϕ^+)	1.00104	58.68	782	7.51
KIN3D@40g (flat)	1.00104	89.49	658	13.62
2D ERANOS@40g (ϕ^+)	1.00172	57.94	768	7.54
2D ERANOS@40g (flat)	1.00172	87.14	658	13.45
MCNP 3D (flat)	1.00185 ± 0.00078	96.71	658	14.88
MCNP 2D (flat)	0.99881 ± 0.00055	90.20	658	13.72
SIMMER@40g (ϕ^+)	1.00026	57.31	786	7.29
SIMMER@40g (flat)	1.00026	92.28	657	14.04
2D ERANOS@172g (ϕ^+)	1.00221	58.08	765	7.59
2D ERANOS@294g (ϕ^+)	1.00012	58.37	765	7.65

Table 17. Comparison among the experimental [69, 70] and calculated kinetic parameters

The results from SIMMER, 3D/2D MCNP, 2D ERANOS, and KIN3D provide a coherent picture, which can be summarized as follows:

- the reduced prompt neutron generation time evaluated by the extended SIMMER code, using the adjoint weighting function, shows a discrepancy of about 3% compared to KIN3D and ERANOS;
- the extended SIMMER results with a constant weighting function show a discrepancy of about 5% and 2% compared to 3D and 2D MCNP results, respectively;
- a consistent difference between adjoint and flat weighting is found for all of the applied codes.

An important result from Table 17 is that there is a reasonable deviation (about 8%) between the extended SIMMER results and the experimental data for the reduced prompt neutron generation time.

ERANOS results with 172 and 294 energy groups show that this deviation can be decreased by a factor of two using a multi-group XS library with larger number of energy groups than employed in SIMMER.

The original SIMMER model has been used to analyse some experimental transients in the SPERT-I D-12/25 configuration [68]. Simulation results showed a reasonable agreement with experiment, but adjustment of kinetic parameters was needed in the original SIMMER model to fit the experimental Λ/β. Therefore the results obtained by using the new technique (Table 17) provide the justification of the adjustments.

4.2.6 Effect of heterogeneity on the kinetic parameters

The values of the kinetic parameters computed by the SIMMER code vary depending on whether or not heterogeneity effects are taken into account in the XSs processing. In fact, the neutron flux distribution (direct and adjoint) is different depending on the XSs processing scheme employed.

The performance of the new method for heterogeneity treatment in the SIMMER code has been investigated by benchmarking the extended SIMMER code against the original SIMMER version and ERANOS.

With this aim, the kinetics parameters β_{eff} and Λ have been computed for 40-energy-groups by using the JEF2.2 reference nuclear data library. The results (Table 18) have been evaluated by means of the 2D ERANOS code, employing homogeneous effective neutron XSs (labelled as 'Homogen'), and by SIMMER using the original XSs processing scheme (labelled as 'Homogen'). The homogeneous results have been compared to the corresponding heterogeneous (labelled as 'Heterogen'), employing the homogeneous equivalent XSs (for 2D ERANOS) and the heterogeneity treatment extension for the SIMMER code. In each case both the adjoint neutron flux (ϕ^+) and a flat flux have been employed as weighting functions.

The results in Table 18 show that the heterogeneity treatment does have a marked impact on the accuracy of the computation of the reduced prompt neutron generation time when compared to the experimental data. If homogeneous models are employed, the calculated Λ/β values show large discrepancies compared to the experimental data (8.1 ± 0.17 msec [10] and 7.93 ± 0.12 msec [72]).

Source	k_{eff}	Λ (μsec)	$\bar{\beta}$ or β_{eff} (pcm)	Λ/β (msec)
2D ERANOS (ϕ^+) (Heterogen)	1.00172	57.94	768	7.54
2D ERANOS (flat) (Heterogen)	1.00172	87.14	658	13.45
2D ERANOS (ϕ^+) (Homogen)	1.03602	52.20	766	6.81
2D ERANOS (flat) (Homogen)	1.03602	80.92	648	12.49
SIMMER (ϕ^+) (Heterogen)	1.00026	57.31	786	7.29
SIMMER (flat) (Heterogen)	1.00026	92.28	657	14.04
SIMMER (ϕ^+) (Homogen)	1.04662	52.81	770	6.86
SIMMER (flat) (Homogen)	1.04662	86.78	657	13.2

Table 18. Comparison of the kinetic parameters computed by the SIMMER and ERANOS codes using the heterogeneous and homogeneous models [69, 70]

Table 18 shows that the SIMMER homogeneous results for Λ/β are in reasonable agreement with the results from the corresponding ERANOS model, with a maximum difference of about 5% when a flat neutron flux is used as weighting function. Nevertheless, when the adjoint flux is used as weighting function, the results from the original SIMMER code show a large discrepancy with respect to the two available experimental data (about 15% and 13 %, respectively) and the reference heterogeneous ERANOS (about 9%).

The important result from Table 18 is that the new method for the heterogeneity treatment allows the SIMMER code to reduce the previously observed disagreement with the experimental values (about 10% and 8%, respectively) and with the reference ERANOS (about 3%).

CONCLUSIONS

A multinational effort is ongoing to renew the European park of Material Test Reactors in order to satisfy the needs for the development of commercial reactors in the next century. With this aim, the Jules Horowitz project [4, 5] has been launched as a new Material Test Reactor (MTR) in Europe to be operative in 2014 in Cadarache (France).

Concerning the safety design, advanced analyses tools are necessary for assessing the reactor behaviour in normal operation as well as during postulated transients or hypothetical accidents. In this context, the capability of the SIMMER multi-physics code systems to cover, in a mechanistic manner, accident scenarios from normal operation conditions up to core disruption represents an important tool. The SIMMER code systems were originally developed for safety analyses of fast metal-cooled reactors, so that their application to safety analyses of thermal reactors requires some extensions particularly in the neutronics model.

The objective of this work is the development of a methodology to take account of the heterogeneity effects in the original SIMMER cross-section processing scheme in order to accurately evaluate the reactivity feedbacks and the kinetic parameters during a transient. The technique takes account properly of the resonance self-shielding effects and the intra-cell neutron flux distribution in space, by employing pre-calculated parameters computed by a reference cell code. The aim is to build tables of pre-calculated parameters with values representing one or more relevant reactor states, e.g. with different coolant density, for use in neutronics/thermal hydraulics-coupled calculations. In this work, the ECCO code has been employed as it shows a high level of accuracy when benchmarked against reference Monte Carlo code MCNP.

This technique improves the original treatment of the resonance self-shielding effect based on the Bondarenko formalism (f-factor) by introducing an escape term in the background cross-section evaluation, which depends on pre-calculated energy dependent parameters (effective mean chord lengths, EMCLs). The effect of the extension is particularly significant for reactors with a relevant contribution of neutrons in the thermal and epithermal energy range, and, as expected, becomes less significant for fast reactors.

Pre-calculated EMCLs describe the effect of resonances of uranium cross-sections better than the classical method employed for fast reactors, based on the mean chord length evaluation. Consequently, the background cross-section σ_0 in the original SIMMER model, which employs infinitely-diluted cross-sections without adjustment, differs from the extended SIMMER model by a factor of about 2, when the pre-calculated parameters (EMCL and neutron flux-ratios) are used. In particular, the σ_0 evaluated using the new technique is lower than in the homogeneous model, leading to lower resonance absorption.

The effect of the spatial distribution of the neutron flux in the fuel, clad, and water has been taken into account by modifying the macroscopic cross-section processing for these components. Pre-calculated non-unity factors, clad-to-fuel and water-to-fuel neutron flux ratios, are applied to the macroscopic cross-sections of the clad and moderator regions, respectively.

The technique has been implemented in the SIMMER code and for validation investigations have been conducted for two systems: a Material Test Reactor fuel sub-assembly and a typical PWR fuel sub-assembly. Moreover, the new technique has been applied to a low enriched Material Test Reactor core model and to the assessment of a neutronics model for the SPERT-I D-12/25 core. The results have been benchmarked against the ECCO/ERANOS and MCNP neutronics reference codes. These investigations point out very important issues in view of transients analyses:

1) the fuel Doppler and the moderator void reactivity effects computed by means of the extended SIMMER code are in good agreement with the ECCO/ERANOS and MCNP reference codes;
2) SIMMER results also show that, if the extended model for heterogeneity treatment is not employed, larger discrepancies arise in the fuel Doppler effect due to the fact that the resonance absorption is overestimated;
3) the pre-calculated parameters show a weak sensitivity to the moderator void fraction and a very weak sensitivity to the moderator and fuel temperatures. Consequently, a relatively simple interpolation scheme could be employed during transient simulations;
4) the technique is also potentially applicable to fast systems.

The performance of the new technique and of the original SIMMER model have been benchmarked in a transient induced by 2.2 $ reactivity insertion in 0.05 s in the Material Test Reactor core model. The results clearly showed that the original SIMMER version is not conservative. In particular, the new technique provides peak power and energy release values of about 30% higher than the original SIMMER model. Results clearly indicate a significant effect of the new method on the evaluation of reactivity feedbacks and kinetic parameters during the transient.

Concerning the investigations for the SPERT-I D-12/25 core configuration, results from the extended SIMMER neutronics model show the capability of the code to describe the SPERT-I core reasonably at near steady-state conditions. In fact:

1) SIMMER results agree with reference codes and with experimental data for both the criticality level and the coolant void effect;
2) experimental neutron flux distributions are reasonably reproduced by SIMMER;
3) kinetics parameters evaluated by SIMMER, mean neutron generation time (Λ), and reduced prompt neutron generation time (Λ/β_{eff}) show an acceptable deviation of about 8% with respect to the available experimental values.

The results of the investigations in the Material Test Reactor core model and SPERT-I D-12/25 core clearly show that the extensions of the SIMMER neutronics model provide a decisive improvement of the neutronics performance of the code compared to the conventional neutron transport codes which usually use homogenized multigroup cross-sections without heterogeneity treatment. This important conclusion is valid at near steady-state conditions for which the pre-calculated parameters for heterogeneity treatment have been evaluated. Therefore, this work represents an important basis for the application of SIMMER to future safety analyses in advanced water-cooled reactors.

REFERENCES

1. http://www.gen-4.org/
2. http://www.iaea.org/INPRO/
3. C. Vitanza, D. Iracane, D. Parrat, Future needs for material test reactors in Europe (FEUNMARR Findings), 7th Int. Topical Meeting on Research Reactor Fuel Management, Aix-en-Provence, France (2003).
4. D. Iracane, The JHR, A New Material Testing Reactor in Europe, *Nucl. Eng. and Tech.*, **38** (2005).
5. D. Iracane, P. Chaix, A. Alamo, Jules Horowitz Reactor: a high performance material testing reactor, C. R. Physique, **9** (2008).
6. P. Trémodeux et al., Jules Horowitz Reactor: General layout, main design options resulting from safety options, technical performances and operating constraints, Proc. TRTR-IGORR10, Gaithersburg, Maryland, USA (2005).
7. J. E. Matos, Foreign Research Reactors Irradiated Nuclear Fuel Inventories Containing HEU and LEU of United States Origin, ANL/RERTR/TM-22, Argonne, USA (1994).
8. J. R. Dietrich, Experimental Investigation of the Self-Limitation of Power During Reactivity Transients in a Subcooled, Water-Moderated Reactor, Borax-I Experiments, 1954, AECD-3688 (1955).
9. J. R. Dietrich, D. C. Layman, Transients and Steady State Characteristics of a Boiling Reactor, The Borax Experiments, 1953, AECD-3840 (1954).
10. R. W. Miller, A. Sola, R. K. McCardell, Report of SPERT-I Destructive Test Program on Aluminum, Plate-Type, Water-Moderated Reactor, Phillips Petroleum Company, IDO-16883 (1964).
11. J. C. Jr. Haire, A Summary Description of the SPERT Experimental Program, *Nuclear Safety Journal*, **3**, pp. 15-23 (1961).
12. G. Biaut, T. Burgois, G. B. Bruna, Reevaluation of BDBA Consequences Of Research Reactors, Proc. TOPSAFE 2008, Dubrovnik, Croatia, September 30-October 3 (2008).

13. S. Pignet, C. Pelissou, R. Meignen, P. Liu, F. Gabrielli, Severe reactivity injection accident simulations for safety assessment of research reactor, Proc. of. the 13th Int. Topical Meeting on Research Reactor Fuel Management (RRFM 2009), Vienna, Austria, March 22-25 (2009).
14. RELAP 4 and 5, A Computer Program for Transient Thermal-Hydraulic Analysis of Nuclear Reactors and Related Systems, ANC-NUREG 1355, U.S. Nuclear Regulatory Commission (1976).
15. K. V. Moore et al., RETRAN A Program for One Dimensional Transient Analysis of Complex Fluid Flow Systems, EPRI CCM-5, Vols. 1-4, Electric Power Research Institute (1978).
16. S. G. Forbes, F. L. Bentzen, P. French, J. E. Grund, J. C. Haire, W. E. Nyer, R. F. Walker, Analysis of Self-Shutdown Behavior in the SPERT I Reactor, IDO-16528, Idaho National Engineering Laboratory (1959).
17. W. J. Turner, calculation of SPERT Transients, *J. Nucl. Energy*, 22, 397 (1968).
18. B. E. Clancy, J. W. Connolly, B. V. Harrington, An Analysis of Power Transients observed in SPERT-I Reactors, Australian Atomic Energy Commission, AAEC/E383 (1976).
19. A. Mohamed Gaheen, S. Elaraby, M. Naguib Aly, M. S. Nagy, Simulation and analysis of IAEA benchmark transients, *Prog. Nucl. Energy*, **49** (2007).
20. W. L. Woodruff, A Kinetics and Thermal Hydraulics Capability for the Analysis of Research Reactor, *Nuclear Technology*, **64**, pp. 196-206 (1984).
21. R. Meignen, Status of the Qualification Program of the Multiphase Flow Code MC3D, Proc. of ICAPP'05, Seoul, Korea, May 15-19 (2005).
22. B. Maugard et al., The BORAX Accident in the JHR, TOPSAFE 2008, Dubrovnik, Croatia, September 30 – October 3 (2008).
23. W. R. Bohl, L. B. Luck, SIMMER-II: A Computer Program for LMFBR Disrupted Core Analysis, Los Alamos National Lab., LA-11415-MS (June 1990).
24. Sa. Kondo, Y. Tobita, K. Shirakawa, SIMMER-III: An advanced computer program for LMFBR severe accident analysis, Proc. of Int. Conf. on Design and Safety of Advanced Nuclear Power Plant, Tokyo, Japan (1992).

25. H. Yamano, S. Fujita, Y. Tobita, K. Kamiyama, et al., SIMMER-IV: A Three-Dimensional Computer Program for LMFR Core Disruptive Accident Analysis, Japan Nuclear Cycle Development Institute, JNC TN9400 2003-070 (2003).
26. Y. Tobita, Sa. Kondo, et al., The Development of SIMMER-III, An advanced computer program for LMFBR severe accident analysis, and its Application to Sodium Experiments, *Nuclear Technology*, **153**, pp. 245-255 (2006).
27. A. Rineiski, V. Sinitsa, W. Maschek, C^4P, a Multigroup Nuclear CCCC Data Processing System for Reactor Safety and Scenario Studies, Proc. of Jahrestagung Kerntechnik, Nuremberg, Germany, May 10-12 (2005).
28. R. D. O'Dell, Standard Interface Files and Procedures for Reactor Physics Codes, Version IV, Los Alamos National Laboratory, LA-6941-MS (1977).
29. K. O. Ott, R. J. Neuhold, Nuclear Reactor Dynamics, ANS, La Grange Park, USA (1986).
30. G. Buckel, E. Hesselschwerdt, E. Kiefhaber, S. Kleinheins, W. Maschek, A New SIMMER-III Version with improved Neutronics Solution Algorithms, FZKA-6290, Karlsruhe, Germany (1999).
31. R. E. Alcouffe, R. S. Baker, F. W. Brinkley, D. R. Marr, R. D O'Dell, W. F. Walters, DANTSYS: A Diffusion Accelerated Neutral Particle Transport Code System, LA-12969-M, Los Alamos, NM, USA, (June 1995).
32. Y. Tobita, Sa. Kondo, et al., Space-time Kinetics Simulation of an Early Burst Phase of the Criticality Accident, International Workshop on the Safety of the Nuclear Fuel Cycle, Tokyo, Japan, May 29-31 (2000).
33. D. Wilhelm, G. Biaut, Y. Tobita, SIMMER Model of a Low-enriched Uranium Non-power Reactor, Nuclear Engineering and Design, **238**, pp. 41-48 (2008).
34. G. Biaut, J. Couturier, D. Wilhelm, P. Liu, Upgrading of the coupled neutronics-fluid dynamics code SIMMER to simulate the research reactors core disruptive RIA, Proceedings of the International Conference on the Physics of Reactors (PHYSOR 2008), on CD-ROM, Interlaken, Switzerland, September 14-19 (2008).
35. J. F. Briesmeister, MCNP4C – A General Monte Carlo Code N-Particle Transport Code, Los Alamos National Lab., LA-13709-M (2000).
36. I. I. Bondarenko, Group Constants for Nuclear Reactor Calculations, Consultants

37. A. E. Waltar, A. B. Reynolds, Fast Breeder Reactors, Pergamon Press, New York (1981).
38. R. B. Kidman, R. E. Schenter, R. W. Hardie, W. W. Little, The Shielding Factor Method of Generating Multigroup Cross Sections for Fast Reactor Analysis, *Nucl. Sci. Eng.*, **48**, pp. 193-201 (1972).
39. F. Gabrielli, A. Rineiski, Development and validation of a cross-section processing scheme for safety studies of thermal reactors, 13th SIMMER-III/IV Review Meeting, O-arai Research and Development Center, JAEA, Mito, Japan, November 20-24 (2006).
40. F. Gabrielli, A. Rineiski, W. Maschek, Computation of Heterogeneity Model Parameters for Analyses of Reactor Transients, Jahrestagung Kerntechnik 2008, Hamburg, Germany, May 27-29 (2008).
41. F. Gabrielli, A. Rineiski, W. Maschek, G. Biaut, Extension of the SIMMER Cross-Section Processing Scheme for Safety Studies of Thermal Reactors, Proc. of the International Conference on the Physics of Reactors (PHYSOR 2008), on CD-ROM, Interlaken, Switzerland, September 14-19 (2008).
42. F. Gabrielli, A. Rineiski, Extension of the SIMMER cross-section processing scheme for safety studies of thermal reactors, 14th SIMMER-III/IV Review Meeting, FZK, Karlsruhe, Germany, September 9-12 (2008).
43. G. Bell, A Simple Treatment for Effective Resonance Absorption Cross-Sections in Dense Lattices, *Nucl. Sci. Eng.*, **5**, 138 (1958).
44. G. Rimpault, Algorithmic features of the ECCO cell code for treating heterogeneous fast reactor assemblies, Proc. Int. Conf on Mathematics and Computations, Reactor Physics, and Environmental Analyses, Portland, Oregon, USA, American Nuclear Society, ISBN 0-89448-198-3, May 1–5 (1995).
45. The MCNPX Team, MCNPX™ User's Manual, Version 2.4.0, LA-CP-02-408, Los Alamos, NM, USA (2002).
46. G. Rimpault, et al., The ERANOS code and data system for fast reactor neutronic analyses, Proc. of the International Conference on the Physics of Reactors (PHYSOR 2002), Seoul, Korea, October 7-10 (2002).

47. N. Hfaiedh, Nouvelle Méthodologie de Calcul de l'Absorption Résonnante, PhD Thesis, Louis Pasteur University, Strasbourg, France (2006).
48. L. W. Nordheim, The Theory of Resonance Absorption, Proc. of Symposia in Applied Mathematics, Vol. XI, p. 58, G. Birkhoff, E. P. Wigner, Editors, Am. Math. Soc. (1961).
49. G. I. Bell, Glasstone, S., Nuclear Reactor Theory, Van Nostrand Reinhold Company, New York, USA (1970).
50. L. Dresner, Resonance Absorption in Nuclear Reactors, Pergamon Press, New York, USA (1960).
51. J. Chernick, R. Vernon, Some Refinements in the Calculation of Resonance Integrals, *Nucl. Sci. Eng.*, **4**, 649 (1958).
52. Oak Ridge National Laboratory, RSICC Peripherical Shielding Routine Collection, PRS-352/SCAMPI (1995).
53. D. C. Wade, R. G. Bucher, Conservation of the adjoint neutron spectrum by use of bilinear-weighted cross sections and its effect on fast reactor calculations, *Nucl. Sci. Eng.*, **64**, pp. 517–538 (1977).
54. E. Kiefhaber, Evaluation and Interpretation of Integral Experiments in Fast Criticals, National Topical Meeting on New Developments in Reactor Physics and Shielding, Kiamesha Lake, NY, USA, September 12-15 (1972).
55. Y. Ronen, Handbook of Nuclear Reactors Calculations, CRC Press, Inc., N. W., Boca Raton, Florida, USA, 1986.
56. OECD/NEA, The JEF-2.2 Nuclear Data Library; JEFF Report 17, France, 2000.
57. T. Nakagawa, K. Shibata, et al., Japanese Evaluated Nuclear Data Library Version 3 Revision-2: JENDL-3.2, *Nucl. Sci. Tech.*, **32**, 1259 (1995).
58. P. F. Rose, ENDF-201, ENDF/B-VI Summary Documentation, BNL-NCS-17541, 4th Edition (1991).
59. S. Rahlfs, Validation physique du nouveau code de cellule européen ECCO pour le calcul des coefficients de réactivité des réacteurs REP et RNR, Phd Thesis, Université de Provence, Marseille, France (1995).
60. T. J. Urbatsch, R. A. Forster, R. E. Prael, R. J. Beckman, Estimation and Interpretation of Keff Confidence Intervals in MCNP, *Nuclear Technology*, **111**, pp.

61. K. Wirtz, Fast Reactors, American Nuclear Society, LaGrange Park, IL, 1973.
62. Y. I. Kim, R. Hill, K. Grimm, G. Rimpault, T. Newton, Z. H. Li, A. Rineiski, P. Mohanakrishan, M. Ishikawa, K. B.. Lee, A. Danilytchev, V Stogov, BN-600 Full MOX Core Benchmark Analysis, Proc. of. The Physics of Fuel Cycles and Advanced Nuclear Systems: Global Developments (PHYSOR 2004), Chicago, IL, USA, April 25-29 (2004).
63. G. Palmiotti, J. M. Rieunier, C. Gho, M. Salvatores, BISTRO Optimized Two Dimensional Sn Transport Code, *Nucl. Sci. Eng.*, **104**, 26 (1990).
64. C. B. Carrico, E. E. Lewis, G. Palmiotti, Three-dimensional Variational Nodal Transport Methods for Cartesian, Triangular and Hexagonal Criticality Calculations, *Nucl. Sci. Eng.*, **111**, 168 (1992).
65. W. E. Nyer, S. G. Forbes, SPERT PROGRAM REVIEW, Phillips Petroleum Co., IDO-16634 (October 1960).
66. SL-1 Accident, U.S. Atomic Energy Commission. SL-1 Accident Investigation Board, U.S Govt. Print. off., Washington, USA (1961).
67. P. Liu, D. Wilhelm, E. Kiefhaber, A. Rineiski, F. Gabrielli, W. Maschek, Implementation of a plate-type fuel pin model to a multi-physics code and Benchmark modelling of special power excursion reactor tests, Proc. of the International Conference on Mathematics, Computational Methods & Reactor Physics (M&C 2009), Saratoga Springs, New York, May 3-7 (2009).
68. P. Liu, D. Wilhelm, E. Kiefhaber, A. Rineiski, F. Gabrielli, W. Maschek, Development of a plate-type fuel pin model for the neutronics and thermal-hydraulics coupled code -SIMMER-III- and its application to the analysis of SPERT, Proc. of the 13th Int. Topical Meeting on Nuclear Reactor Thermal Hydraulics (NURETH-13), Kanazawa, Japan, September 27 – October 2 (2009).
69. F. Gabrielli, G. Lohnert, A. Rineiski, W. Maschek, P. Liu, E. Kiefhaber, Impact of SIMMER neutronics modelling options on transient simulations for SPERT, 13th Int. Topical Meeting on Nuclear Reactor Thermal Hydraulics (NURETH-13), Kanazawa, Japan, September 27 – October 2 (2009).

70. F. Gabrielli, G. Lohnert, A. Rineiski, W. Maschek, P. Liu, E. Kiefhaber, Neutronics Model for SPERT, Proc. of the Jahrestagung Kerntechnik, Dresden, Germany, May 12-14 (2009).
71. A. W. Krass, K. L. Goluoglu, Experimental Criticality Benchmarks for SNAP 10A/2 Reactor Cores, Oak Ridge National Laboratory, ORNL/TM-2005/54, Vol. **I** (2005).
72. R. L. Johnson, A Statistical Determination of the Reduced Prompt Neutron Generation Time, $\Lambda/\overline{\beta}$, in the SPERT IV Reactor, Phillips Petroleum Company, IDO-16903 (1963).
73. G. R. Keepin, Physics of Nuclear Kinetics, Addison Wesley Publishing Company, Reading, Massachusetts, USA (1965).
74. A. Rineiski, KIN3D: Module de cinétique spatiale et de perturbations pour TGV2, Commissariat à l'Énergie Atomique (CEA), SPRC/LEPh 97-203 (1997).
75. F. Brown, B. Kiedrowski, W. Martin, G. Yesilyurt, Advances in Monte Carlo Criticality Methods, Proc. of the International Conference on Mathematics, Computational Methods & Reactor Physics (M&C 2009), Saratoga Springs, NY, USA, May 3-7 (2009).
76. G. D. Spriggs, R. D. Busch, K. J. Adams, D. K. Parsons, L. Petrie, J. S. Hendricks, On the Definition of Neutron Lifetimes in Multiplying and Non-Multiplying Systems, Los Alamos National Lab., LA-UR-97-1073 (1997).
77. C. M. Persson, Reactivity Determination and Monte Carlo Simulation of the Subcritical Reactor Experiment – "Yalina", MSc Thesis, Royal Institute of Technology, Stockholm, Sweden (2005).